JIMMA UNIVERSITY
JIMMA INSTITUTE OF TECHNOLOGY
SCHOOL OF GRADUATE STUDIES
FACULTY OF CIVIL AND ENVIRONMENTAL ENGINEERING
STRUCTURAL ENGINEERING STREAM

FINITE ELEMENT ANALYSIS OF REINFORCED CONCRETE CONTINUOUS DEEP BEAMS WITH OPENINGS

A Thesis Submitted to School of Graduate Studies, Jimma University in Partial Fulfillment of the Requirements for the Degree Master of Science in Structural Engineering

By

Helen Teklay Gebrekirstos

January, 2020
Jimma, Ehtiopia

JIMMA UNIVERSITY
JIMMA INSTITUTE OF TECHNOLOGY
SCHOOL OF GRADUATE STUDIES
FACULTY OF CIVIL AND ENVIRONMENTAL ENGINEERING
STRUCTURAL ENGINEERING STREAM

FINITE ELEMENT ANALYSIS OF REINFORCED CONCRETE CONTINUOUS DEEP BEAMS WITH OPENINGS

A Thesis Submitted to School of Graduate Studies, Jimma University in Partial Fulfillment of the Requirements for the Degree Master of Science in Structural Engineering

Adisor: Engr. Elmer C. Agon, Asso, Prof.

Co - Advisor: Engr. Habtamu Gebremedhin, Msc

January, 2020
Jimma, Ethiopia

DECLARATION

I declare that this research entitled "Finite Element Analysis of Reinforced Concrete Continuous Deep Beams with Openings" is my own original work, and has not been submitted as a requirement for the award of any degree in Jimma University or elsewhere.

Helen Teklay Gebrekirstos _____ _____

NAME SIGNATURE DATE

As research Adviser, I hereby certify that I have read and evaluated this thesis paper prepared under my guidance, by Helen Teklay Gebrekirstos entitled "FINITE ELEMENT ANALYSIS OF REINFORCED CONCRETE CONTINUOUS DEEP BEAMS WITH OPENINGS" and recommend and would be accepted as a fulfilling requirement for the Degree Master of Science in Structural Engineering.

Advisor: Engr. Elmer C. Agon, Asso. Prof. _____ _____

NAME SIGNATURE DATE

Co - Advisor: Engr. Habtamu Gebremedhin, Msc _____ _____

NAME SIGNATURE DATE

ABSTRACT

Now a day, numerical models for the assessment of behavior of structures become more accurate and reliable. A finite element modeling approach which is used to predict the behavior of structures is becoming more popular instead of conducting the full experimental tests, since the efficiency of the model can be evaluated by the experimental results, the numerical models shows a good agreement with the experimental program.

In this study a finite element approach was taken for assessing the response of reinforced concrete continuous deep beams with openings subjected to two point loads. The responses such as failure mode, ultimate load and deflection from the load-mid span displacement graph were verified with the experimental result.

Parametric study was carried out using the developed finite element model. In the parametric study the effects of opening size, shape and location on the load deflection behavior of deep beam was investigated.

From the study it can be conclude that the load carrying capacity of deep beams is greatly affected by the occurrence of openings or discontinuities. The inclusion of 9% rectangular opening at the exterior and interior shear span between the support and loading point on the deep beam causes a 21.08% and 52.33% reduction in the load carrying capacity respectively. In addition this study has compared different types of opening size, shapes and locations and from those shapes the circular one was with better load carrying capacity and regarding the location of openings placing openings at the center of the exterior shear span near to the exterior support was more advantageous in this study.

Keywords — Finite element model, load carrying capacity, Load deflection graph

ACKNOWLEDGEMENT

First and foremost, I would like to thank the Almighty God, who is always there for me through the times of trouble and good times. Secondly, I would to express my sincere thanks and appreciation to my advisor Engr. Elmer C. Agon (Ass.Prof.) and Co-advisor Engr. Habtamu Gebremedhin (Msc) for their advice, patience and guidance throughout the process of completing this research work.

Finally, I would like to extend my sincere gratitude to my families for their great encouragement and support during my study.

TABLE OF CONTENTS

Contents **Page**

LIST OF TABLES

LIST OF FIGURES

ABBREVIATION

ACI	American Concrete Institute
ANSYS	Analysis system
A_{st}	Area of longitudinal bottom reinforcement
A'_{st}	Area of longitudinal top reinforcement
a	Shear span distance measured from center of support to center of loading point
b_w	Width of beam
CAE	Complete Analysis Environment
CFRP	Carbon fiber reinforced polymer strips
C3D8R	Continuum three dimensional eight node brick element with reduced integration, hourglass control
CDP	Concrete damage plasticity
d	Effective depth of beam
d_c	Concrete compression damage parameter
d_t	Concrete tension damage parameter
e	Eccentricity
EC	European code
E_{cm}	Modulus of elasticity of concrete
E_s	Elastic modulus of reinforcement
f'_c	Cylinder compressive strength of concrete
f_{su}	Tensile strength of reinforcement
f_y	Yield strength of reinforcement
f_{bo}	Biaxial compressive strength of concrete

f_{cm}	Average compressive strength of concrete
f_{co}	Uniaxial compressive strength of concrete
ε_{c1}	Strain at average compressive strength
ε_{cu}	Ultimate strain
${\varepsilon_c}^{pl}$	Plastic strain
ε_y	Yield strain of reinforcement
FEA	Finite element analysis
FEM	Finite element method
G_f	Total energy supply
K	Second stress invariant ratio
K_c	Ratio of biaxial compressive strength to uniaxial compressive strength
K_e	Element stiffness matrix
$\{\delta_e\}$	Nodal displacement vector of the element
$\{F_e\}$	Nodal force vector
GFRP	Glass fiber reinforced polymer
h	Overall depth of beam
L	Span length
l_p	Width of loading plate
l_n	Clear span
ρ_s	Longitudinal bottom reinforcement ratio
${\rho'}_s$	Longitudinal top reinforcement ratio
RC	Reinforced concrete
T3D2	Two node linear 3-D truss
Ψ	Dilation angle

CHAPTER ONE

INTRODUCTION

1.1. Background of the Study

Beam is a structural member that is designed to resist forces acting perpendicular to its axis. In general, Beam can be classified into three categories as per its span-to- depth ratio namely shallow or normal beam, moderate deep beam and deep beam. Shallow beams are characterized by linear strain distribution and most of the applied load is transferred through a fairly uniform compression field.

Moderate deep beams differ from shallow beams considerably. There is a significant effect of normal pressure on stress distribution. The assumption made in simple bending (i.e. plane section remains plane after bending) becomes wrong due to nonlinear strain distribution. In moderate deep beam, the flexure capacity and shear capacity of the beam is nearly same.

Deep beams are often used as structural members in civil engineering work. A deep beam is a beam in which a significant amount of the load is carried to the supports by a compression strut joining the load and the reactions. According to ACI 318-08 Code, Deep beams are defined as members loaded on one face and supported on the opposite face so that compression struts can develop between the loads and the supports. Their clear spans are either equal to or less than four times the overall member depth or regions with concentrated loads within twice the member depth from the face of the support. The EC 203-2006 adopts the same definition as ACI 318-08, whereas the BS EN1992-1-1: 2004 Euro Code defines a deep beam as a member whose span is less to or equal to 3 times the overall section depth.

Deep beams play a very significant role in design of large as well as small structures. Some times for architectural purposes buildings are designed without using any column for a very large span. In such case if ordinary beams are provided they can cause failure such as flexural failure. In addition, most widely popular application of deep beams in

construction industry is in construction of transfer girders in offshore structures and foundation pile caps, wall footings, walls of bunkers, tanks, load bearing walls in buildings, plate elements in folded plates, pile caps, floor diaphragm and shear walls are the most important once. Particularly, the use of deep beams at the lower levels in tall buildings for both residential and commercial purposes has increased rapidly because of their convenience and economic efficiency. A deep beam in a building is shown in Fig. 1.1 as an example.

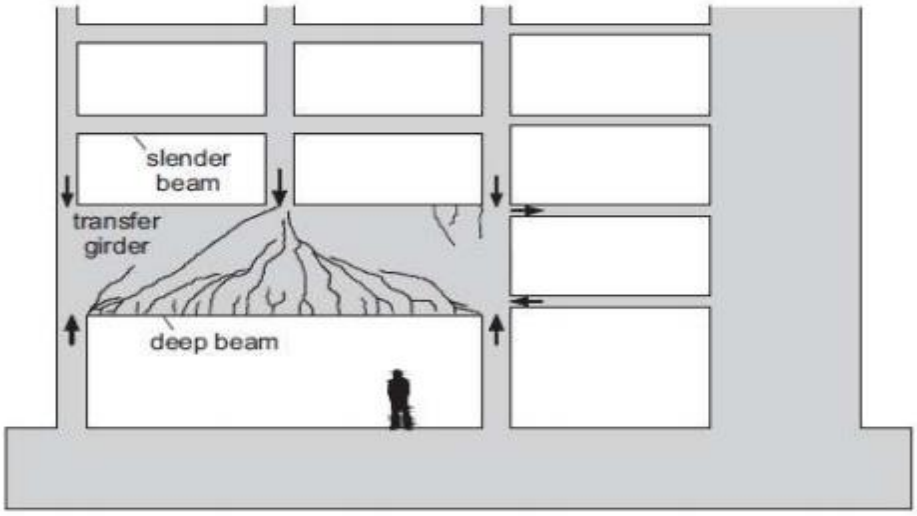

Figure 1.1 A deep beam in a building (Mihaylov, 2015)

Research on concrete deep beams has been carried out for more than five decades. From the time when research on deep beams started in 1965 until the present day, many researchers studied the behavior of deep beams.

RC deep beam can be classified into simply supported deep beam and continuous deep beam. This research was mainly focused on RC continuous deep beams.

Reinforced concrete continuous deep beams are fairly known structural elements which have a shear span to depth ratio less than 2.5, where the shear span is the clear span (l_n) of the beam for distributed load and the distance between the point of application of the load and the face of the support for concentrated load. They are used as foundation walls, transfer girders and pile caps. Figure 1.2 shows examples of continuous deep beams.

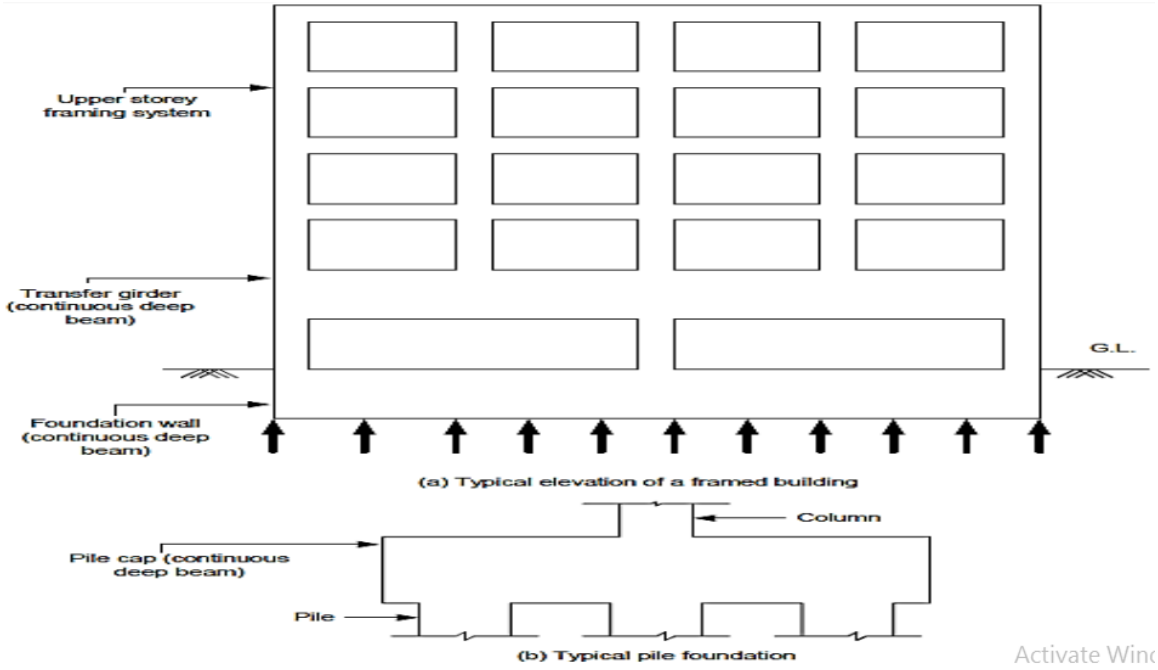

Figure 1.2 Examples of continuous deep beams (Kong, 2003)

In many cases there have been trends that RC deep beams with openings are implanted for ease the installation of building services. Building services are installed through the RC deep beam with web openings. RC deep beam with different shape of openings are used for different kind of building services such as for the installation of piping, ducts, computer networks, telephone circuits, power cable and air-conditioning.

Openings can lead to major cost saving for the construction project in the end. Advantages of openings are length of piping and ducts can be reduced by passing the piping and ducts utility through the RC deep beams with openings. Moreover, openings reduced the headroom, height of the building and slightly in weight of concrete beams which bring to such advantages. But web openings have an effect on the behavior of the structural concrete members if they are not properly provided.

Behavior of RC deep beam such as ultimate load capacity, first cracking and cracks pattern, mode of failure and load-deflection curve are affected with openings through itself. So, this effect can be minimizing by considering the appropriate size, shape and location of opening.

1.2. Statement of the Problem

The use of deep beams at lower levels in tall buildings for both residential and commercial purpose as well in the construction of bridges as transfer girders has increased rapidly because of their convenience and economic efficiency. In order to install different building services different openings in size, shape and location can introduce which lead to major cost saving for the construction project in the end.

A large number of studies have been performed regarding the effects of opening on the simple supported deep beams using both experimentally and FEA, but very limited data have been reported on continuous deep beams with web opening using FEA.

Introducing the opening in these beams is very significant. In the case that openings are provided on the beam web, their effects on the behavior of the beam become more considerable. Due to unexpected alterations in the sectional configuration, opening corners are subject to high stress concentration that may lead to cracking which is unacceptable from aesthetic and durability viewpoints. According to Mansur (2006) the reduced stiffness of the beam may give rise to excessive deflection under service load and result in a considerable redistribution of internal forces and moments in a continuous beam. The proper provisions of the web openings may be critical on the strength of deep beams. So study on continuous RC deep beam with openings using FEA is significant.

1.3. Research Questions

The research was mainly focused to answer the following research questions:

- What type of finite element model is used for the simulation of RC continuous deep beam?
- What is the effect of opening size, shape and location on the load carrying capacity of RC continuous deep beam?
- What is the difference behavior between control (solid) RC continuous deep beam and RC continuous deep beam with opening?

1.4. Objectives of the Study

1.4.1. General objective

- To conduct a nonlinear finite element analysis of two span continuous RC deep beams with openings subjected to two point concentrated load using finite element software package ABAQUS.

1.4.2. Specific objectives

- To develop finite element model which is capable of simulating the behavior of two span RC continuous deep beams?
- To investigate the effects of size, location and shape of openings on the load carrying capacity of the RC continuous deep beam.
- To identify the difference behavior between control (solid) RC continuous deep beams and RC continuous deep beams with opening.

1.5. Significance of the Study

In an experimental study, in order to acquire more realistic results in terms of RC member behavior, dimensions of a deep beam should not be lower than some certain values. It results very big specimen dimensions and that makes the experimental study of deep beams more difficult. Therefore performing such an experimental study of a deep beam requires bigger test setup, more instrumentation, and extra human labor and budget but conducting a finite element analysis in comparison with an experimental study is very preferable and reliable technique from the viewpoint of difficulty, time saving, human force and budget.

In addition to the above, this study will have a significant value to select appropriate size, location and shape of openings for continuous deep beams. Finally it helps to minimize the gap for other researchers.

1.6. Scope and Limitation of the Study

It is necessary to define the scope of the research topic since RC deep beams are concerned with different number of span and loading condition that can be occurred in

buildings. Accordingly, the scope of this research was to simulate two span continuous RC rectangular deep beams with different size, location and shape of openings loaded monotonically with two concentrated loads by using FEA ABAQUS 6.13-1 software package to obtain the load-deflection and compare the result of the opening deep beams with the solid deep beam. There will be other type of behavior of deep beams which are not occur on the two span continuous RC deep beams but they may be occur on deep beams which have number of span greater than two and on other loading condition of continuous deep beams but they are not covered in this study. Furthermore, this study was limited to the investigation of the effect of openings on the two span continuous RC deep beams under two point concentrated loading condition.

CHAPTER TWO

REVIEW OF RELATED LITERATURE

2.1. General

The study on deep beams is not a recent task by investigators. To mention some of literatures which are in connection with this study and showing advancements in the field of study is considered to be important.

The study on deep beams is started by experimental studies conducted on wall type beams behavior in 1965 and 1966. They carried out the study in the form of numerical methods and this has contributed further the numerical study on deep beam is as a significant. After these, significant numbers of experimental studies have been reported on RC deep beam behavior with or without opening in the web, beams under different load condition as well as simple or continuous deep beams.

In addition to experimental studies on RC deep beams behavior, numerical simulation with finite element method is another important issue here to discuss about. Since 1962 which finite element method was first applied in analysis of concrete structures, it was rapidly developed in both theory and application.

2.2. Research on Reinforced Concrete Continuous Deep Beam with Openings

Previous studies which carried out by various researchers on deep beam with openings are:-

Yang et al. (2006) mentioned that, the strengths at diagonal crack appearance stage and at failure load are closely related to the angle of the inclined plane joining the support and the corner of the web opening. Also, the influence of concrete strength on the ultimate shear strength remarkably decreases in deep beams with openings rather than solid deep beams.

Yoo et al. (2007) studied the behavior of pre stress RC deep beam with web opening. They found that the mode of failure of deep beams with web openings was like as solid

concrete deep beams with minor cracks occurring below and above the outer edge of openings.

Keun and Ashraf (2007) tested ten reinforced concrete continuous deep beams that had web openings in order to investigate several variables such as shear span to overall depth (a/h) ratio, size and position of web openings. There were two types of failure affected by the position and size of web openings regardless of the shear span to overall depth (a/h) ratio. The load capacity of beams that had web opening (ratio of opening area to shear span area=0.025) in external shear spans was almost equal to those of continuous deep beams that had no opening at all.

Lee et al. (2008) tested RC continuous deep beams to evaluate the shear strength with various location of web opening, in total five specimens with circular web opening have been cast and tested in the laboratory it has been observed that the specimens with web opening have about 90% of shear strength of the specimen without web opening, in general the span with web opening is less stiff than have the span without web opening.

Campione and Minafo (2012) studied the influence of small circular web opening on RC deep beams. The variables were the amount of reinforcement and the location of web opening. They found that the effect of web opening was depending on its position and the importance of the presence of reinforcement was depending on its arrangement. Yoo et al. (2013) studied the behavior of high strength RC deep beams with varies location of small web opening. They found that the increasing in concrete compressive strength (f'_c) has a significant effect on improving the behavior and load carrying capacity of RC deep beams with web opening.

Mohamed et al. (2014) tested twelve two-span continuous deep beams with and without web openings. The parameters of the study were the percentage of horizontal web reinforcement, position and number of the web openings in addition to their strengthening by using GFRP. Test results showed that the existence of web square openings within an interior or exterior shear spans had significant effects on the behavior and capacity.

Chin et al. (2015) tested three specimens of reinforced concrete deep beams, where the

first specimen was without openings, the second specimen was with large circular web opening. While, the third one was with the same opening size as in the second specimen but it strengthened with CFRP in shear regions. They found that, the reduction of load carrying capacity for unstrengthen specimen with opening compared to solid reinforced concrete deep beam was 51%.

Based on the test results presented in AL-Bayati et al. (2016) work it was concluded that, as the opening was positioned at the center of the shear span, the behavior of the beams was significantly influenced regardless the value of the (a/d) ratio and the opening size. Also it was found that, when the opening of a large diameter shifted away from the load path either to the top or to the bottom regions of the beam, the cracking and ultimate loads were dramatically reduced.

Waleed et al. (2018) mentioned that, the overall stiffness and deformability of the reinforced concrete deep beams with openings in shear spans was dramatically dropped after the occurrence of diagonal and flexural cracks in comparison with solid deep beams. Thus, comparatively the mid span section deflection was larger in these specimens.

Waleed et al. (2019) conducted experimental and numerical analysis of five simply supported RC deep beam with and without opening and the main variable were size and location of web openings. Tests showed that, as the opening size increased the dropping in the load capacity was increased. Also, this increasing led to considerable decreasing in the overall stiffness of the reinforced concrete deep beams and, as a result, significant reduction in the first diagonal and first flexural cracking loads. The failure of the investigated deep beam was characterized by either diagonal splitting mode of failure or shear-compression mode of failure.

2.3. Finite Element Method

The facts associated for choosing nonlinear finite element analysis as validation tool can be verified in the following paragraphs.

The finite element analysis is a numerical technique. In this method all the complexities of the problems, like varying shape, boundary conditions and loads are maintained as

they are but the solutions obtained are approximate. Because of its diversity and flexibility as an analysis tool, it is receiving much attention in engineering. The fast improvements in computer hardware technology and slashing of cost of computers have boosted this method, since the computer is the basic need for the application of this method. A number of popular brand of finite element analysis packages are now available commercially (Bhavikatti, 2005).

In engineering problems there are some basic unknowns. If they are found, the behavior of the entire structure is predicted. The basic unknowns or the field variables which are encountered in the engineering problems are displacements in solid mechanics, velocities in fluid mechanics, and electric and magnetic potentials in electrical engineering and temperatures in heat flow problems. In a continuum, these unknowns are infinite. The finite element procedure reduces such unknowns to a finite number by dividing the solution region into small parts called elements and by expressing the unknown field variables in terms of assumed approximating functions (Interpolating functions/Shape functions) within each element. The approximating functions are defined in terms of field variables of specified points called nodes or nodal points. Thus in the finite element analysis the unknowns are the field variables of the nodal points. Once these are found the field variables at any point can be found by using interpolation functions (Bhavikatti, 2005).

After selecting elements and nodal unknowns next step in finite element analysis is to assemble element properties for each element. For example, in solid mechanics, the force-displacement i.e. stiffness characteristics of each individual element have to be found (Bhavikatti, 2005).

Mathematically this relationship is of the form,

$[K]_e[\delta]_e = [F]_e$ ……. eqn 2.1 (Bhavikatti, 2005)

Where $[K]_e$ is element stiffness matrix

$[\delta]_e$ is nodal displacement vector of the element

$[F]_e$ is nodal force vector

The exact analysis of reinforced concrete deep beams with web openings presents formidable problems. Existing methods of predicting deep beam behavior involves either elastic theory or semi–empirical equation, neither of which entirely satisfactory (Yoo, et al., 2004). The basic assumption that plane sections remain plane after loading and that the material is homogeneous and elastic do not hold for deep beams. Some recommendations have been made following experimental investigations of the subjects; of particular note is the truss analogy which led to the development of a semi-empirical design equations for ultimate strength. Tan et al. (2003) and Yang et al. (2006) mentioned that these equations are found complicated, approximate and a more rigorous solution to the problem is desirable and cannot be used to predict the failure modes of deep beams. It is recognized that finite element methods can provide realistic and satisfactory solutions for nonlinear behavior of reinforced concrete structures.

Singh et al. (1980) and Tan et al. (2003) mentioned that FEM offers a powerful and general analytical tool for studying the behavior of reinforced concrete deep beams.

Demir et al. (2016) proposed a numerical finite element model, as well as a reliable finite element modeling technique and constitutive material models to simulate nonlinear behavior of reinforced concrete deep beams. The results demonstrated that finite element analysis is a highly effective and consistent tool to simulate nonlinear behavior of reinforced concrete deep beams.

2.4. ABAQUS Software

ABAQUS is a suite of powerful engineering simulation programs, based on the finite element method that can solve problems ranging from relatively simple linear analyses to the most challenging nonlinear simulations. ABAQUS contains an extensive library of elements that can model virtually any geometry. It has an equally extensive list of material models that can simulate the behavior of most typical engineering materials including metals, rubber, polymers, composites, reinforced concrete, crushable and resilient foams, and geotechnical materials such as soils and rock. Designed as a general-purpose simulation tool, ABAQUS can be used to study more than just structural (stress/displacement) problems. It can simulate problems in such diverse areas as heat

transfer, mass diffusion, thermal management of electrical components (coupled thermal-electrical analyses), acoustics, soil mechanics (coupled pore fluid-stress analyses), and piezoelectric analysis. ABAQUS offers a wide range of capabilities for simulation of linear and nonlinear applications. Problems with multiple components are modeled by associating the geometry defining each component with the appropriate material models and specifying component interactions. In a nonlinear analysis ABAQUS automatically chooses appropriate load increments and convergence tolerances and continually adjusts them during the analysis to ensure that an accurate solution is obtained efficiently (ABAQUS 2008).

2.5. Research on Reinforced Concrete Continuous Deep Beam using FEA

Dirar and Morley (2005) describes a series of nonlinear finite element analyses carried out using the commercial package, DIANA7 to predict the ultimate load and mode of failure for three different types of reinforced concrete continuous two-span deep beams. Only one parameter, the shear retention factor, was varied during the analysis. They concluded that the finite element method is capable of modeling the behavior of the reinforced concrete deep beams and the predictions of the ultimate load are within an accuracy region of 5%.

Sabale et al. (2014) study the behavior of deep beams of various span to depth ratio using finite element analysis under two point loading of 50KN. The detailed analysis has been carried out by using non-linear finite element method and design of deep beam by using I.S 456-2000. The objectives of this study are to observe deflection, cracking of deep beams subjected to two point loading of 50KN.They conclude that deflection of beams increases as span to depth ratio decreases and as span to depth ratio goes on decreasing the load at failure goes decreasing.

Wissam (2015) describes a series of finite element analyses carried out using ANSYS to predict the behavior and strength of continuous reinforced concrete deep beams. Main variables investigated were beam depth (h), ranged from 400 mm to720 mm, compressive strength of concrete, f'_c, and shear span-to-overall depth ratio, a/h . He concludes that the

finite element method is used for the nonlinear analysis and design of such elements very efficiently and accurately. The mean ratio of experimental to predicted values for ultimate load capacities is equal 1.04.

Kassim et al. (2015) implemented nonlinear finite element to examine ten reinforced concrete deep beams with single large web opening under one point loading. These beams were strengthened by using CFRP sheets except one which was referred as a reference beam (i.e., beams without strengthening). The dimension of single web opening was (381×381) mm and located near the left support of the beam. The considered variables were the CFRP sheets configuration and their thickness. The CFRP sheets configuration was vertical, horizontal and (U) type configuration. These CFRP sheets were varied in thickness which were (0.7, 1.4 and 2.8) mm. They found that the percentage of increasing in the ultimate load compared to the reference beam was (26, 53 and 59 %), (55, 78 and 90 %) and (86, 92 and 97%) for vertical, horizontal and (U) type configurations of CFRP sheets thickness of (0.7, 1.4 and 2.8) mm, respectively.

Mohamed and Ahmed (2019) studied the behavior of bottom loaded continuous deep beams (CDB) numerically by using finite element modeling. Main variables investigated were position of web openings and percentage of web reinforcement ratio. They conclude that ultimate capacity of CDB with web openings increased when the position of web openings was at either the top or bottom of the center of load path. On the other hand, the top position of the web openings is more sufficient than bottom web openings. Opening types has insignificant effect on ultimate capacity of CDB. Further, it observed from the results that, additional reinforcement around the opening had insignificant effect on ultimate capacity of CDB.

Based on a detailed literature survey, it is observed that the behavior of reinforced concrete continuous deep beams containing openings loaded up to failure through finite element analysis is limited. The robust finite element analysis in terms of simulating nonlinear behavior of reinforced concrete continuous deep beams with different size, shape and location of opening is also found limited. In the present study, the numerical investigations will be carried out on two span reinforced concrete continuous deep beams

with and without opening against static loading to demonstrate the accuracy and effectiveness of the finite element based numerical models and to predict the effect of openings in deep beams. Even though many experimental studies have been reported, no researches widely study on two span continuous reinforced concrete deep beams with opening by simulation.

CHAPTER THREE

RESEARCH METHODOLOGY

3.1. Research Design

This study uses the finite element approach to gather the relevant data regarding the behavior of reinforced concrete continuous deep beams with openings using ABAQUS software. Yang and Ashour (2007) experimental result was used to check whether the simulation results reflect the real world.

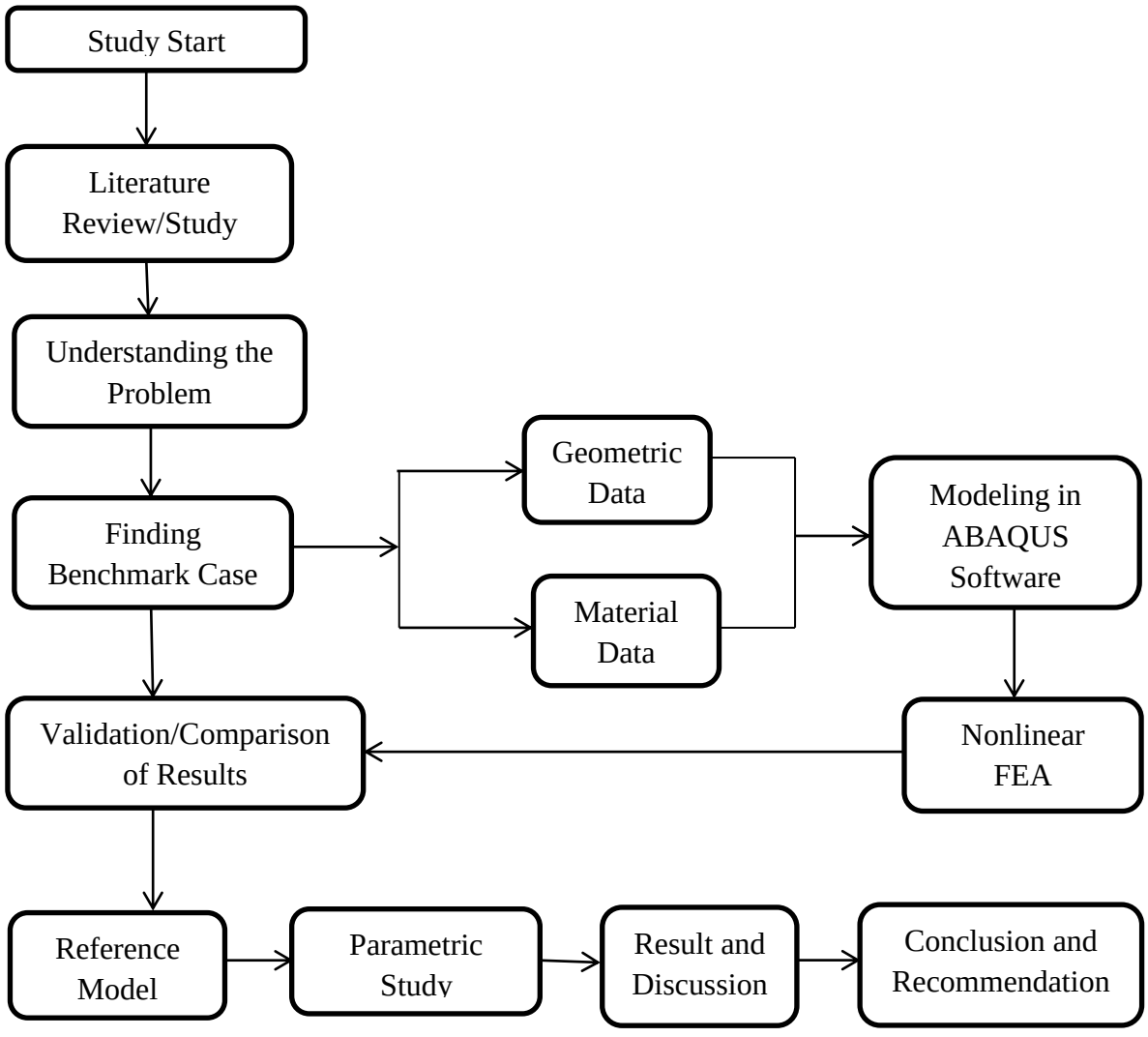

Figure 3.1 Flow chart showing methodology used

3.2. Study Variables

The dependent variable include

- Performance of RC continuous deep beam

The independent variables include

- Size of openings
- Shape of openings
- Location of openings

3.3. Sample detailing

This research was concerned with a maximum of seventy three sample models of rectangular RC continuous deep beams as shown in Table 3.1, 3.2 and 3.3.

Table 3.1 Sample detailing for opening provide at center between support and loading point

Beam notation	Size of opening (mm)	Opening size (%)	Shape of opening	Location of opening
L10-60	-	-	-	-
B1	101.554125	1	Circular	Exterior shear span
B2	203.1082501	4	Circular	Exterior shear span
B3	304.6623751	9	Circular	Exterior shear span
B4	101.554125	1	Circular	Interior shear span
B5	203.1082501	4	Circular	Interior shear span
B6	304.6623751	9	Circular	Interior shear span
B7	90 X 90	1	Square	Exterior shear span
B8	180 X 180	4	Square	Exterior shear span
B9	270 X 270	9	Square	Exterior shear span
B10	90 X 90	1	Square	Interior shear span
B11	180 X 180	4	Square	Interior shear span
B12	270 X 270	9	Square	Interior shear span
B13	100 X 81	1	Rectangular H	Exterior shear span
B14	190 X 170.527	4	Rectangular H	Exterior shear span
B15	280 X 260.358	9	Rectangular H	Exterior shear span
B16	100 X 81	1	Rectangular H	Interior shear span
B17	190 X 170.527	4	Rectangular H	Interior shear span
B18	280 X 260.358	9	Rectangular H	Interior shear span
B19	81 X 100	1	Rectangular V	Exterior shear span
B20	170.527 X 190	4	Rectangular V	Exterior shear span
B21	260.358 X 280	9	Rectangular V	Exterior shear span
B22	81 X 100	1	Rectangular V	Interior shear span
B23	170.527 X 190	4	Rectangular V	Interior shear span
B24	260.358 X 280	9	Rectangular V	Interior shear span

Table 3.2 Sample detailing for opening provide at center near to support

Beam notation	Size of opening (mm)	Opening size (%)	Shape of opening	Location of opening
B25	101.554125	1	Circular	Exterior shear span
B26	203.1082501	4	Circular	Exterior shear span
B27	304.6623751	9	Circular	Exterior shear span
B28	101.554125	1	Circular	Interior shear span
B29	203.1082501	4	Circular	Interior shear span
B30	304.6623751	9	Circular	Interior shear span
B31	90 X 90	1	Square	Exterior shear span
B32	180 X 180	4	Square	Exterior shear span
B33	270 X 270	9	Square	Exterior shear span
B34	90 X 90	1	Square	Interior shear span
B35	180 X 180	4	Square	Interior shear span
B36	270 X 270	9	Square	Interior shear span
B37	100 X 81	1	Rectangular H	Exterior shear span
B38	190 X 170.527	4	Rectangular H	Exterior shear span
B39	280 X 260.358	9	Rectangular H	Exterior shear span
B40	100 X 81	1	Rectangular H	Interior shear span
B41	190 X 170.527	4	Rectangular H	Interior shear span
B42	280 X 260.358	9	Rectangular H	Interior shear span
B43	81 X 100	1	Rectangular V	Exterior shear span
B44	170.527 X 190	4	Rectangular V	Exterior shear span
B45	260.358 X 280	9	Rectangular V	Exterior shear span
B46	81 X 100	1	Rectangular V	Interior shear span
B47	170.527 X 190	4	Rectangular V	Interior shear span
B48	260.358 X 280	9	Rectangular V	Interior shear span

All the seventy three sample model of reinforced concrete continuous deep beams had overall depth of 600mm, section width of 160mm and span length of 1200mm.

The size of the opening for circular shape was given as a diameter. And the opening size 1%, 4% and 9% indicate that the percentage of the opening size from the total area of the reinforced concrete continuous deep beams. All sample models have the same cylindrical compressive strength of concrete, reinforcement properties and arrangements with L10-60 beam (experimental tested beam).

Table 3.3 Sample detailing for opening provide at center near to loading point

Beam notation	Size of opening (mm)	Opening size (%)	Shape of opening	Location of opening
B49	101.554125	1	Circular	Exterior shear span
B50	203.1082501	4	Circular	Exterior shear span
B51	304.6623751	9	Circular	Exterior shear span
B52	101.554125	1	Circular	Interior shear span
B53	203.1082501	4	Circular	Interior shear span
B54	304.6623751	9	Circular	Interior shear span
B55	90 X 90	1	Square	Exterior shear span
B56	180 X 180	4	Square	Exterior shear span
B57	270 X 270	9	Square	Exterior shear span
B58	90 X 90	1	Square	Interior shear span
B59	180 X 180	4	Square	Interior shear span
B60	270 X 270	9	Square	Interior shear span
B61	100 X 81	1	Rectangular H	Exterior shear span
B62	190 X 170.527	4	Rectangular H	Exterior shear span
B63	280 X 260.358	9	Rectangular H	Exterior shear span
B64	100 X 81	1	Rectangular H	Interior shear span
B65	190 X 170.527	4	Rectangular H	Interior shear span
B66	280 X 260.358	9	Rectangular H	Interior shear span
B67	81 X 100	1	Rectangular V	Exterior shear span
B68	170.527 X 190	4	Rectangular V	Exterior shear span
B69	260.358 X 280	9	Rectangular V	Exterior shear span
B70	81 X 100	1	Rectangular V	Interior shear span
B71	170.527 X 190	4	Rectangular V	Interior shear span
B72	260.358 X 280	9	Rectangular V	Interior shear span

3.4. Explanation of the experimental test

3.4.1. Test specimen

The details of geometrical dimensions and reinforcement for test specimen of Yang and Ashour (2007) is shown in Table 3.4 and Fig. 3.2. Main variables investigated were beam depth, h, ranged from 400 mm to 720 mm, compressive strength of concrete, f'_c, and shear span-to-overall depth ratio, a/h. The beams tested were to the concrete compressive strength: L-series for concrete design strength of 27 MPa and H-series for concrete design strength of 60 MPa. The beam notation given in Table 3.4 includes three parts. The first part refers to concrete strength: L for low concrete strength. The second part is used to identify the shear span-to-overall depth ratio and the third part gives the section

overall depth in cm. For example, L10–60 is a continuous deep beam having a low concrete strength, shear span-to-overall depth ratio of 1.0 and overall depth of 600 mm (Yang, and Ashour, 2007).The L10-60 beam was used as a validation beam with the finite model of this research.

The section width, b_w, of L10-60 beam is 160 mm and longitudinal top and bottom reinforcement ratios were 1%. The total length of test specimen is given in Table 3.4. The distance between the soffit of beam and center of longitudinal reinforcement was 45 mm. The longitudinal bottom reinforcement was continuous over the full length of the beam and the longitudinal top reinforcement was anchored within the outside of exterior supports by 90^0 hooks as shown in Fig. 3.2 (Yang, and Ashour, 2007).

Table 3.4 Details of test specimen (Yang, and Ashour, 2007)

Specimen	f'_c (MPa)	a/h	h (mm)	a (mm)	d (mm)	L (mm)	A_{st} =A'_{st} (mm^2)	$\rho_s = \rho'_s$
L10–60	32.1	1	600	600	555	1200	861	0.0097

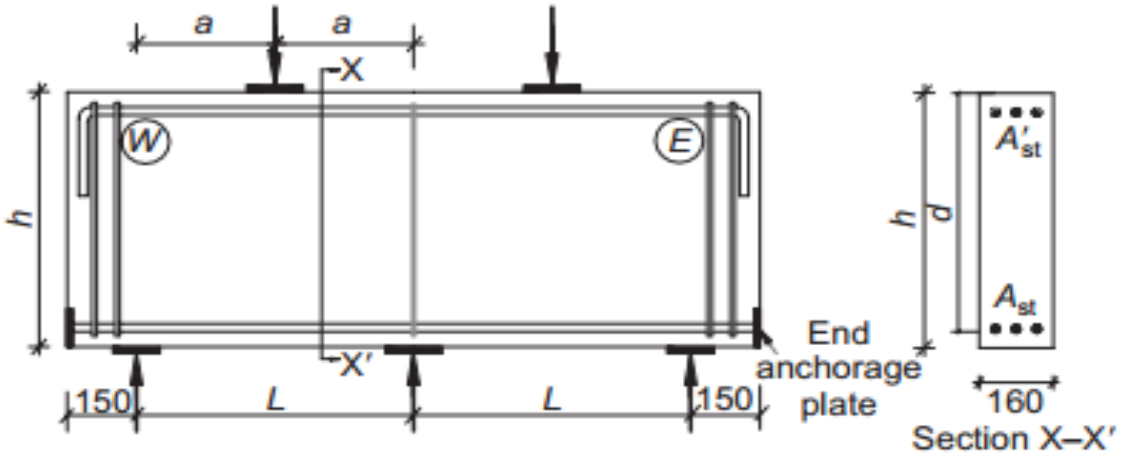

Figure 3.2 Details of beam geometry and arrangement of reinforcements (Yang, and Ashour, 2007)

3.4.2. Material properties

Figure 3.3 shows the stress–strain relationship of the 19 mm diameter steel reinforcing bar used in test specimen.

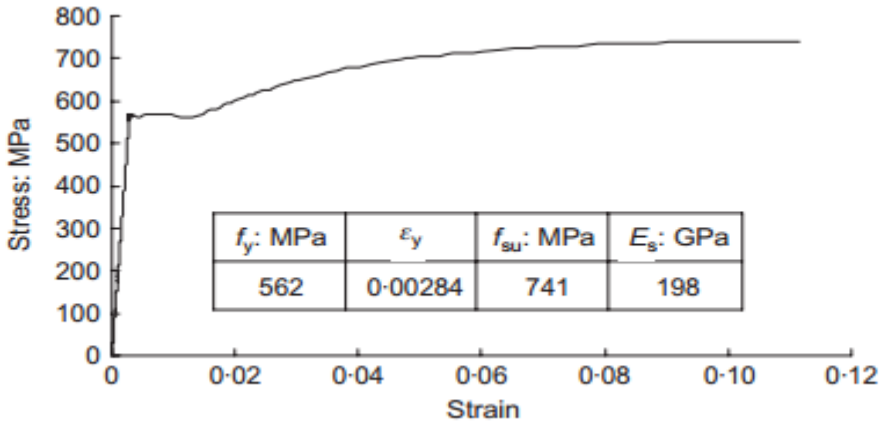

Figure 3.3 Stress–strain curve of longitudinal reinforcement (Yang, and Ashour, 2007)

3.4.3. Test set-up

Loading and support arrangements are shown in Fig. 3.4. The beam were tested to failure under two-point symmetrical top loads with loading rate of 3 kN/min using a 3000 kN capacity universal testing machine. The two exterior end supports are designed to allow horizontal and rotational movements, whereas the intermediate support prevents horizontal movement but allows rotation. At the location of loading or support point, a steel plate of 100 mm or 200 mm wide was provided to prevent premature crushing or bearing failure as shown in Fig. 3.4 (Yang, and Ashour, 2007).

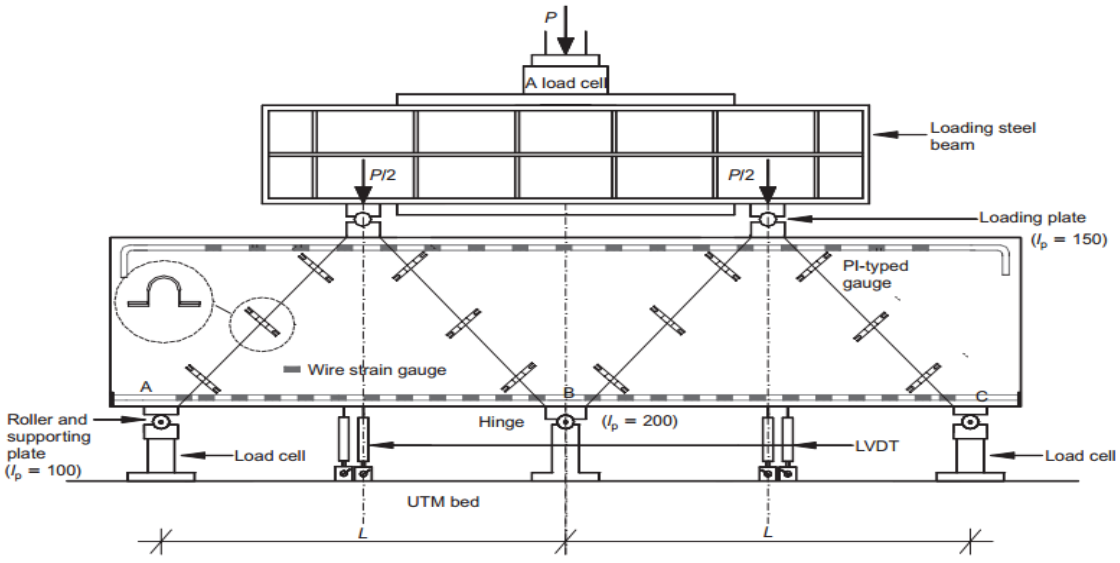

Figure 3.4 Test set-up of specimen (dimensions in mm) (Yang, and Ashour, 2007)

3.5. Description of finite element model

3.5.1. Element types

Different types of 3D solid elements were provided by finite element package. In this study C3D8R (continuum three dimensional eight node brick element with reduced integration, hourglass control) are used for both concrete and steel plate and T3D2 (A two node linear 3-D truss).

3.5.2. Reinforcement bars

For elastic design analysis, the reinforcement was usually neglected in the finite element modeling since the stiffness contribution of concrete is much greater than the reinforcement but in the non-linear analysis the modeling of reinforcement is needed basically in determining the ultimate capacity of a structure. In this study the reinforcing bars are modeled as truss elements that are one dimensional line elements in three dimensional space that have stiffness associated with deformation in the line. Both elastic and plastic properties were included the ELASTIC option used to assign the modulus of elasticity and Poisson's ratio and in the PLASTIC option the true stress and strain values were used to model its plastic property.

Mechanical properties of reinforcing bars which are used in this simulation was directly taken from the experimental program as given in Table 3.5.

Table 3.5 Mechanical properties of reinforcement bars (Yang, and Ashour, 2007)

	Area(mm^2)	Yield stress (Mpa)	Yield strain(Mpa)	Tensile stress(Mpa)	Modulus of Elasticity (Gpa)
Main reinforcement	283.528737	562	0.00284	741	198

3.5.3. Concrete elements and constitutive relations

Concrete exhibits non-linearity both in compression and tension this poses difficulties in numerical analysis. Parameters needed to model concrete under compound stress are included in ABAQUS software in concrete damaged plasticity model.

One of the strength hypothesis most often applied to concrete is the Drucker-prager hypothesis. According to it, failure is determined by non-dilatational strain energy and the boundary surface itself in the stress space assumes the shape of a cone. The advantage of using this criterion is surface smoothness and thereby no complications in numerical application. The drawback is that it is not fully consistent with the actual behavior of concrete (Sumer, and Aktas, 2015).

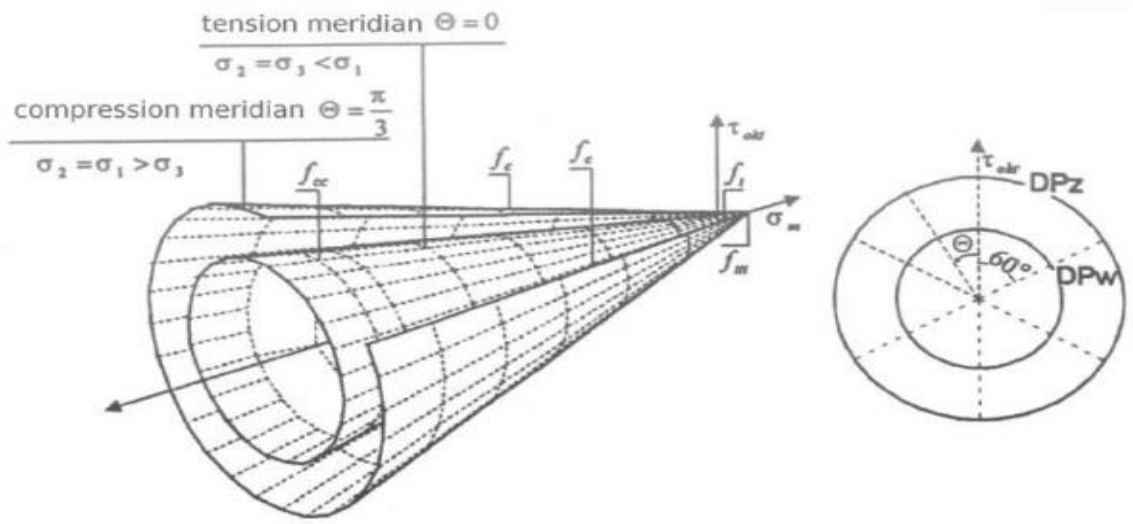

Figure 3.5 Drucker-prager boundary surface and deviatoric cross-section (Sumer, and Aktas, 2015)

The CDP model used in ABAQUS software is a modification of Drucker-prager strength hypothesis. In recent years it has been modified further that shows the failure surface in the deviatoric cross section needs not to be a circle and it is governed by parameter K. The parameter K is interpreted as a ratio of the distances between the hydrostatic axis and the compression meridian and tension meridian in the deviatoric cross section. The CDP model recommends to assume K =2/3. This shape is similar to the strength criterion formulated by William and Warnke (1975) (Sumer, and Aktas, 2015).

Similarly, the shape of the plane's meridians in the stress space changes, experimental results indicate that the meridians are curves. In the CDP model the plastic potential surface in the meridians plane assumes the form of a hyperbola. The shape is adjusted through eccentricity. The CDP model recommends to assume e = 0.1 (Sumer, and Aktas, 2015).

Another parameter describing the state of the point in which the concrete undergoes failure under biaxial compression in other words it is a ratio of the strength in the biaxial state to the strength in the uniaxial state. ABAQUS user manual species default value of 1.16 (Sumer, and Aktas, 2015).

The last parameter characterizing the performance of concrete under compound stress is dilation angle which is concrete internal friction angle usually assumed as 36° (Sumer, and Aktas, 2015).

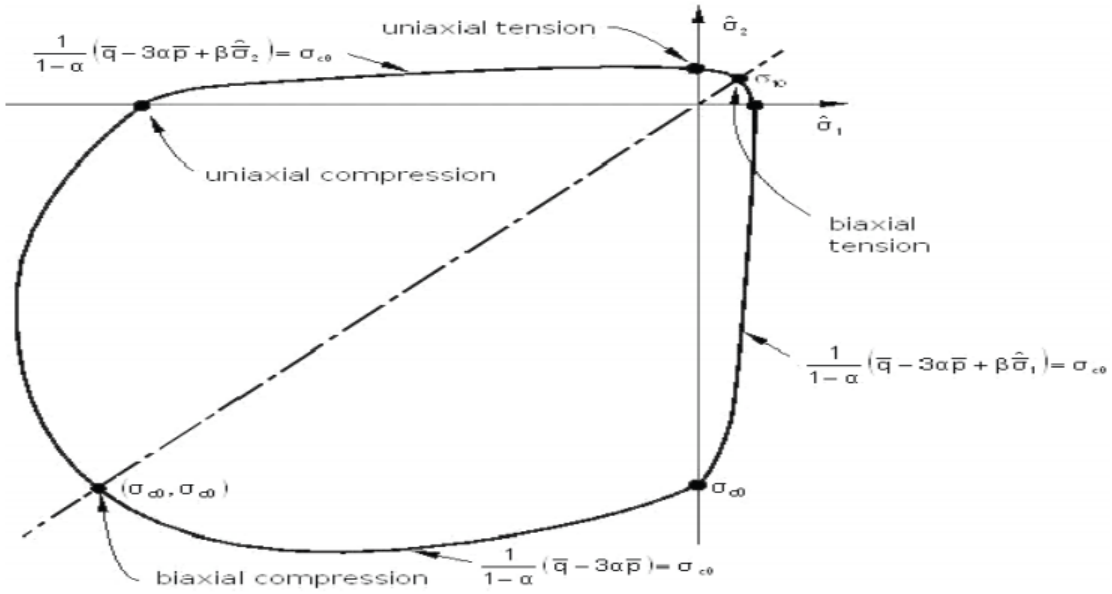

Figure 3.6 Strength of concrete under biaxial stress in CDP (Kmieck, and Kaminski, 2011)

Table 3.5 Default parameters of CDP model under compound stress (Kmieck, and Kaminski, 2011)

Parameter name	Value
Ψ(dilatation angle)	36^0
e (eccentricity)	0.1
fbo/fco (ratio of biaxial to uniaxial compressive strength)	1.16
K (second stress invariant ratio)	0.667
Viscosity parameter	0

3.5.4. Stress strain curve for uniaxial compression

When there is no test result the only available quantity is average compressive strength of concrete (f_{cm}) so other quantities can be calculated from

$$E_{cm} = 22(0.1f_{cm})^{0.3} \qquad eqn\ 3.1$$

$$\varepsilon_{c1} = 0.7(f_{cm})^{0.31} \qquad eqn\ 3.2$$

$$\varepsilon_{cu} = 3.5\,{}^{0}/_{00} \qquad eqn\ 3.3$$

Where f_{cm} is in (Mpa)

E_{cm} is the longitudinal modulus of elasticity (Gpa)

ε_{c1} is the strain at average compressive strength

ε_{cu} is the ultimate strain

The formulas 3.2 and 3.3 are applicable to concrete grade of C50/60 at the most. On the basis of experimental results Majewski proposed the following approximating formulas;

$$\varepsilon_{c1} = 0.0014[2 - exp(-0.024f_{cm}) - exp(-0.14f_{cm})] \qquad eqn\ 3.4$$

$$\varepsilon_{cu} = 0.004 - 0.0011[1 - exp(-0.0215f_{cm})] \qquad eqn\ 3.5$$

After knowing these values points at which the graph intersect is determined

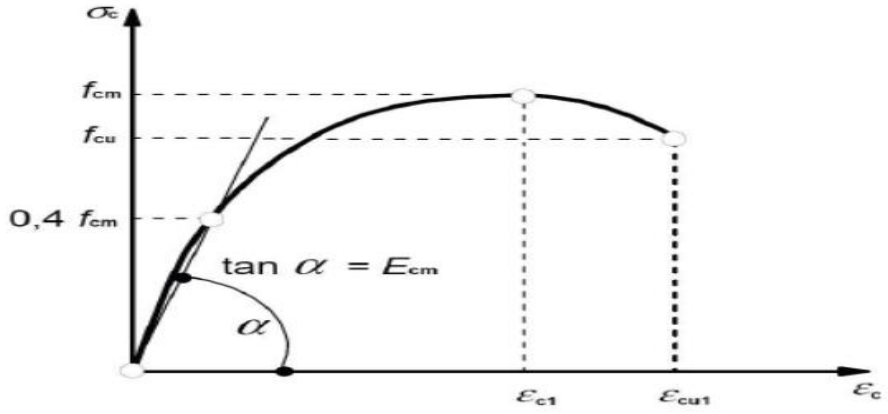

Figure 3.7 Stress-strain diagram for analysis of structures according to Eurocode 2 (EC 2-02, 2002)

The compressive stresses will be calculated using the formula given below

$$\frac{\sigma_c}{f_{cm}} = \frac{k\eta - \eta^2}{1 + (k-2)\eta} \qquad eqn\ 3.6$$

Where $\eta = {}^{\varepsilon_c}/_{\varepsilon_{c1}}$

ε_{c1} = is the Strain at the peak stress

$$k = 1.05E_{cm} \times {}^{|\varepsilon_{c1}|}/_{f_{cm}}$$

Once a graph is obtained the variables should be transformed to inelastic strains which are used in CDP model so in order to find the inelastic strain the elastic strain should be deducted from the total strain.

$$\varepsilon_c{}^{in} = \varepsilon_c - \varepsilon_{oc}{}^{el} \qquad eqn\ 3.7$$

$$\varepsilon_{oc}{}^{el} = \frac{\sigma_c}{E_o} \qquad eqn\ 3.8$$

Having defined the yield stress-inelastic strain pair of variables degradation variable d_c which ranges from zero for undamaged material to one for total loss of load bearing capacity is determined.

$$d_c = 1 - \frac{\sigma_c}{f_{cm}} \qquad eqn\ 3.9$$

And finally the plastic strain will be calculated by the ABAQUS software itself.

$$\varepsilon_c{}^{pl} = \varepsilon_c{}^{in} - \frac{d_c}{(1-d_c)}\frac{\sigma_c}{E_O} \qquad eqn\ 3.10$$

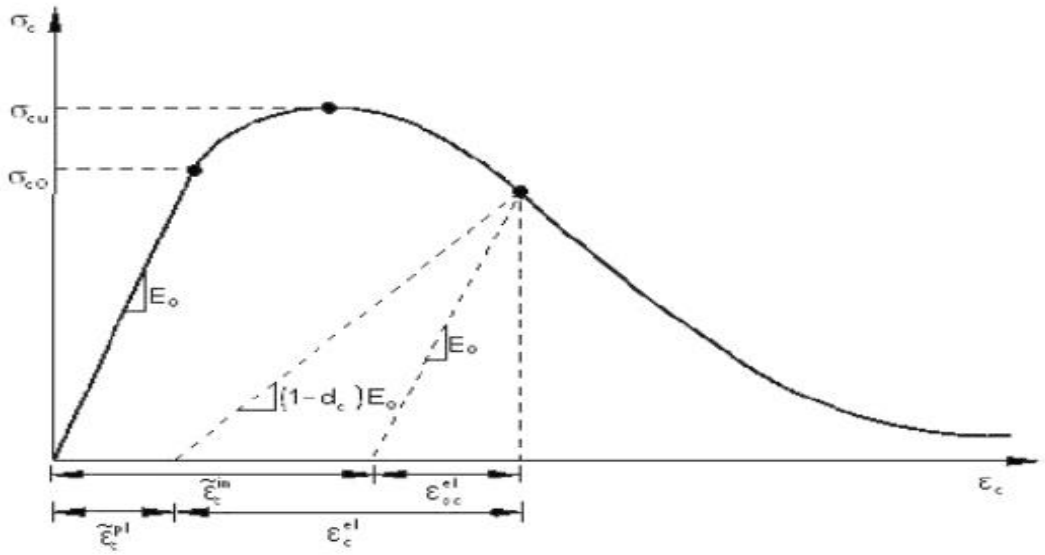

Figure 3.8 Response of concrete to uniaxial loading in compression (Kmieck, and Kaminski, 2011)

3.5.5. Stress strain curve for uniaxial tension

Bilinear model shown in figure was adopted for tensile behavior of concrete. Cracking opening was used instead of tensile strain and calculated as a ratio of total energy supply (G_f) per unit area required to create crack in concrete. Thus brittle behavior of concrete was defined by stress –cracking displacement rather than a stress-strain response (Sumer, and Aktas, 2015).

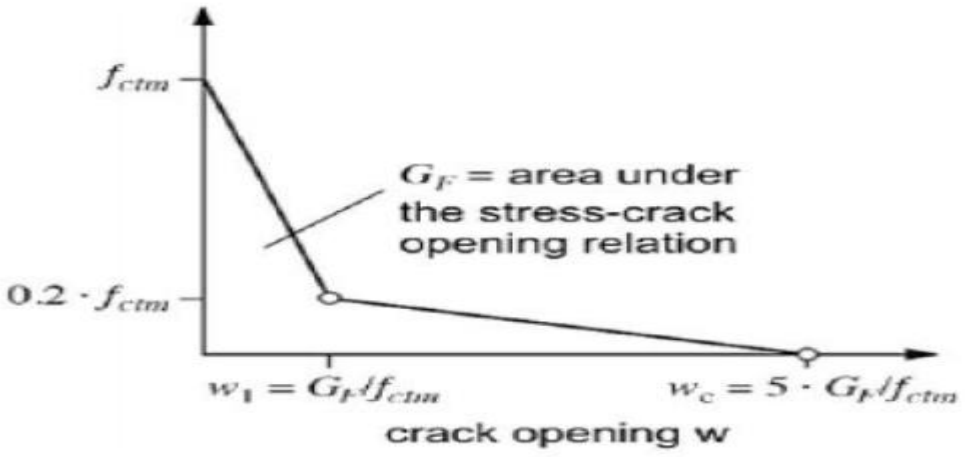

Figure 3.9 Stress-crack opening relation for uniaxial tension (Sumer, and Aktas, 2015)

The concrete damaged plasticity model assumes that the reduction of the elastic modulus is given in terms of a scalar degradation variable d as

$$E = (1 - d)E_o \qquad eqn\ 3.11$$

Where E_o is the initial (undamaged) modulus of elasticity

In this study all damage properties of concrete were derived from a single known quantity average compressive strength of concrete (f_{cm}).

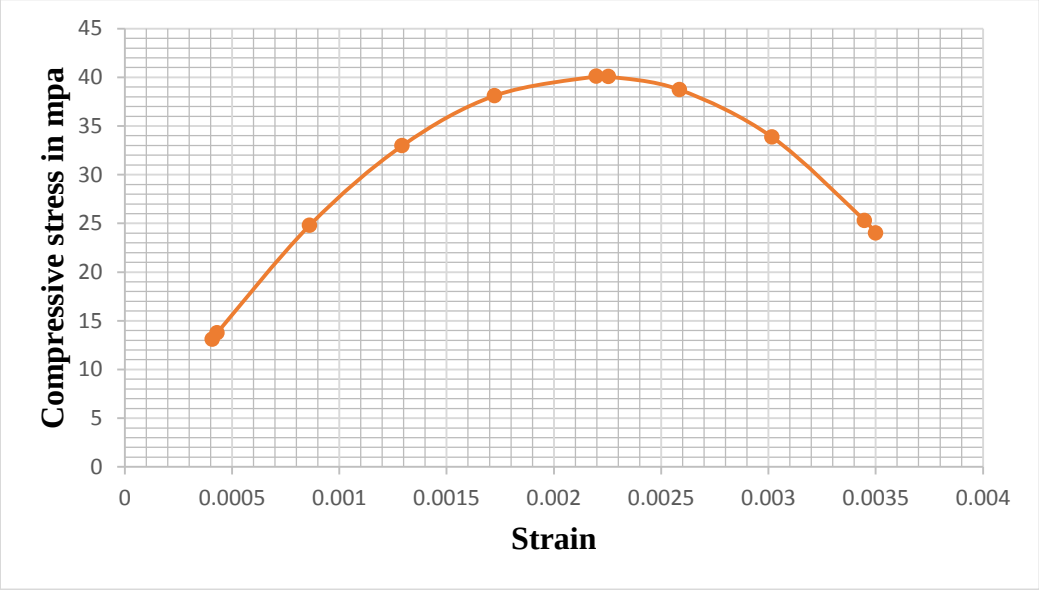

Figure 3.10 Compressive behavior of the analyzed concrete

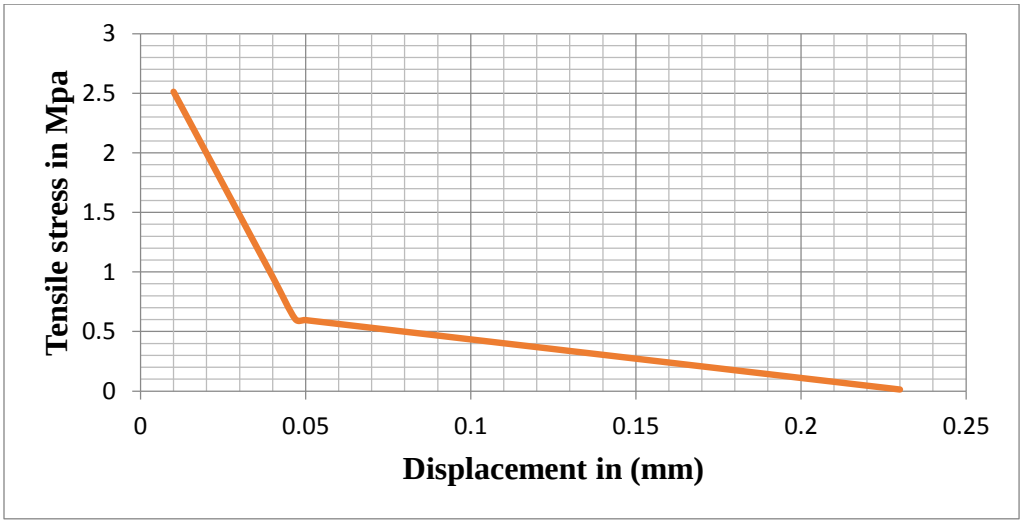

Figure 3.11 Tensile behavior of analyzed concrete

3.5.6. Finite element model

After defining the material properties the geometry of deep beam with steel plates was plotted as shown in Figure 3.12.

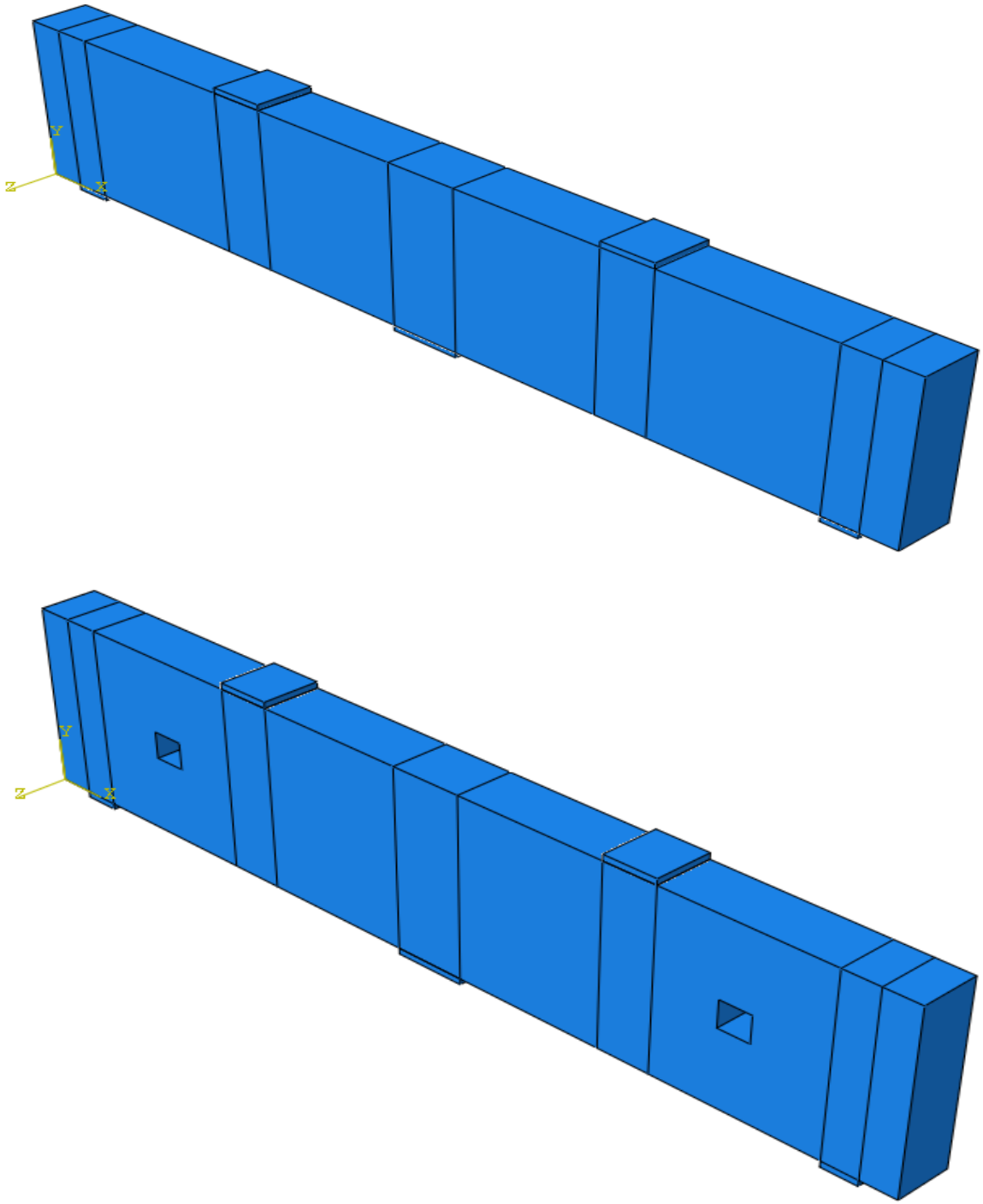

Figure 3.12 Geometric model of continuous deep beam with and without opening

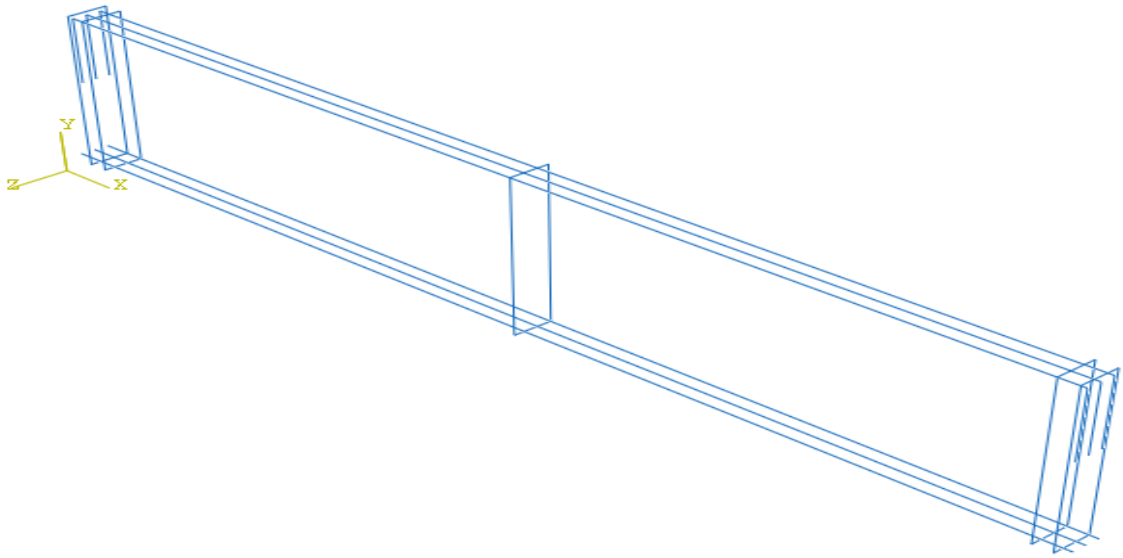

Figure 3.13 Embedded reinforcement of the deep beam

The individual elements are connected properly after assembling all elements in the simulation and the reinforcements have been modeled as embedded elements in concrete region so that the interaction between reinforcement and concrete elements assumed fully bonded. And steel plates were directly tied to the beam using the option tie constraint.

After modeling and assembling the section appropriate boundary condition were created using the boundary condition option using the initial step. The two exterior end supports are designed to allow horizontal and rotational movements, whereas the intermediate support prevents horizontal movement but allows rotation.

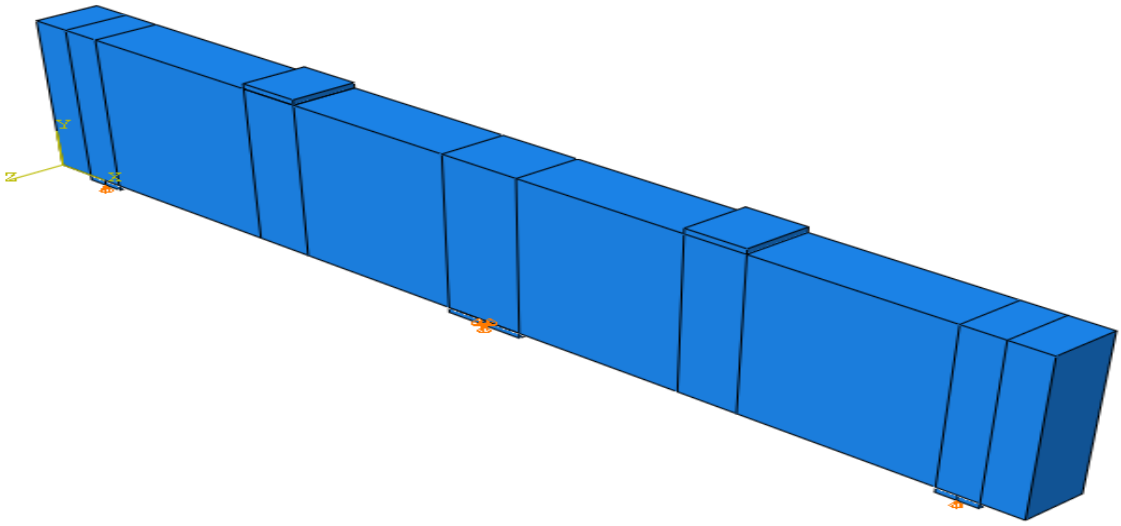

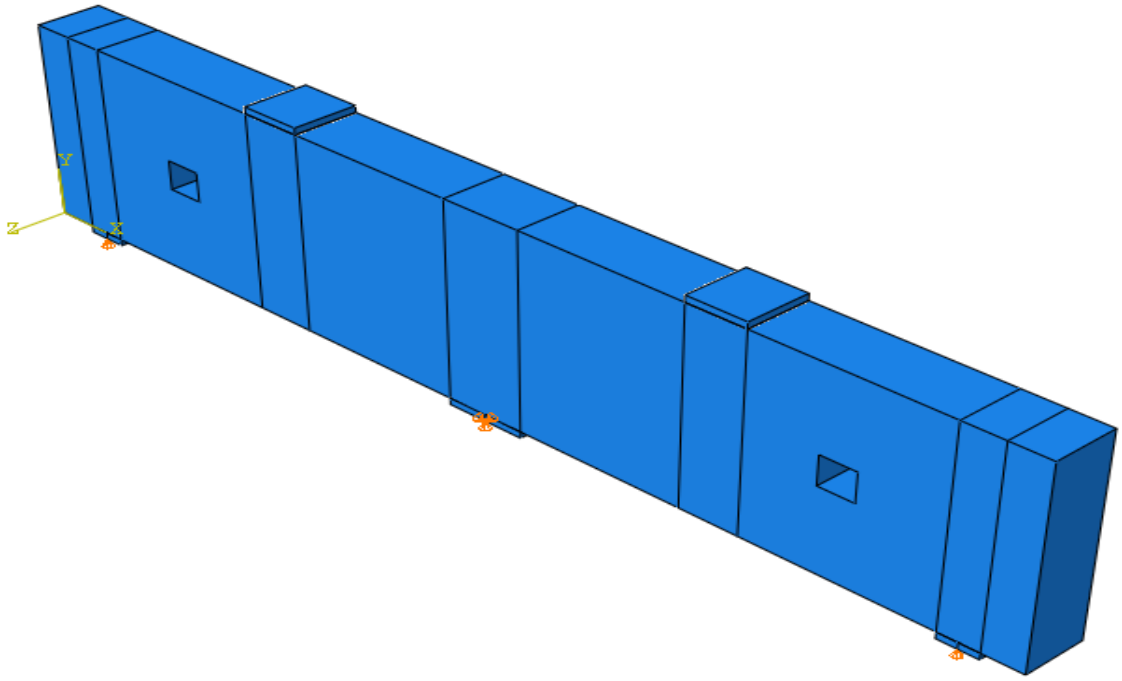

Figure 3.14 Boundary support conditions of the model

The load was applied as a point load that was kept constant throughout the analysis. The interaction between the reference point (RP) and the load plate were coupling constraint in order to distribute the point load to the load plate.

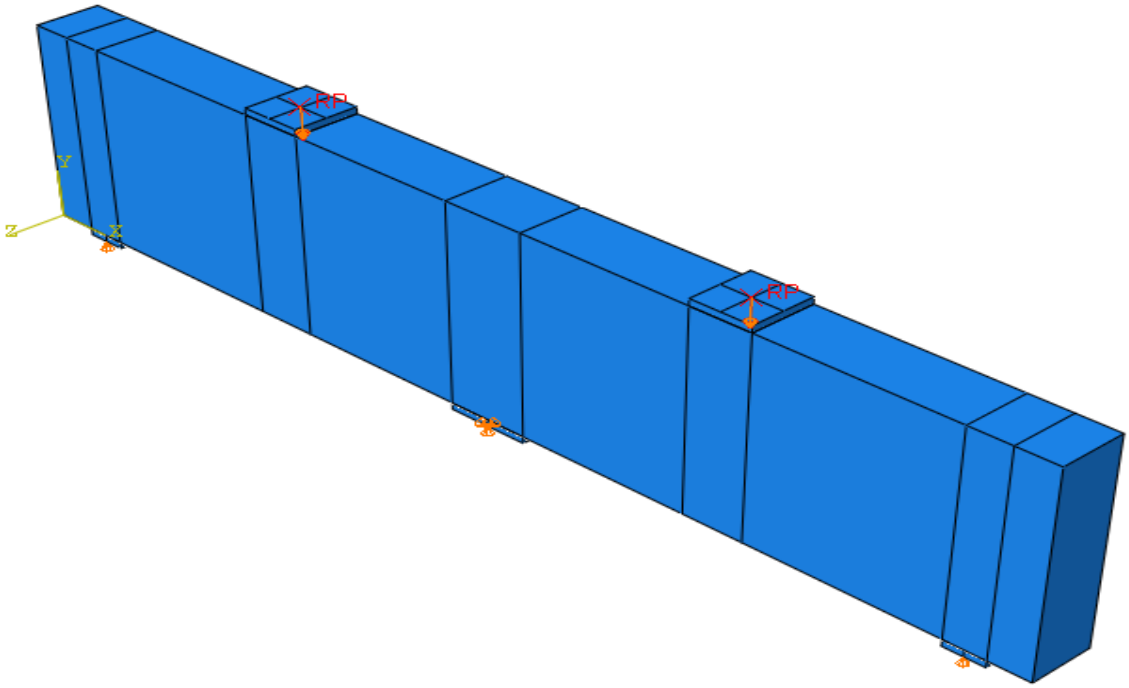

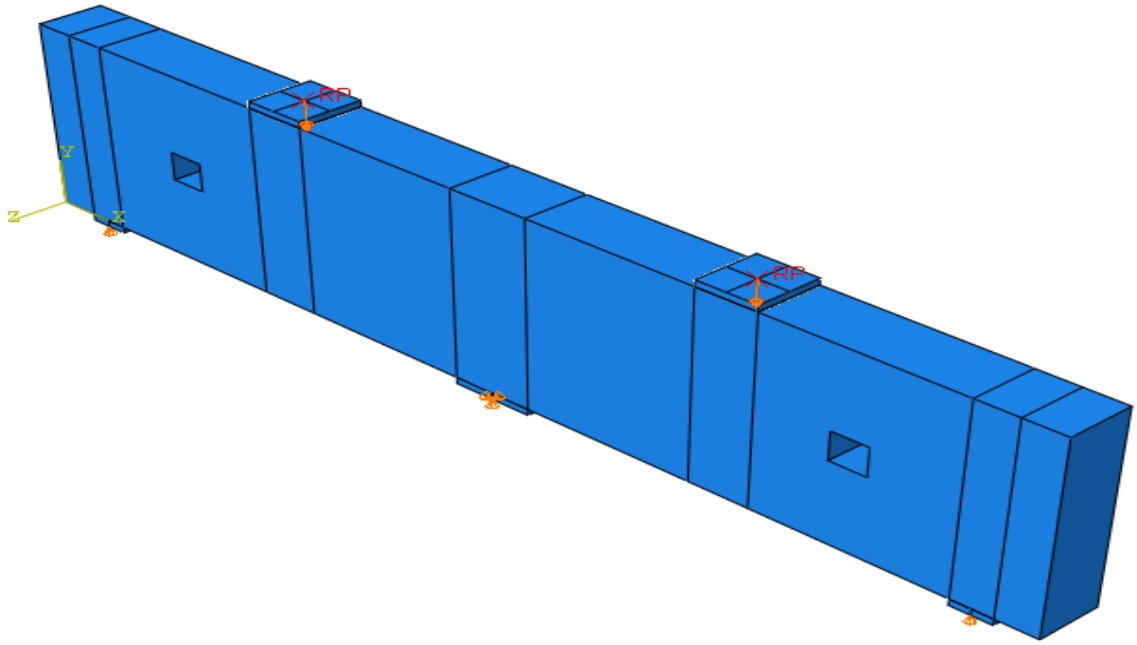

Figure 3.15 Applied load as a point

In simulation using finite element modeling the size of mesh is very important factor in accuracy of analysis result. Coarse mesh may yield less accurate results and the finer one may increase the analysis cost since there is no definite rule regarding size of mesh an iterative procedure were used to determine the adequate size of mesh to the model. In this study a mesh size of 50mm was appropriate both to concrete and reinforcement bars generated using mesh module.

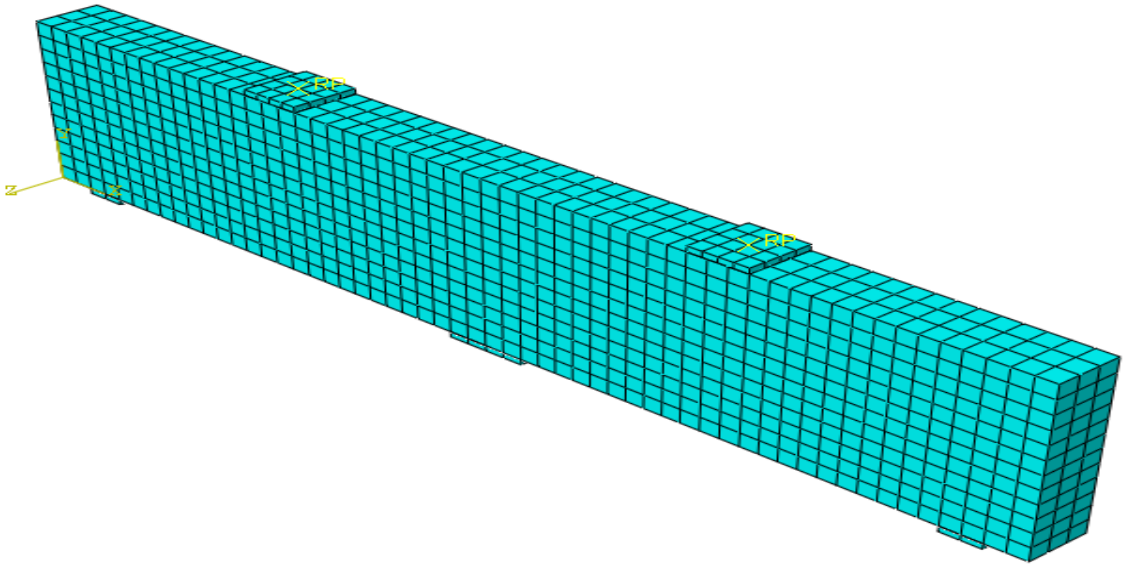

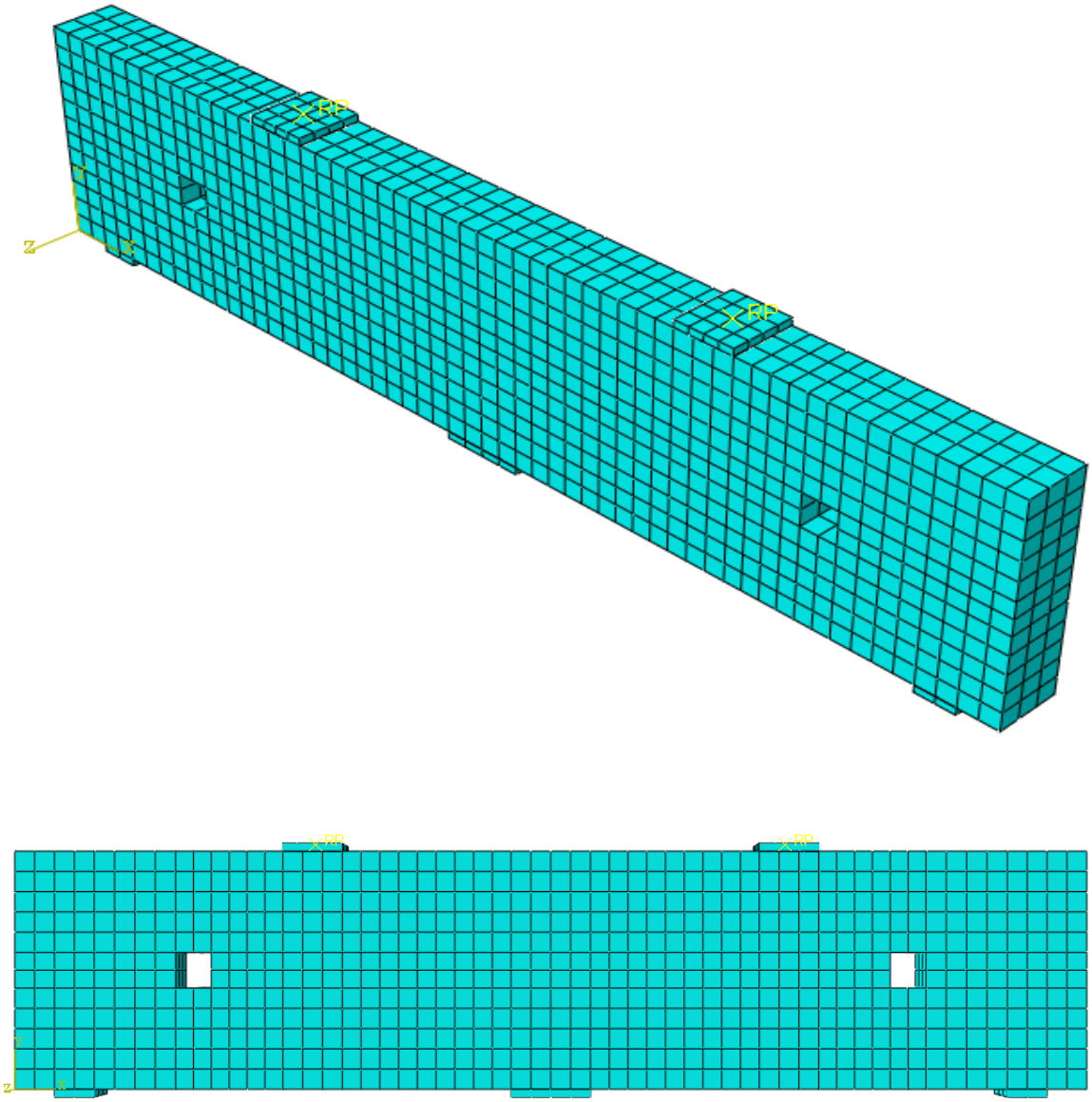

Figure 3.16 Finite element mesh of the model

.

CHAPTER FOUR

VALIDATION, RESULTS AND DISCUSSION

4.1. General

4.1.1. Comparison of finite element analysis and experimental result

Damage occurrences at the ultimate level for both experimental and numerical studies are displayed in Figs 4.1 and 4.2 in terms of tensile damage (DAMAGET) respectively.

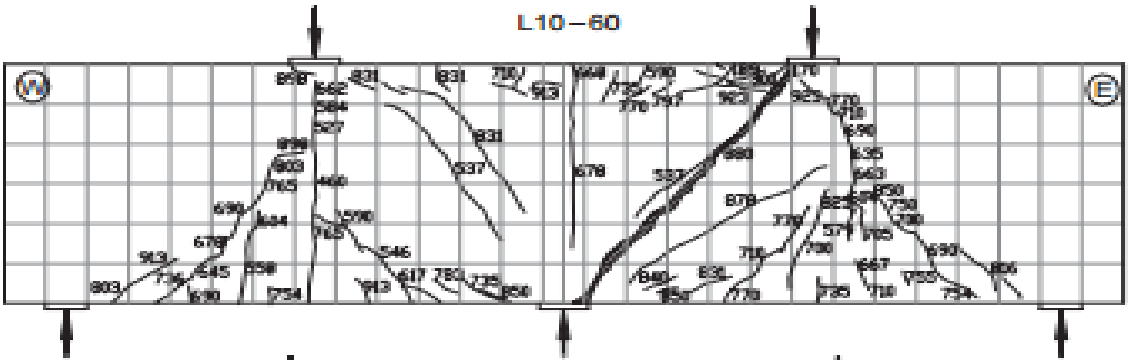

Figure 4.1 Crack patterns and failure mode for tested deep beam (Yang and Ashour, 2007)

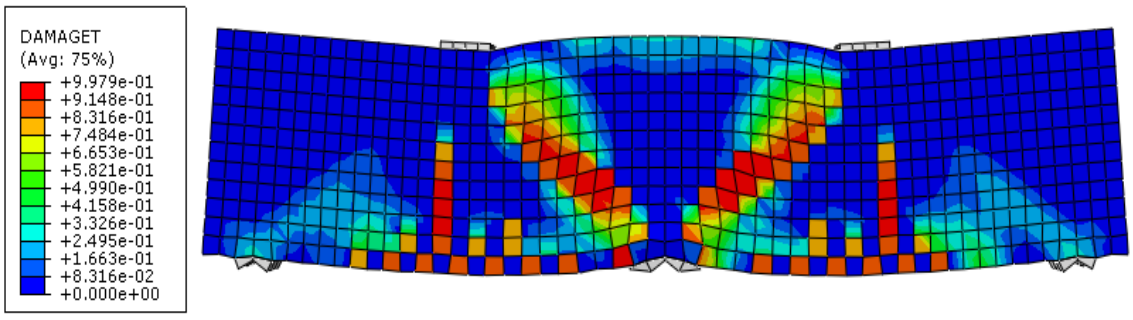

Figure 4.2 Crack pattern and failure mode for the numerical finite element model

As it seen from the above figure both the experimental tested deep beam and the numerical finite element model was failed by a diagonal crack which connecting the edges of the load and intermediate support plate.

The comparison of ultimate strength and ultimate deflection of the deep beam is shown in the Table 4.1.

Table 4.1 Comparison of finite element simulation and experimental result

Test specimen	Parameters	Finite element model	Experiment	% difference
L10-60	Ultimate load (KN)	899.8214	880	2.25%
	Displacement ((mm)	1.533988	1.624	5.54%

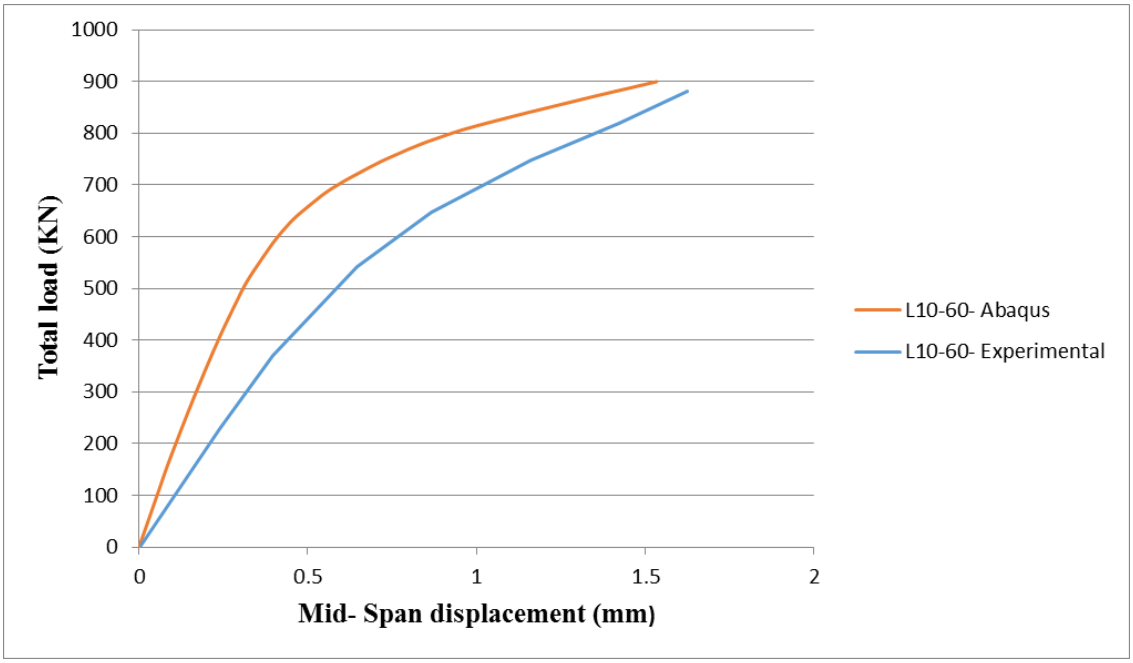

Figure 4.3 Total load plotted against mid-span displacement for experimental and FE model

The result of the finite element model is stiffer than the experimental result. There are several effects that may cause the higher stiffness in the finite element models. The major factor is micro cracks which are present in the concrete for experimental deep beams, and could be produced by drying shrinkage in the concrete and handling of the deep beams. But the finite elements do not include the micro cracks. So the micro cracks reduce the stiffness of the experimental deep beam.

After the verification of the finite element model the effects of opening size, opening location and opening shape analysis have taken and finally the results are presented in this section.

4.2. Load Deflection Behavior

4.2.1. Control beam

The load deflection graph indicates that a reinforced concrete continuous deep beam has a nonlinear strain distribution. This nonlinear strain distribution is occurring due to the depth of the deep beam.

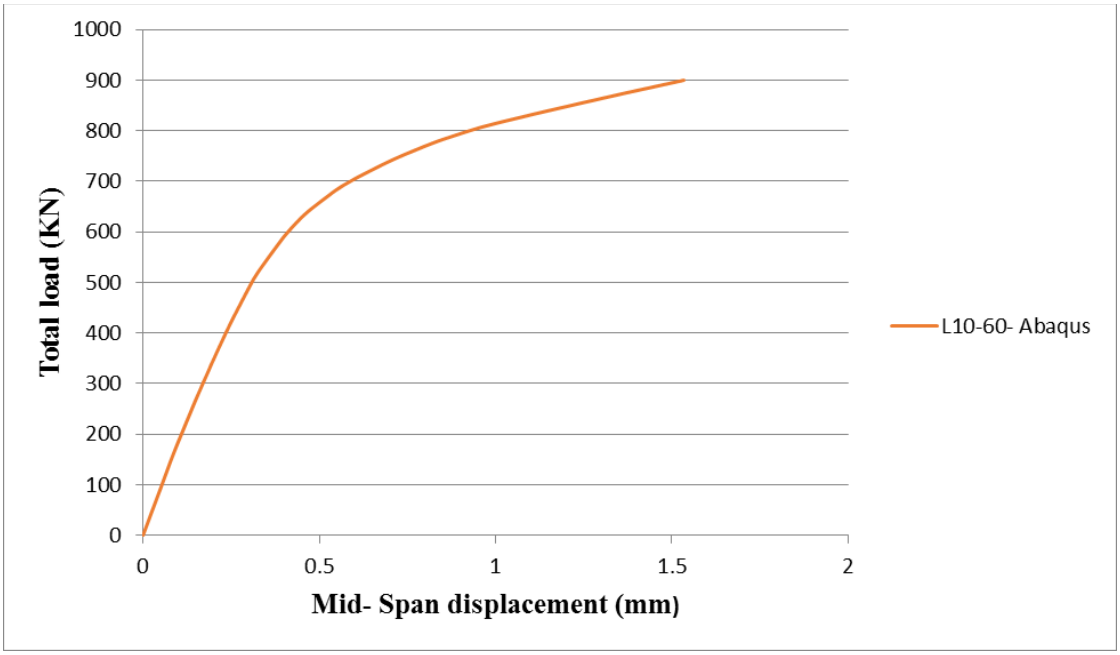

Figure 4.4 Total load plotted against mid- span displacement for control beam

4.2.2. Beam with opening

4.2.2.1. Effects of opening size and location

To investigate the effect of opening size on reinforced concrete continuous deep beam three different opening sizes were considered 1%, 4% and 9 % of the total area of the beam. These openings were placed at the center near to support, between support and loading point and near to loading point of the interior and exterior shear span.

It can be seen from figure 4.5, 4.6, 4.7 and 4.8 that as opening size increases in the deep beam there is a reduction in its load carrying capacity. When 1%, 4% and 9% circular opening are provided between supports and loading point in the exterior shear span of the deep beam, the load carrying capacity becomes 885.20KN, 844.19KN and 807.31KN

respectively. And when 1%, 4% and 9% circular opening are provided between supports and loading point in the interior shear span of the deep beam, the ultimate load becomes 750.91KN, 682.78KN and 568.78KN respectively.

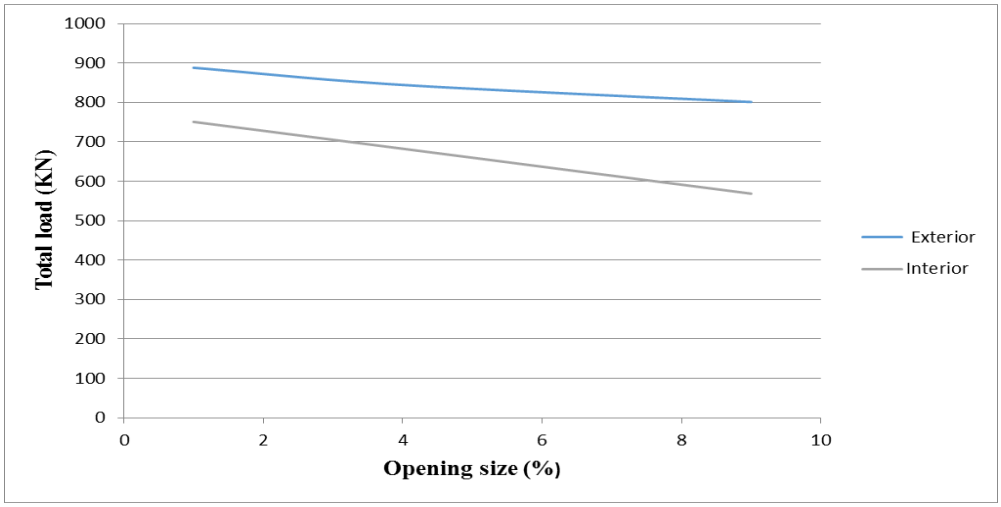

Figure 4.5 Total load plotted against opening size for circular opening deep beam

The inclusion of 1%, 4%,9% square opening between supports and loading point in the exterior shear span of the deep beam causes a reduction of load carrying capacity to 838.21KN, 794.72KN and 743.09KN respectively. And The inclusion of 1%, 4%,9% square opening between supports and loading point in the interior shear span of the deep beam causes a reduction of load carrying capacity to 668.01KN, 542.15KN and 439.71KN respectively.

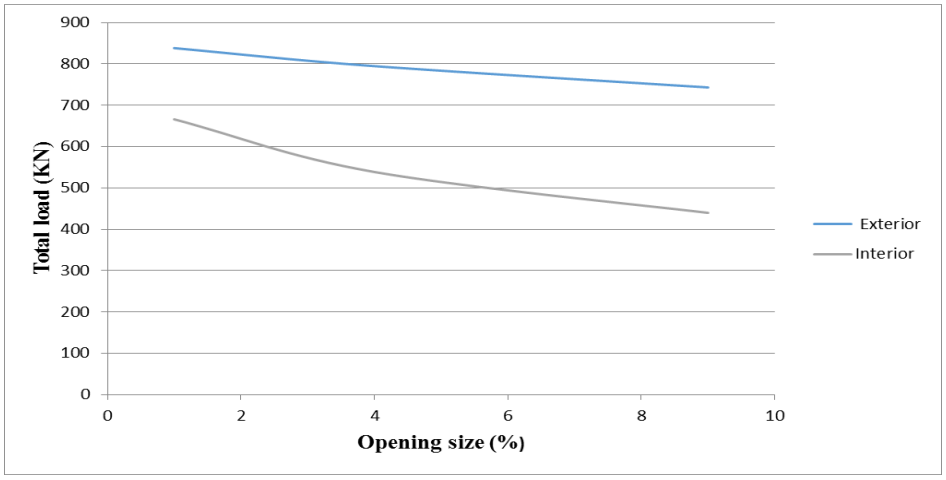

Figure 4.6 Total load plotted against opening size for square opening deep beam

When 1%, 4% and 9% horizontal rectangular opening are provided between supports and loading point in the exterior shear span of the deep beam, the load carrying capacity becomes 855.07KN, 826.04KN and 762.13KN respectively. And when 1%, 4% and 9% horizontal rectangular opening are provided between supports and loading point in the interior shear span of the deep beam, the ultimate load becomes 676.80KN, 558.58KN and 452.52KN respectively.

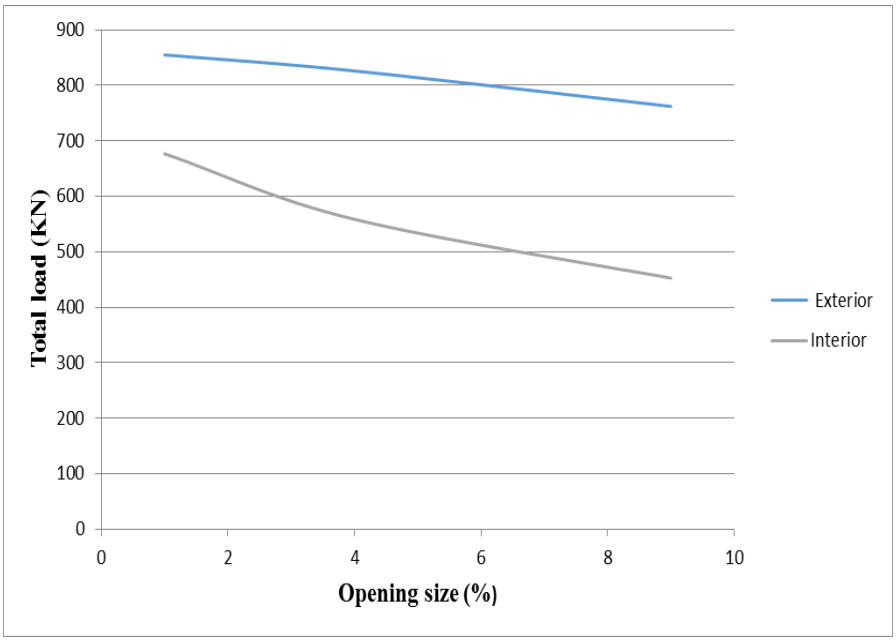

Figure 4.7 Total load plotted against opening size for horizontal rectangular opening deep beam

The inclusion of 1%, 4%,9% vertical rectangular opening between supports and loading point in the exterior shear span of the deep beam causes a reduction of load carrying capacity to 832.04KN, 787.21KN and 710.15KN respectively. And the inclusion of 1%, 4%,9% vertical rectangular opening between supports and loading point in the interior shear span of the deep beam causes a reduction of load carrying capacity to 666.01KN, 538.61KN and 428.97KN respectively.

Figure 4.5, 4.6, 4.7 and4.8 shows that RC continuous deep beams that have openings in the exterior shear span has higher load carrying capacity than RC continuous deep beams that have openings in the interior shear span.

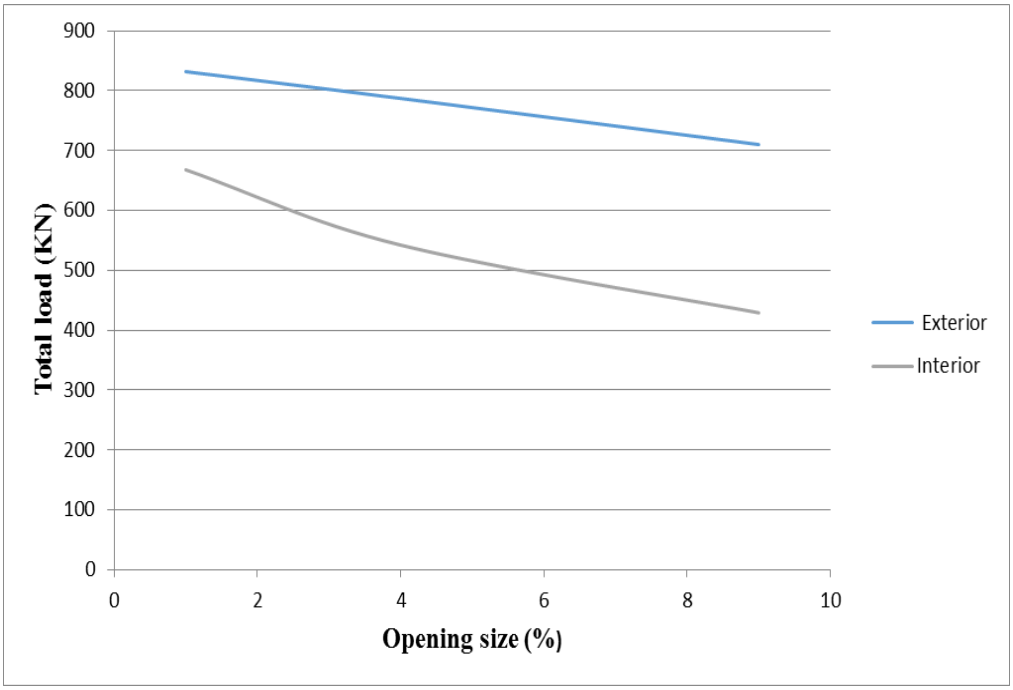

Figure 4.8 Total load plotted against opening size for vertical rectangular opening deep beam

4.2.2.2. Effects of opening size and shape

The effect of shape of opening was investigated by considering square, circular and rectangular openings. As it seen from Figure 4.9 and Figure 4.10 for the inclusion of 1%,4% and 9% opening, the circular one has a high load carrying capacity which have 885.20KN, 844.19KN and 807.31KN in exterior shear span and 750.91KN, 682.78KN and 568.78KN interior shear span respectively.

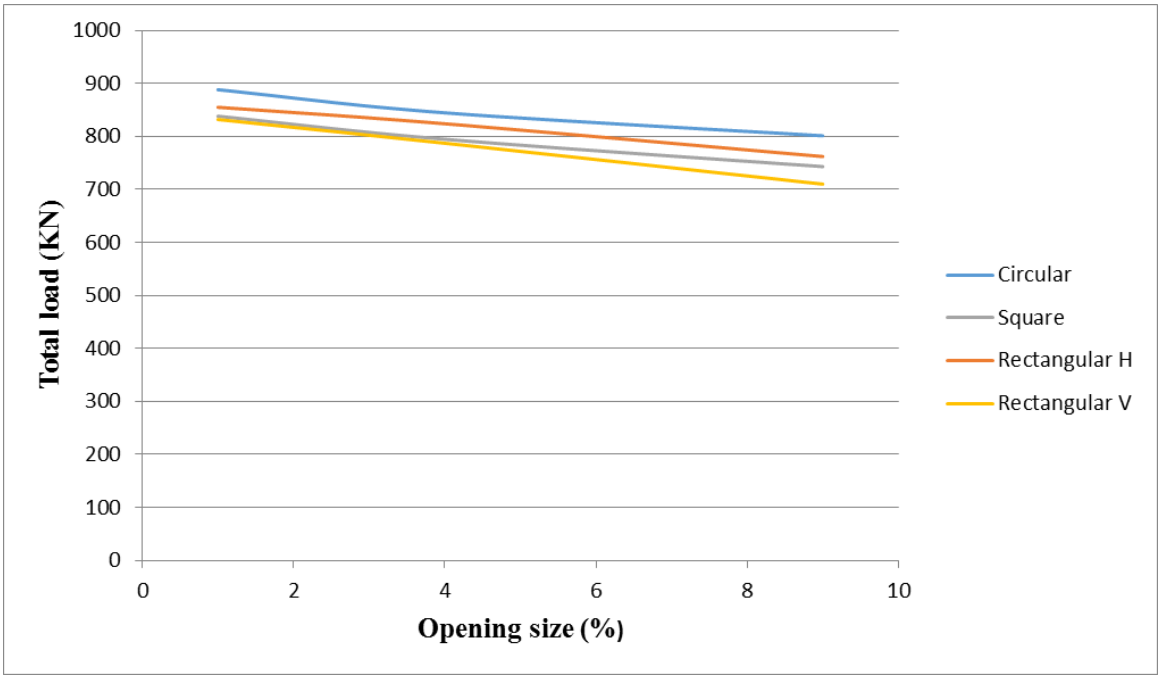

Figure 4.9 Total load plotted against opening size at exterior shear span of deep beam

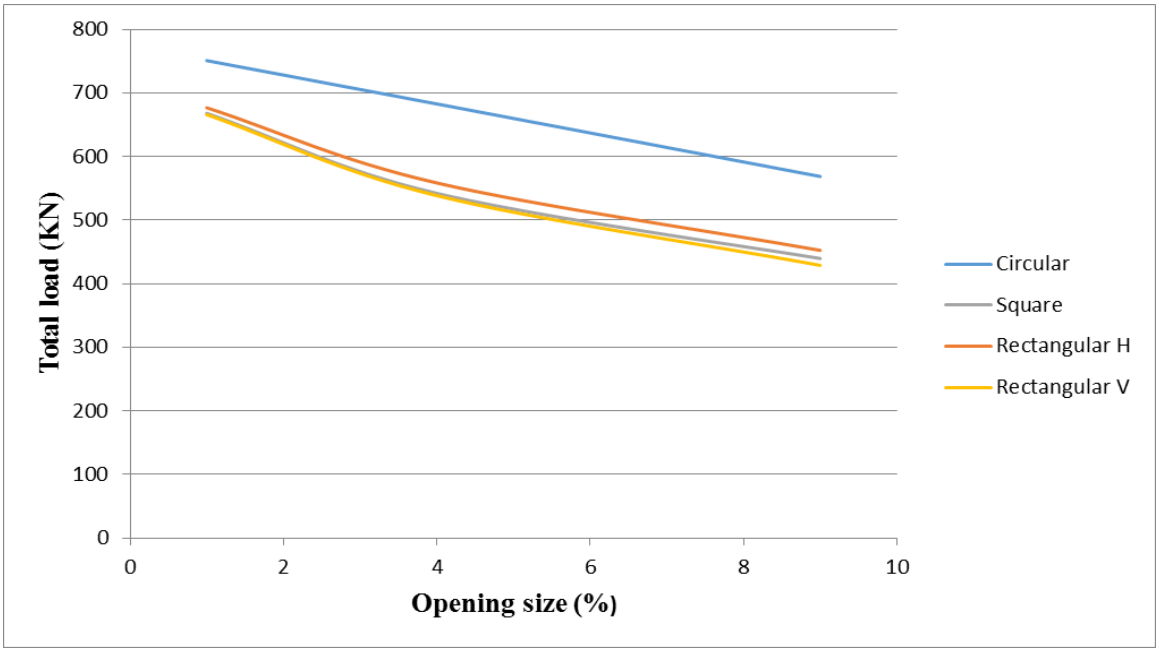

Figure 4.10 Total load plotted against opening size at interior shear span of deep beam

Figure 4.11 and Figure 4.12 shows that the load deflection graphs of beams with circular opening at the exterior shear span. When 1% opening provide near to support, near to loading point and between support and loading point, the ultimate load becomes

893.28KN, 888.97KN and 885.20KN respectively. And when 4% and 9% opening provide near to support, near to loading point and between support and loading point, the ultimate load becomes 860.6KN and 842.14KN, 857.37KN and 830.37KN, 844.19KN and 807.31KN respectively. So providing openings near to the support shows a better load carrying capacity. In more detail, the openings should be kept away from the natural load path joining the reaction and loading points.

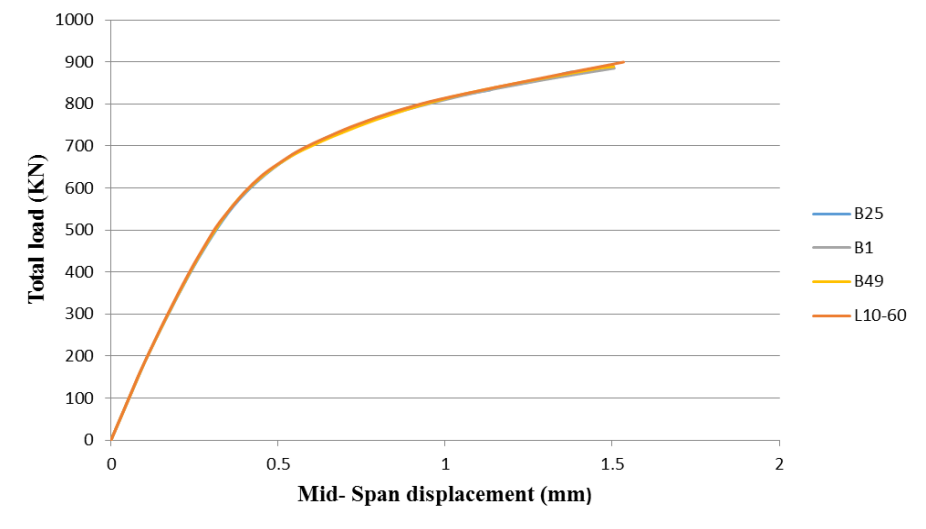

Figure 4.11 Total load plotted against mid- span displacement for deep beam with 1% circular opening at exterior shear span

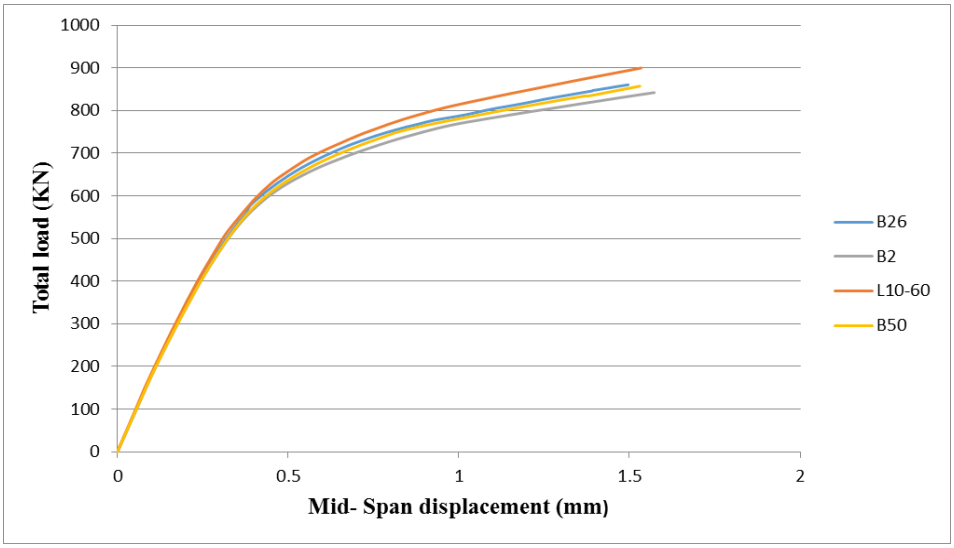

Figure 4.12 Total load plotted against mid- span displacement for deep beam with 4% circular opening at exterior shear span

4.2.3. Comparison of control beam and beams with opening

4.2.3.1. Circular opening

As it seen in the figure the total load carrying capacity of the deep beam was decrease as the opening size increase. The numerical simulation shows that the inclusion of 1%, 4% and 9 % circular opening in the exterior shear span of RC continuous deep beams deep beam causes a 1.63 %, 6.18% and 10.28% reduction in the load carrying capacity of the deep beam respectively. And the inclusion of 1%, 4% and 9 % circular opening in the interior shear span of RC continuous deep beams deep beam causes a 16.55 %, 24.12% and 36.79% reduction in the load carrying capacity of the deep beam respectively.

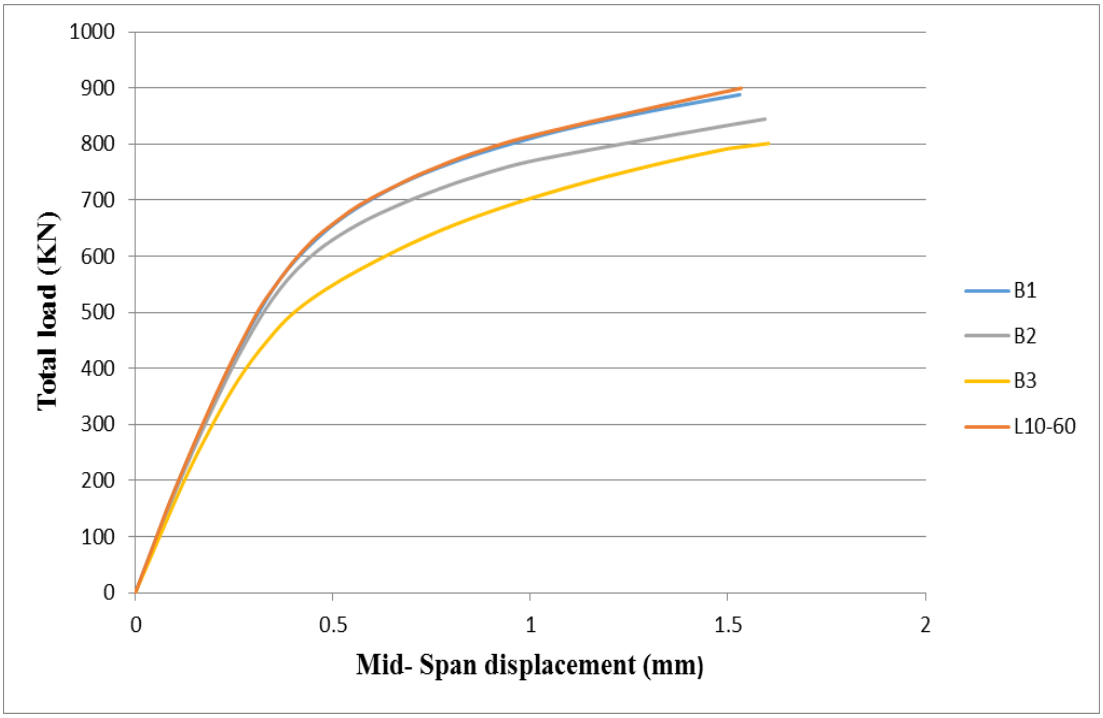

Figure 4.13 Total load plotted against mid-span displacement for opening beam at exterior shear span

Figure 4.13 and 4.14 shows that when opening size increase the load deflection graph becomes more and more nonlinear. The nonlinear strain distribution was greater in RC continuous deep beams with openings at the interior shear span when compared to RC continuous deep beams with openings at the exterior shear span.

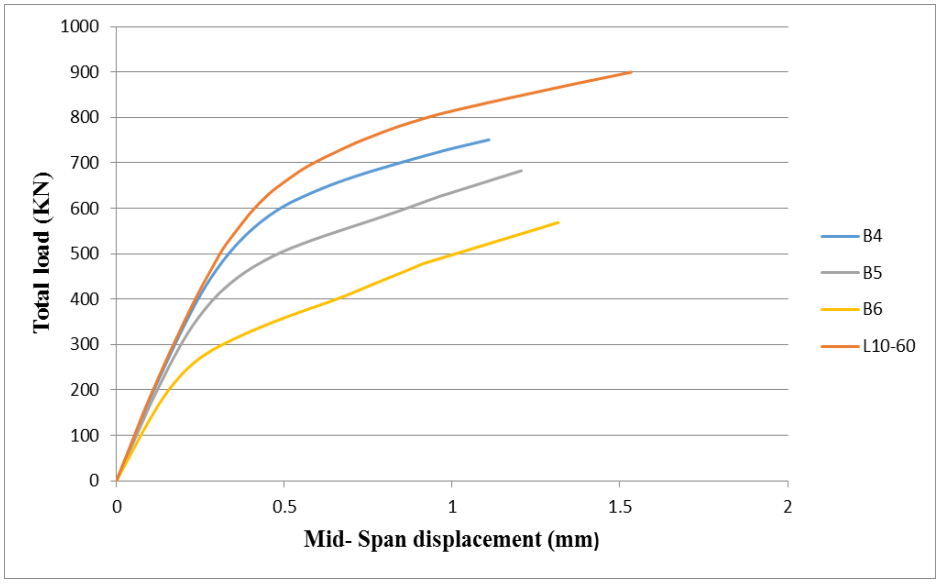

Figure 4.14 Total load Plotted against mid-span displacement for opening beam at interior shear span

4.2.3.2. Square opening

As it seen in the figure the inclusion of 1%, 4% and 9 % square opening in the exterior and interior shear span RC continuous deep beams deep beam causes a 6.85%, 11.68 %, 17.42% and 25.76%, 39.75, 51.13 % reduction in the load carrying capacity of the deep beam respectively.

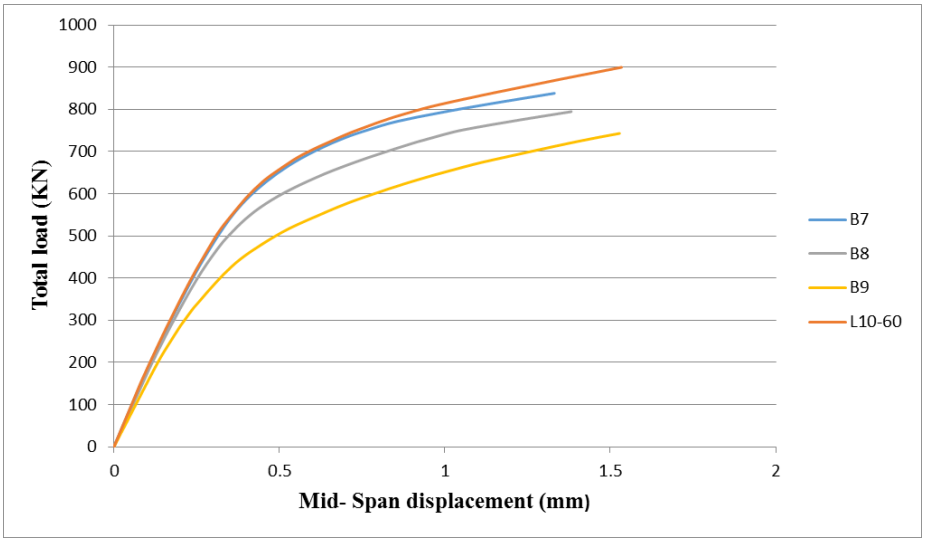

Figure 4.15 Total load plotted against mid-span displacement for opening beam at exterior shear span

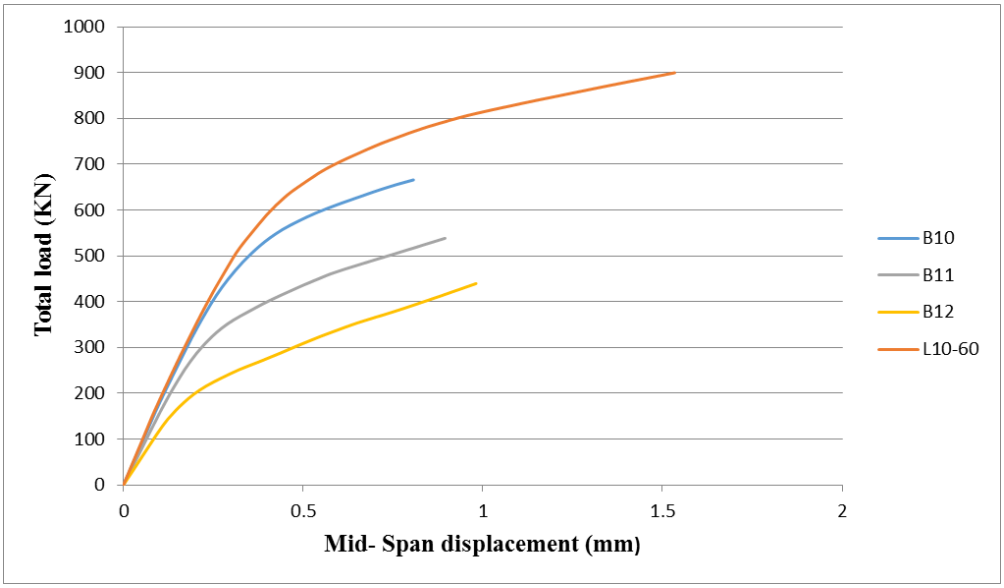

Figure 4.16 Total load plotted against mid-span displacement for opening beam at interior shear span

4.2.3.3. Rectangular opening in the horizontal

For the inclusion of 1%, 4% and 9 % opening in the exterior and interior shear span of RC continuous deep beams causes a 4.97%, 8.2%, 15.3% and 24.79%, 37.92, 49.71 % reduction in the load carrying capacity of the deep beam respectively.

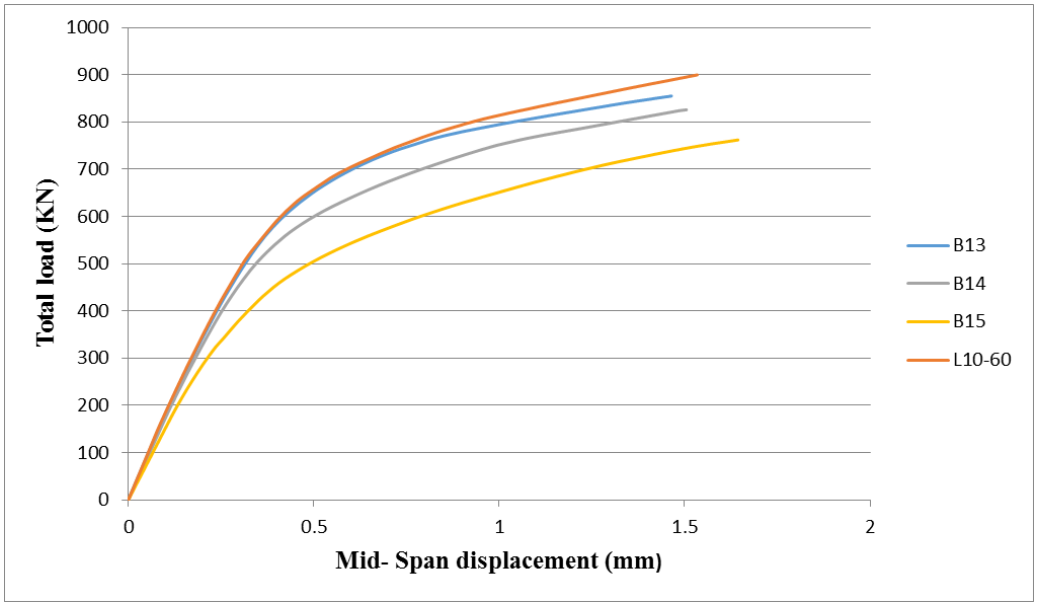

Figure 4.17 Total load plotted against mid-span displacement for opening beam at exterior shear span

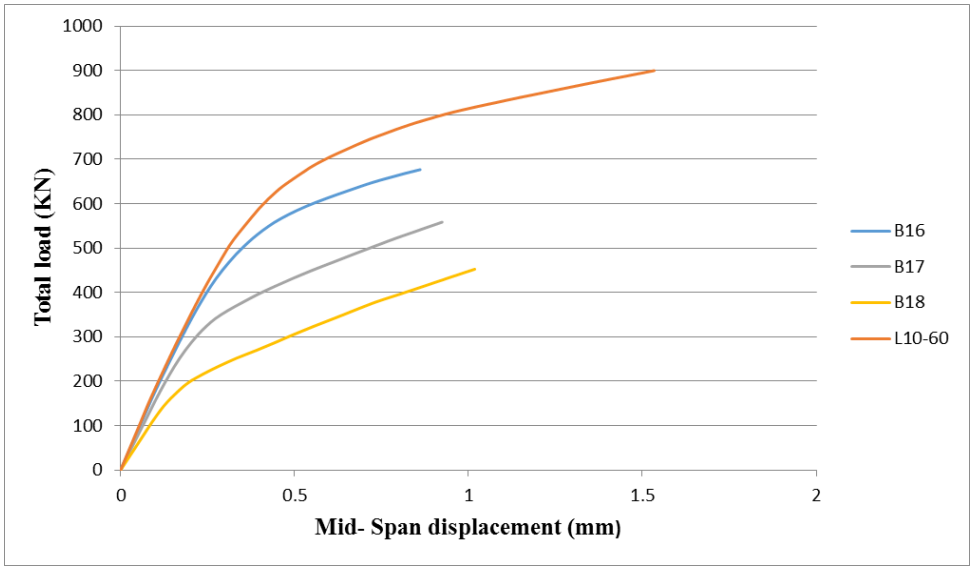

Figure 4.18 Total load Plotted against mid-span displacement for opening beam at interior shear span

4.2.3.4. Rectangular opening in the Vertical

For the inclusion of 1%, 4% and 9 % opening in the exterior and interior shear span of RC continuous deep beams causes a 7.53%, 12.51%, 21.08 % and 25.99%, 40.14%, 52.33% reduction in the load carrying capacity of the deep beam respectively.

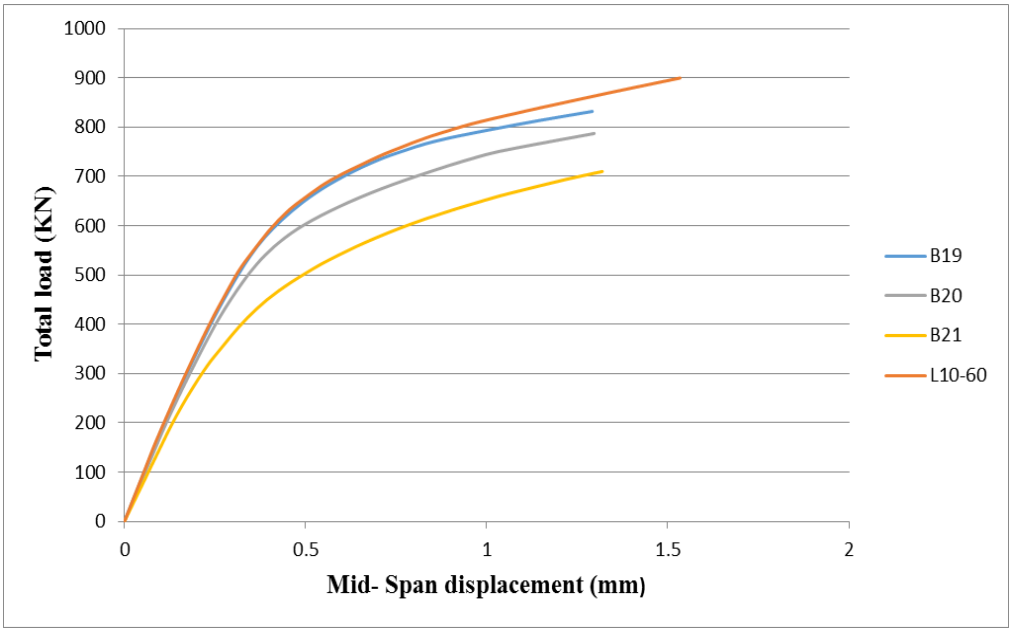

Figure 4.19 Total load plotted against mid-span displacement for opening beam at exterior shear span

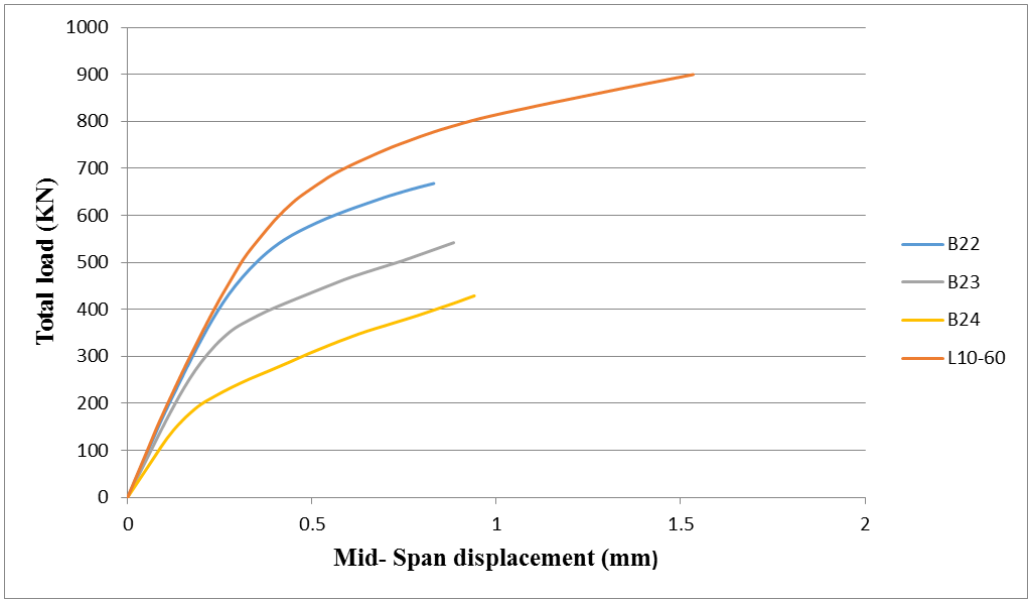

Figure 4.20 Total load plotted against mid-span displacement for opening beam at interior shear span

4.3. Crack pattern and mode of failure

The main mode of failure for control beam and beams with opening at exterior shear span was characterized by the formation of two symmetrical inclined cracks emanating from the edges of the central support bearing plate to the edges of the loading plates. There was also additional formation of inclined cracks at opening corners for RC continuous deep beams with opening at the exterior shear span. When openings provided on RC continuous deep beams, inclined cracks was occurred around the corner of the opening.

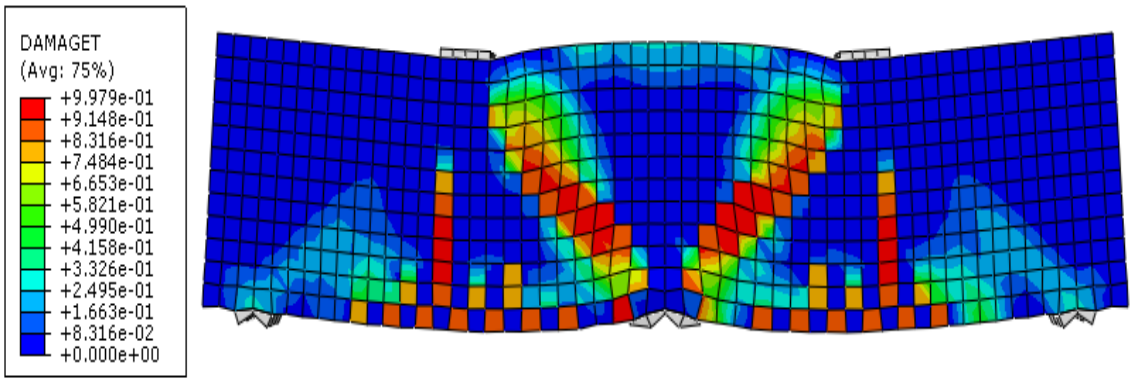

Figure 4.21 Crack patterns and failure mode for control deep beam

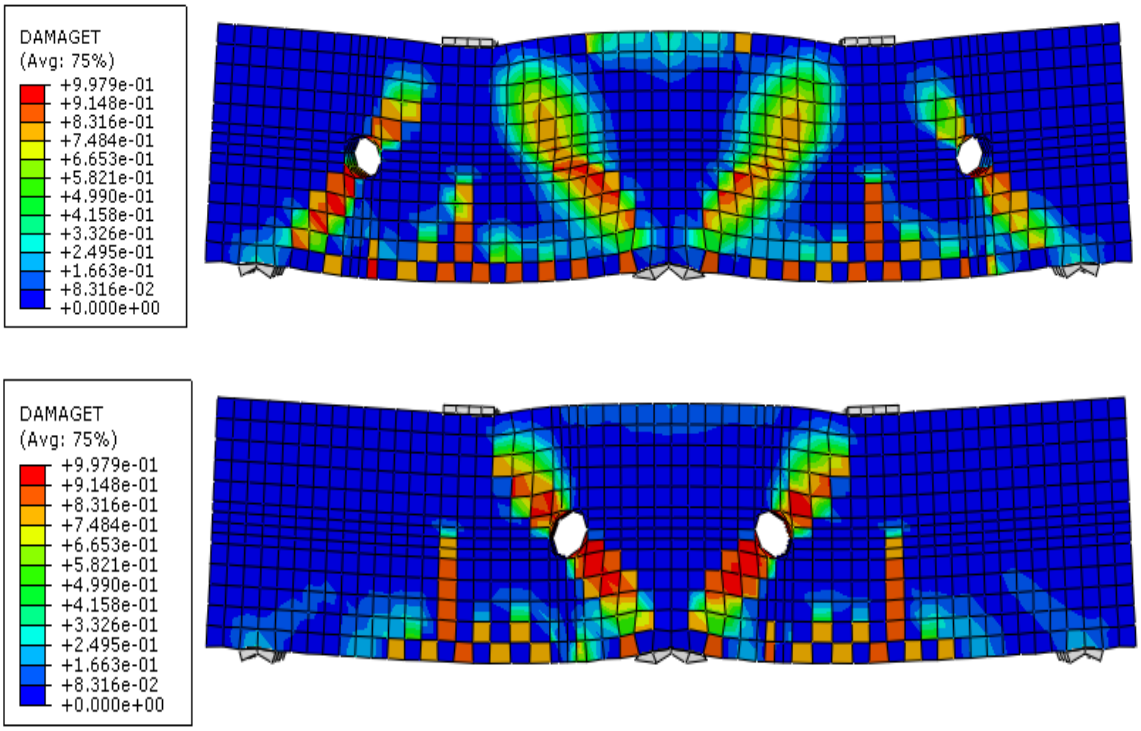

Figure 4.22 Crack pattern and failure mode for deep beam with circular opening

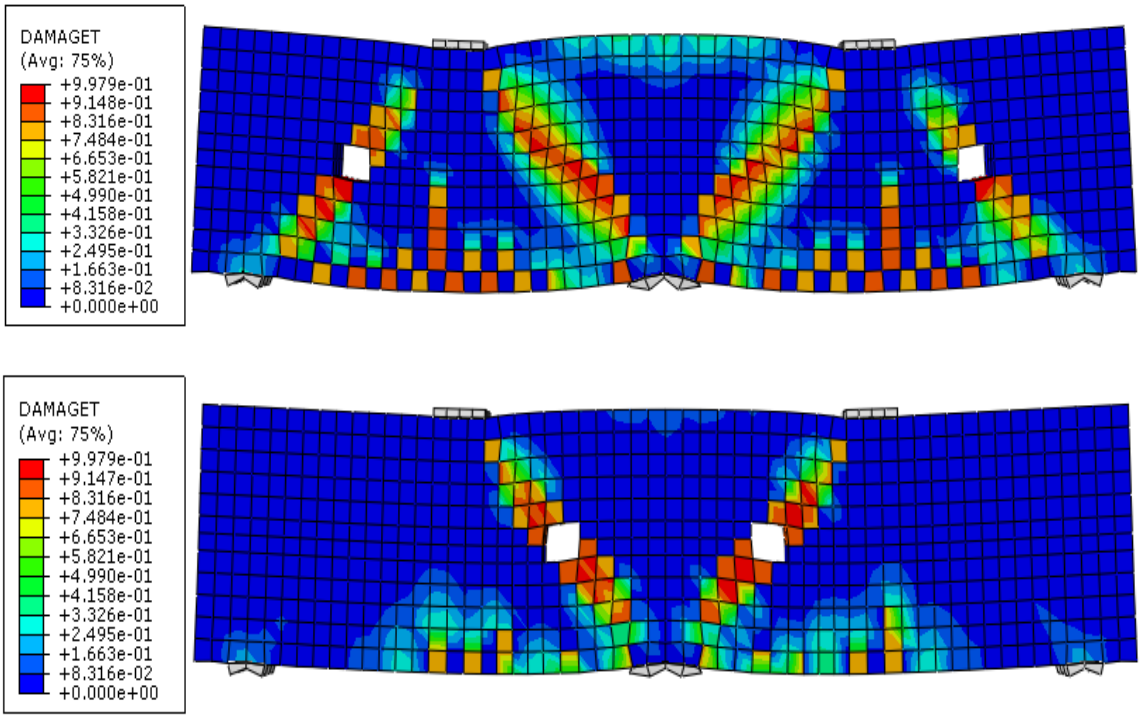

Figure 4.23 Crack pattern and failure mode for deep beam with horizontal rectangular opening

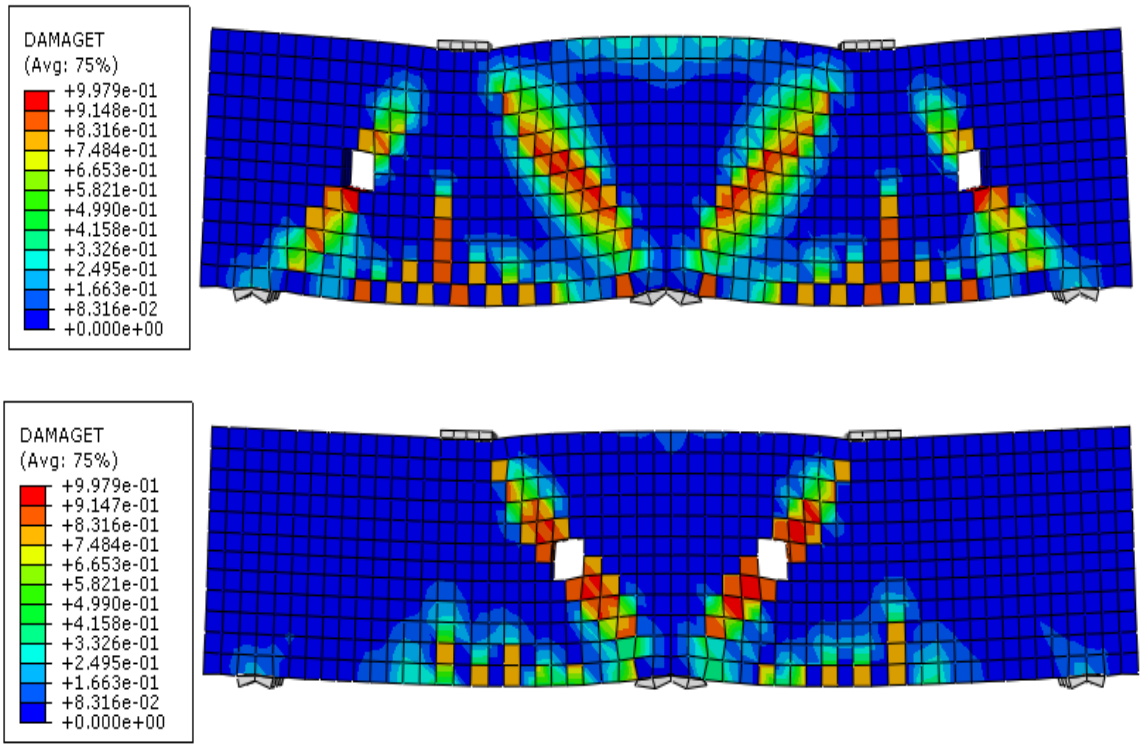

Figure 4.24 Crack pattern and failure mode for deep beam with square opening

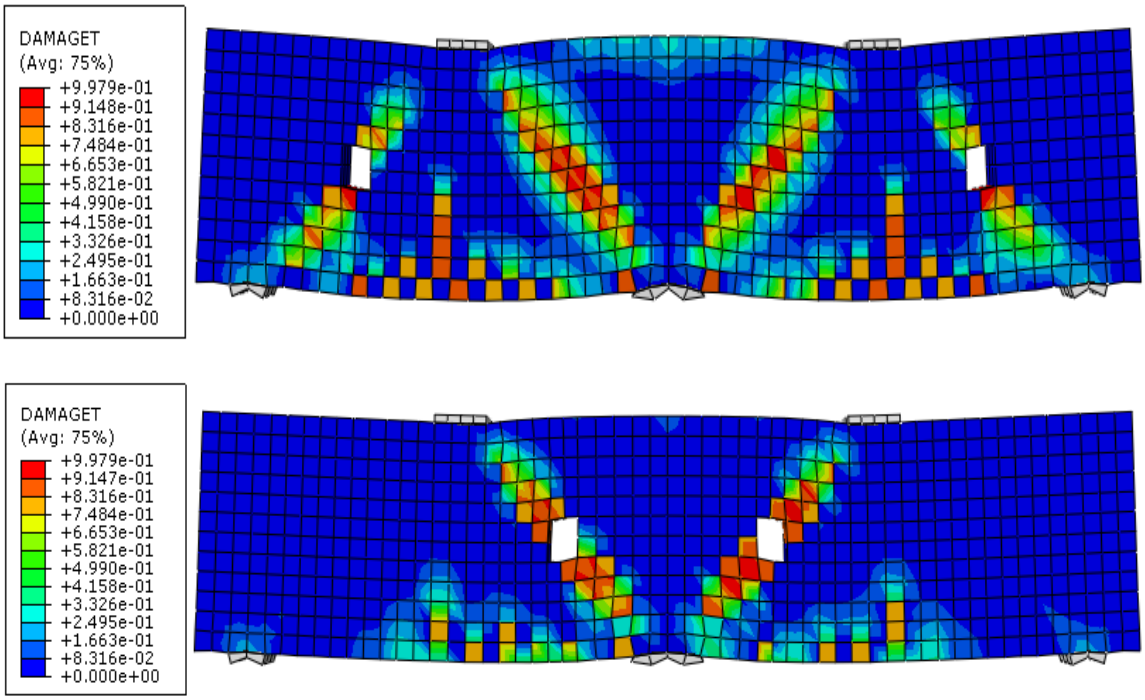

Figure 4.25 Crack pattern and failure mode for deep beam with vertical rectangular opening

CHAPTER FIVE

CONCLUSION AND RECOMMENDATION

6.1. Conclusion

The performance of reinforced concrete continuous deep beams specified in this study was investigated using nonlinear finite element method. The effect of opening size, location and shape on the RC continuous deep beams was assessed. After the careful inspection of the analysis results, the following conclusions are drawn.

- Numerical simulation by using ABAQUS software is capable of developing reasonable and acceptable estimations in order to investigate the load deflection behavior and mode of failure of reinforced concrete continuous deep beams.
- Four types of opening shapes were included under this study. The inclusion of 9% opening on exterior shear span causes a 10.28%, 17.42%, 15.3% and 21.08% reduction of load carrying capacity for circular, square, rectangular in horizontal and vertical opening respectively and the inclusion of 9% opening on interior shear span causes a 36.79%, 51.13%, 49.71% and 52.33% reduction of load carrying capacity for circular, square, rectangular in horizontal and vertical opening respectively. As a result the higher load carrying capacity was observed in the circular one.
- This study compared two major opening locations. The inclusion of 9% circular opening on exterior and interior shear span causes a 10.28% and 36.79% reduction of load carrying capacity respectively. So, opening located in the exterior shear span showed better load carrying capacity than opening located in the interior shear span.
- The inclusion of 9% circular opening at exterior shear span near to the support, near to loading point and between support and loading point causes a reduction of 6.41%, 7.72% and 10.28% load carrying capacity of RC continuous deep beams.
- Finally, providing openings away from the load path near to the exterior support gives a better load carrying capacity.

6.2. Recommendation

The following recommendations are suggested for future researches which are not covered in the present study:

- Based on the finite element method, future studies can include different types of loading to further test the design method with continuous beams more than two spans and multiple loads or other loading system in the RC continuous deep beams.
- The effect of parameters such as number of opening, span to depth ratio, concrete grade and steel grade on load carrying capacity, stiffness, crack pattern and mode of failure should be included in the future study.
- The effect of openings on RC continuous deep beams with different span to depth ratio should be included in the future study.
- Strengthening of the opening in the RC deep beams with composite sheets and additional steel reinforcement around the opening can be investigated and simulated by finite element software in the future study.

REFERENCES

ACI 318-08, Building Code Requirements for Structural Concrete and Commentary American Concrete Institute, Detroit, USA.

AL-Bayati, Nabeel, A., Bassman, R., Muhammad, and Ahmed, S. H.(2016). Structural Behavior of Self Compacting Reinforced Concrete Deep Beams Containing Openings. Engineering and Technology Journal. 34 (12): 2310-2317.

Ashour, A. F., and Go Rishi. (2000). Tests of reinforced concrete continuous deep beams with web openings. Structural Journal. 97 (3): 418-426.

Bhavikatti, S.(2005). Finite Element Analysis. India, New Age International Publisher.

BS EN1992-1-1(2004), Eurocode 2: Design of concrete structures – Part 1-1: General rules and rules for buildings.

Campione, G. and Minafo, G. (2012). Behaviour of concrete deep beams with openings and low shear span-to-depth ratio. Engineering Structures. 41: 294–306.

Chin, Siew, C., Fadzil, M. Y., DOH, S. I., Andri, K., and Wen, K. C. (2015) .Experimental study on shear strengthening of rc deep beams with large openings using CFRP. In International Conference on Architecture, Structure and Civil Engineering.

Demir, A., Ozturk, H. and Dok, G. (2016). 3D numerical modelling of RC deep beam behavior nonlinear finite element analysis. Disast. Sci. Eng. 2(1): 13-18.

Dirar, and Morley, C.T. (2005). Nonlinear Finite Element Analysis of Reinforced Concrete Deep Beams. International Conference on Computational Plasticity.

EC, Egyptian Code for the Design and Construction of Concrete Structures (203-2006).

Getting started with ABAQUS (2008). Unite states of America; Simulia corp.

Kassim, M., Salahaldin, A. and Ali, M.(2015). Analysis of Fiber Reinforced Concrete Deep Beams with Large Opening Strengthened by CFRP Laminates. Kirkuk University Journal. 10(1): 29-46.

Keun, H.Y. and Ashraf, F.A. (2007). Structural behavior of reinforced concrete continuous deep beams with web openings. Magazine of Concrete Research. 59(10): 699–711.

Kmieck, P. and Kaminski, M.(2011). Modeling of RC structures and composite structures with concrete degradation taken into consideration. Archives of civil and mechanical engineering. 6(3): 623-629.

Kong, F. K.(2003). "Continuous deep beams",in Reinforced Concrete Deep Beams, New York.

Lee, J. K., Li, C. G. and Lee, Y.T. (2008). Experimental Study on Shear Strength of Reinforced Concrete Continuous Deep Beams with Web Opening. The 14th World Conference on Earthquake Engineering.

Mansur, M.A.(2011). Design of reinforced concrete beams with web openings. Structural Engineering and Construction Conference. 6: 5 – 6.

Mihaylov, B. (2015). Five spring model for complete shear behavior of deep beams, Structural Concrete.(1):71-83.

Mohamed, S. and Ahmed, M. (2019). Finite Element Analysis of Bottom Loaded Continuous Deep Beams with and without Web Openings. IOSR Journal of Mechanical and Civil Engineering (IOSR-JMCE). 16 (1): 01-11.

Mohamed, M. R., Aly, A. Z., Ali, M. A. and Mahmoud, A. M. (2014). Behavior Of High Performance Continuous RC Deep Beams With Openings And Its Strengthening. Journal of Engineering Sciences. 42 (5):1138 – 1162.

Nie, X. F., Shi, S. Z., Jin, G. T. and Chen, G. M. (2018). Experimental study on RC T-section beams with an FRP-strengthened web opening. Composite Structures. 185: 273-285.

Sabale,V. D., Borgave, M.D. and Prof. Joshi, P. K. (2014). Non-Linear Finite Element Analysis of Deep Beam. International Journal of Engineering Research & Technology (IJERT). 3 (5): 2134-2138.

Singh, R., Ray, S. P. and Reddy, C. S. (1980). Some tests on reinforced concrete deep beams with and without opening in the web .The Indian concrete journal. 54 (7): 189 – 194.

Sumer, Y. And Aktas, M.(2015). Defining parameters for concrete damage plasticity model. Turkey, Challenge journal of strucrtural mechanics. 149-155.

Tan, K. H., Tong, K. and Tang, C. Y. (2003). Consistent strut-and-tie modeling of deep beams with web openings. Magazine of Concrete Research. 55 (1):572-582.

Waleed, A. J., Abbas A. A. and Nazar, K. O. (2018). Strength and Serviceability of Reinforced Concrete Deep Beams with Large Web Openings Created in Shear Spans. Civil Engineering Journal. 4: 2560-2574.

Waleed, A. J., Abbas A. A. and Nazar, K. O. (2019). Effect of Size and Location of Square Web Openings on the Entire Behavior of Reinforced Concrete Deep Beams. Civil Engineering Journal. 5 (1): 209-226.

Wissam, D. S. (2015). Nonlinear Behavior of Reinforced Concrete Continuous Deep Beam. International Journal of Engineering Research & Technology (IJERT). 4(4): 249-255.

Yang, K.H., Eun, H.C. and Chung, H. S. (2006). The Influence of Web Openings on the Structural Behavior of Reinforced High-Strength Concrete Deep Beams. Engineering Structures. 28 (13): 1825–1834.

Yang, K. H., Chung, H. S. and Ashour, A. F. (2007). Influence of Section Depth on the Structural Behavior of Reinforced Concrete Continuous Deep Beams. Magazine of Concrete Research. 59(8): 575–586.

Yoo, T. M., Doh, J. H. and Guan, H. (2004). Experimental work on Reinforced and Prestressed Concrete Deep Beans with Various Web Openings. Griffith school of Engineering, Griffith University Gold Coast Campus, Queensland, Australia.

Yoo, T.M., Doh, J.H., Guan, H. and Fragomeni, S. (2007). Experimental work on Reinforced and Pre-Stressed Concrete Deep Beams with Various Web Openings. Griffith School of Engineering.

APPENDIXES

APPENDIX A

The compressive and tensile behavior of concrete used in the beam model is described below.

Characteristics of C-32.1 concrete used for beams

Table a.1 Compressive behavior and damage behavior

Compressive behavior		Compressive damage behavior	
Yield stress	Inelastic strain	Compressive damage parameter	Inelastic strain
		0	0
13.7742742	0	0	1.82351E-05
24.80812737	0.000118591	0	0.000118591
32.96767001	0.000305079	0	0.000305079
38.11014623	0.000581978	0	0.000581978
40.1	0.000996577	0	0.000996577
40.07088883	0.001054221	0.000725964	0.001054221
38.72398964	0.001425583	0.034314473	0.001425583
33.85840399	0.002002387	0.155650773	0.002002387
25.29993156	0.002689853	0.369079013	0.002689853
24.00829818	0.002780559	0.401289322	0.002780559

Table a.2 Tensile behavior and damage behavior

Tensile behavior		Tensile damage behavior	
Yield stress	Displacement	Tension damage parameter	Displacement
3.030106849	0	0	0
2.512360522	0.01	0.17086735	0.01
1.994614196	0.02	0.341734699	0.02
1.47686787	0.03	0.512602049	0.03
0.959121544	0.04	0.683469398	0.04
0.60602137	0.046819946	0.8	0.046819946
0.595730985	0.05	0.803396047	0.05
0.56337184	0.06	0.814075256	0.06
0.531012694	0.07	0.824754465	0.07
0.498653549	0.08	0.835433675	0.08
0.466294404	0.09	0.846112884	0.09
0.433935258	0.1	0.856792093	0.1
0.401576113	0.11	0.867471303	0.11
0.369216968	0.12	0.878150512	0.12
0.336857822	0.13	0.888829721	0.13
0.304498677	0.14	0.899508931	0.14
0.272139531	0.15	0.91018814	0.15
0.239780386	0.16	0.92086735	0.16
0.207421241	0.17	0.931546559	0.17
0.175062095	0.18	0.942225768	0.18
0.14270295	0.19	0.952904978	0.19
0.110343805	0.2	0.963584187	0.2
0.077984659	0.21	0.974263396	0.21
0.045625514	0.22	0.984942606	0.22
0.013266368	0.23	0.995621815	0.23

APPENDIX B

Sample models with different opening size, shape and location are illustrated below

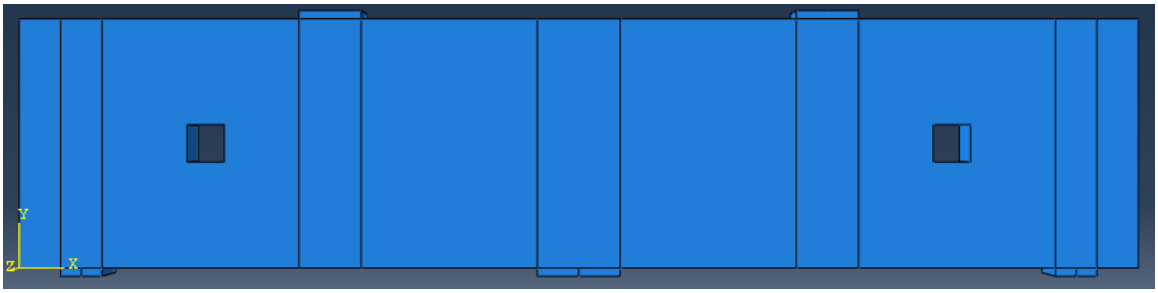

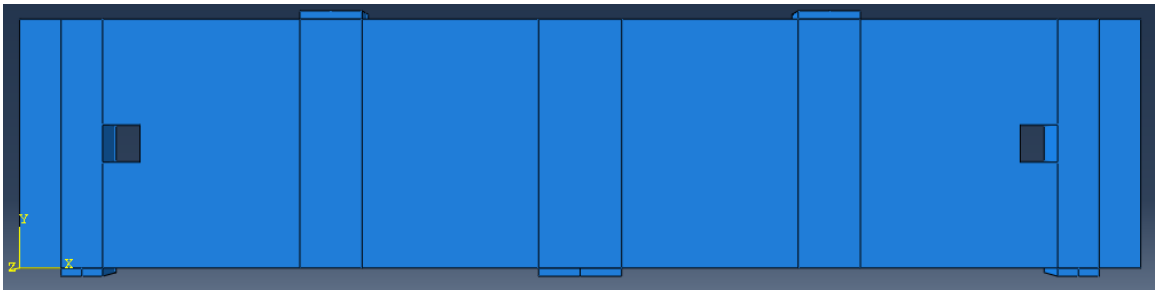

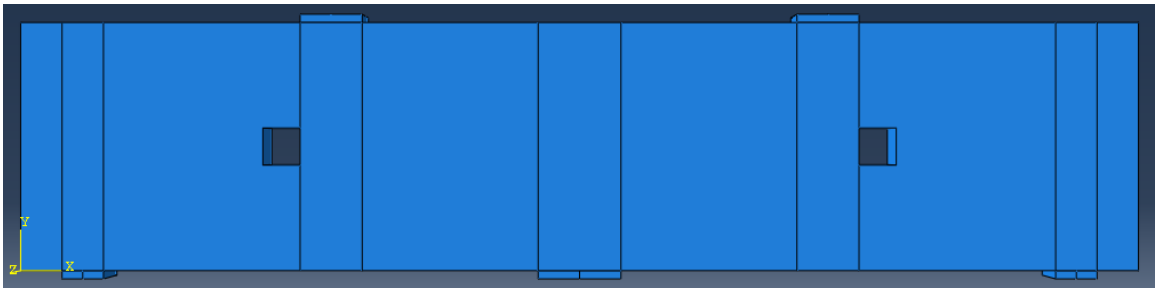

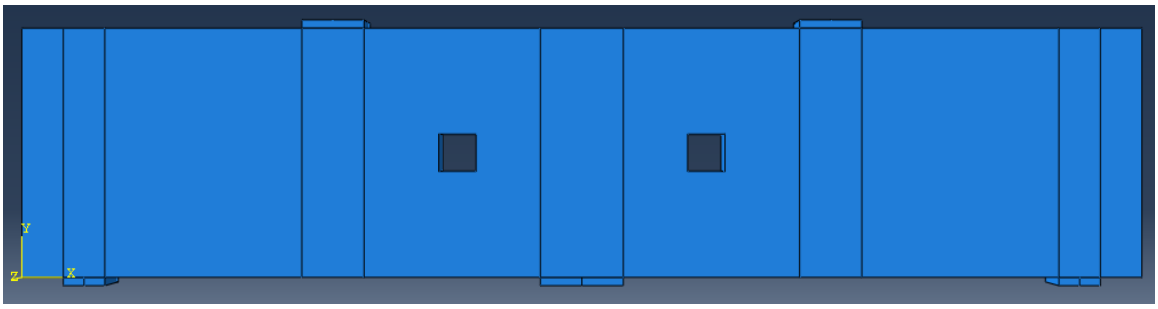

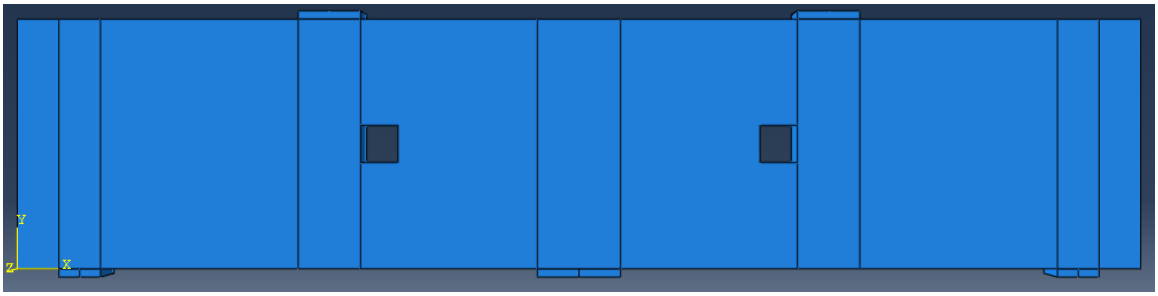

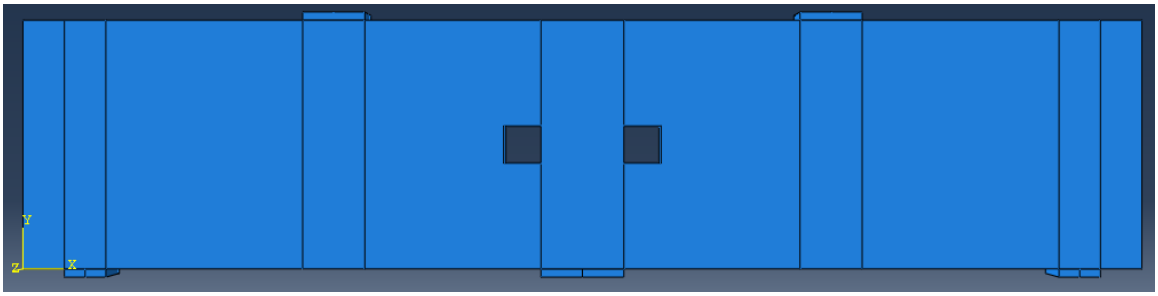

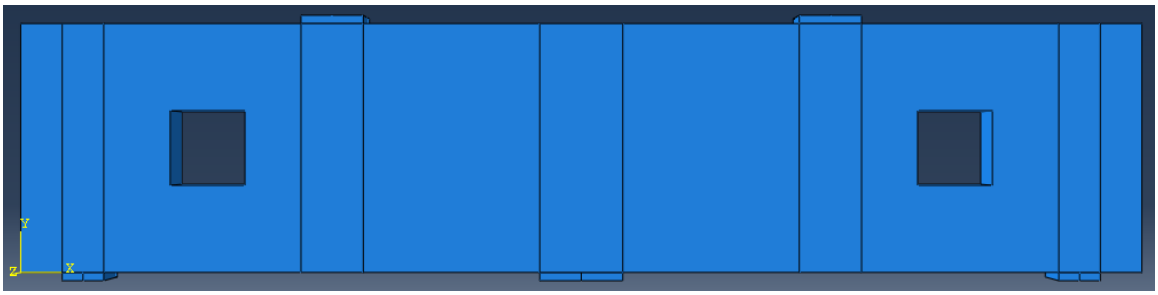

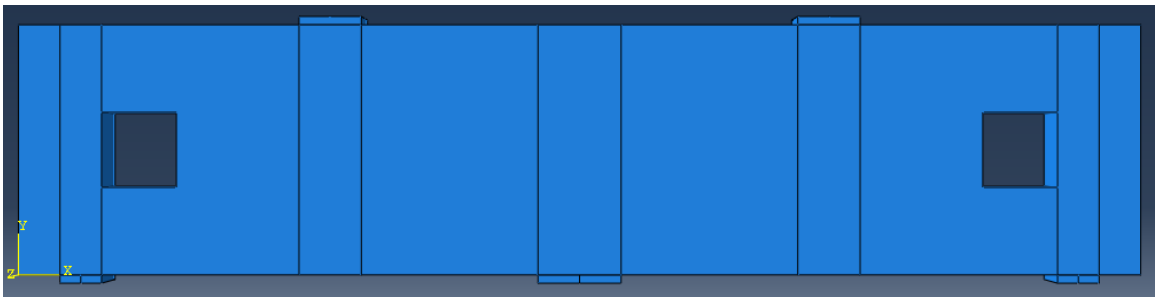

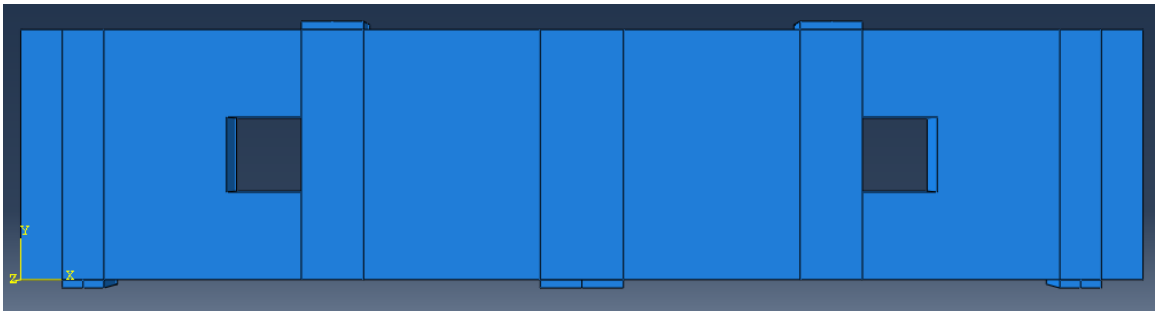

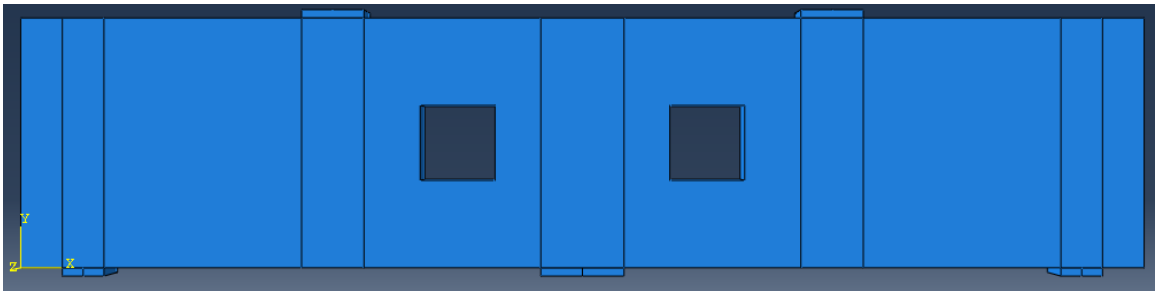
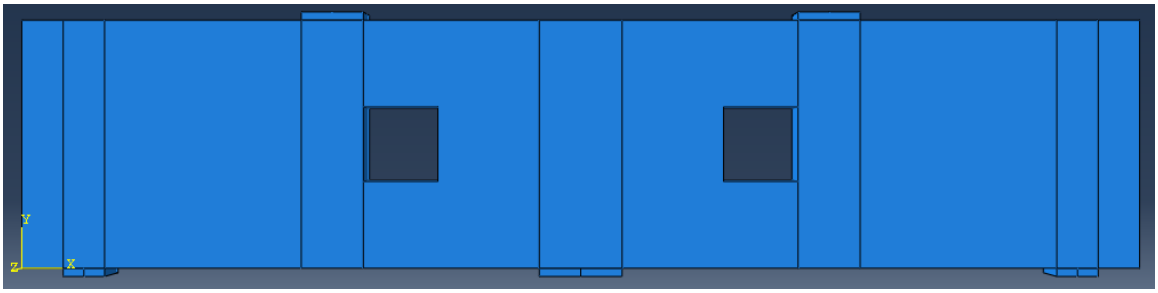
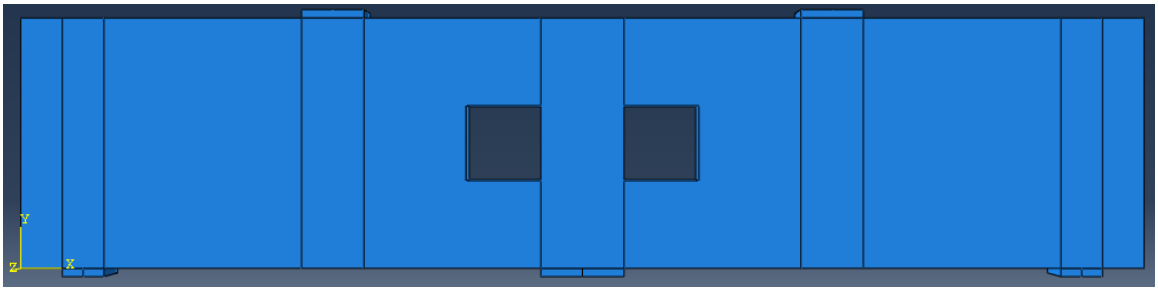
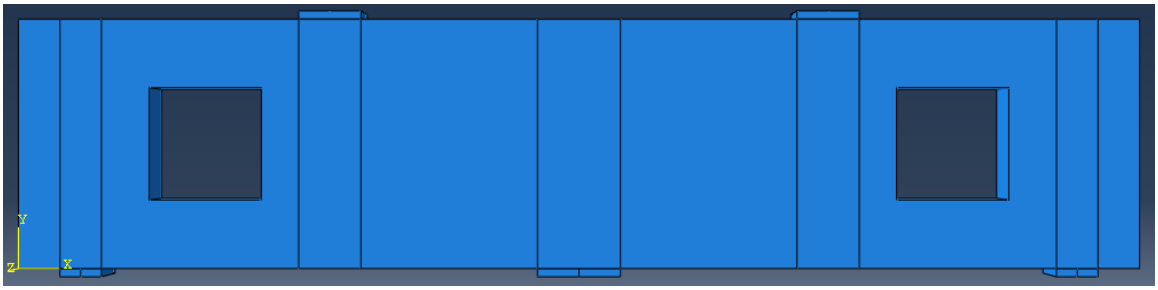
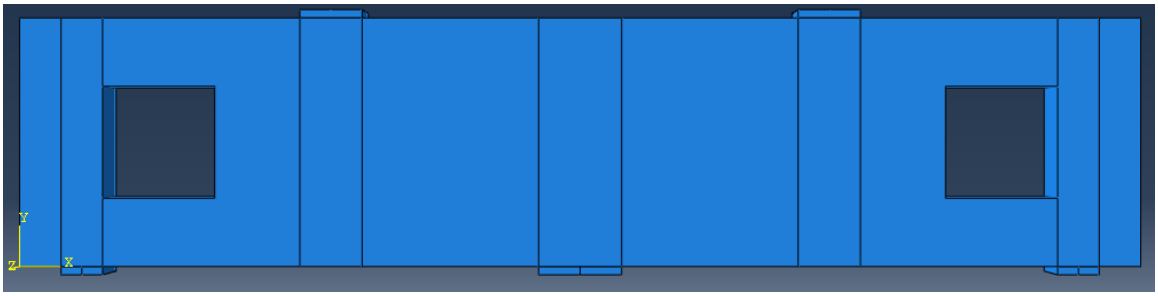

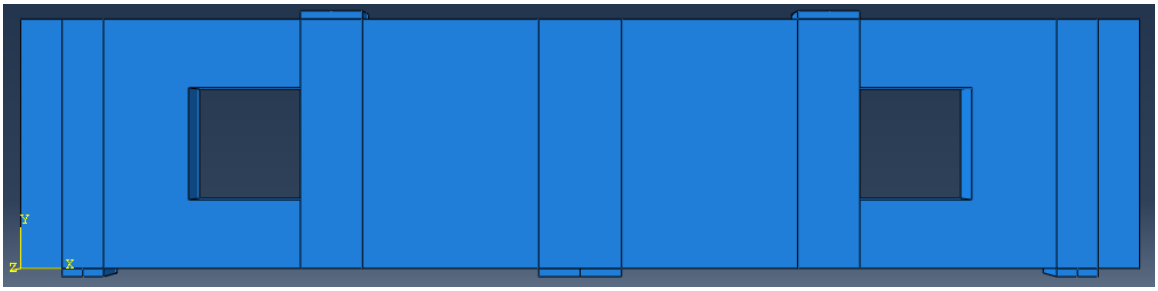
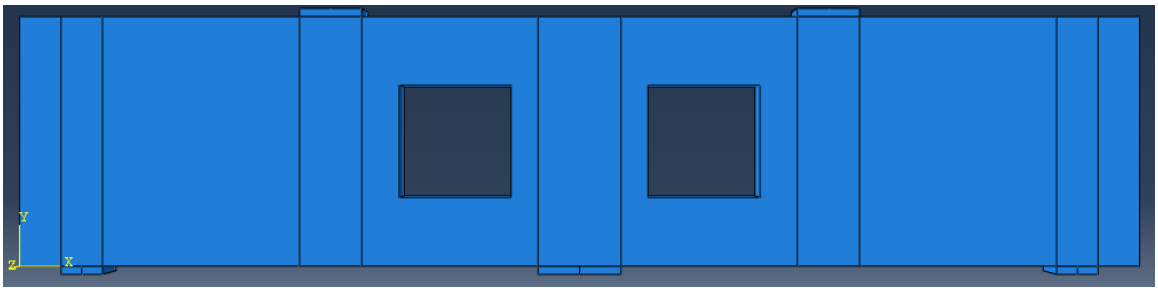
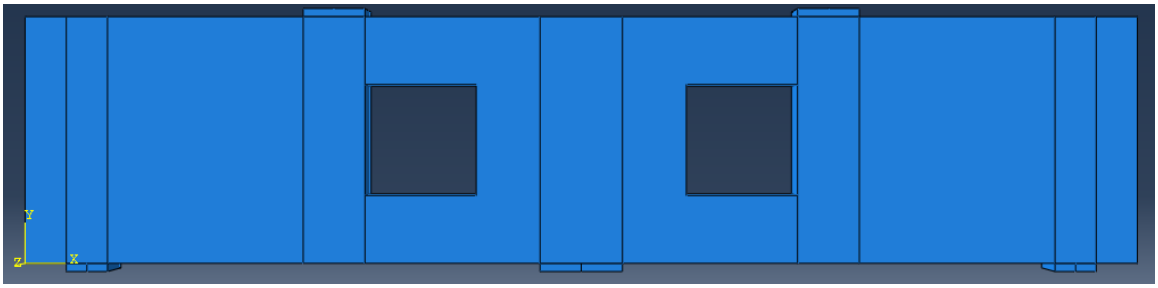
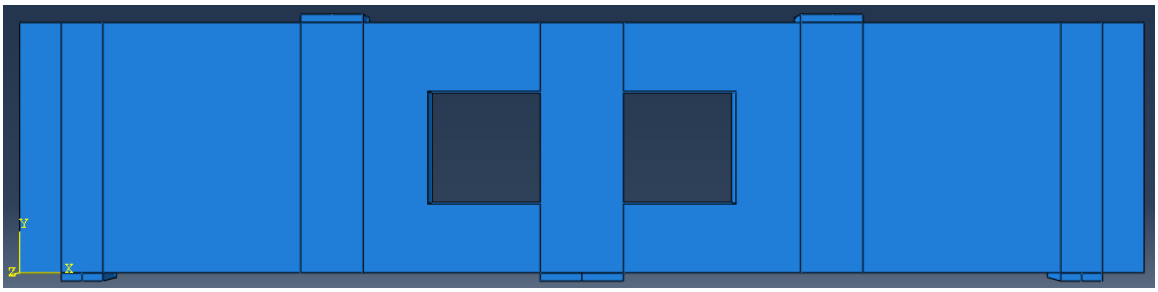
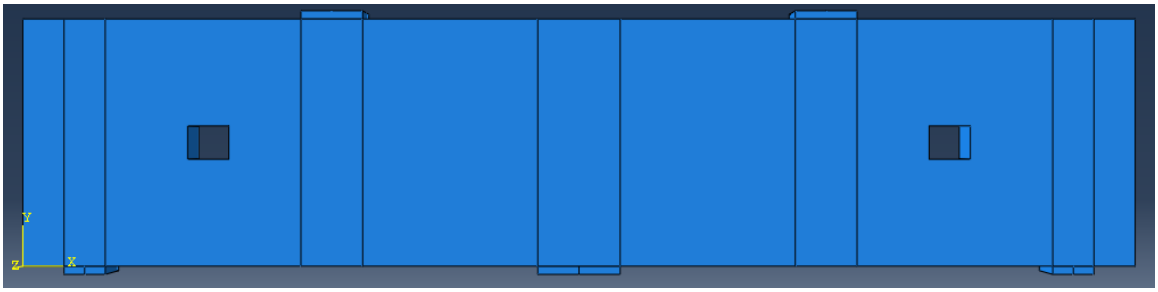

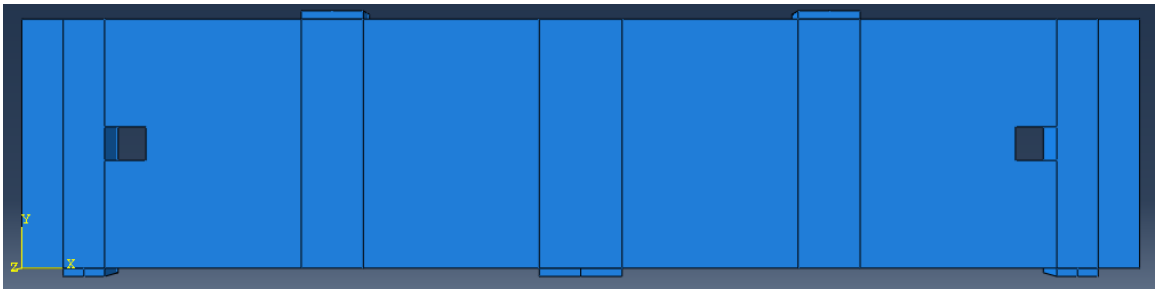

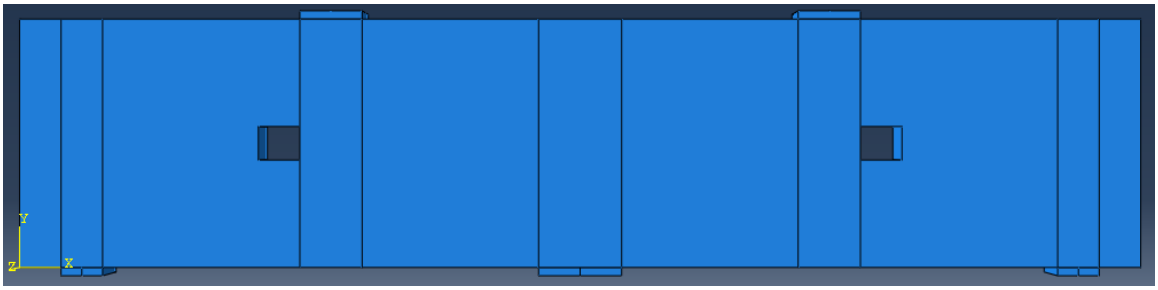

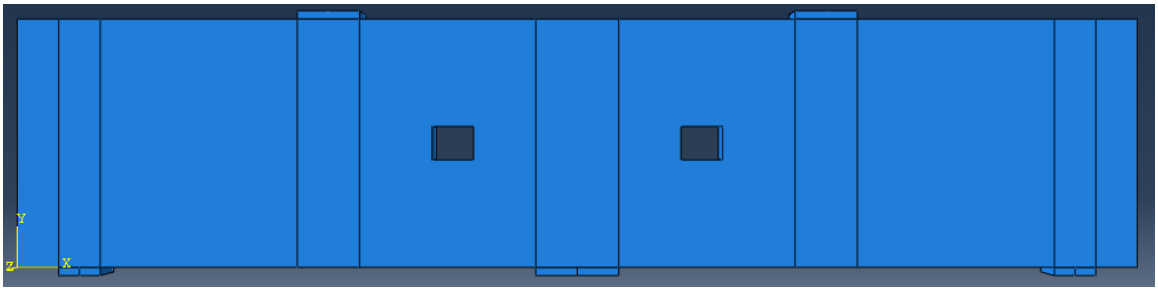

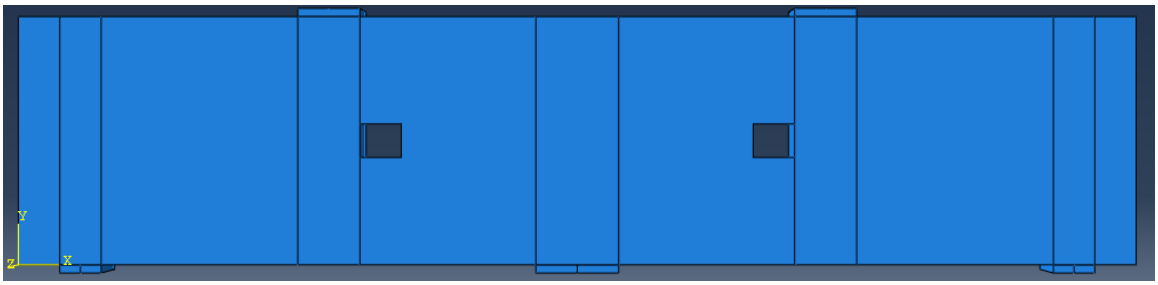

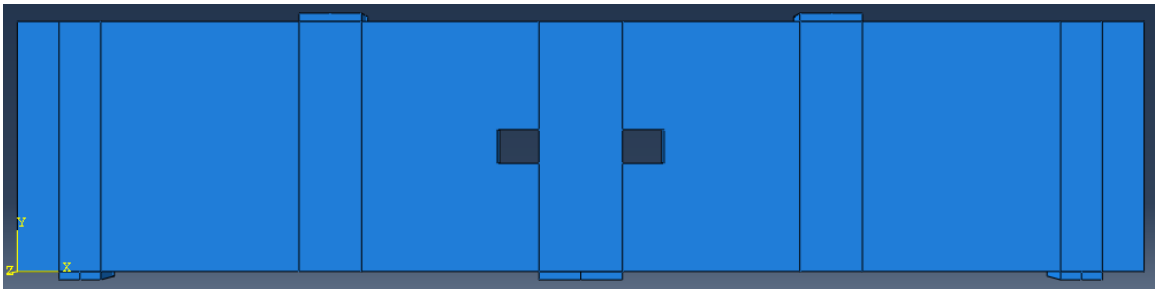

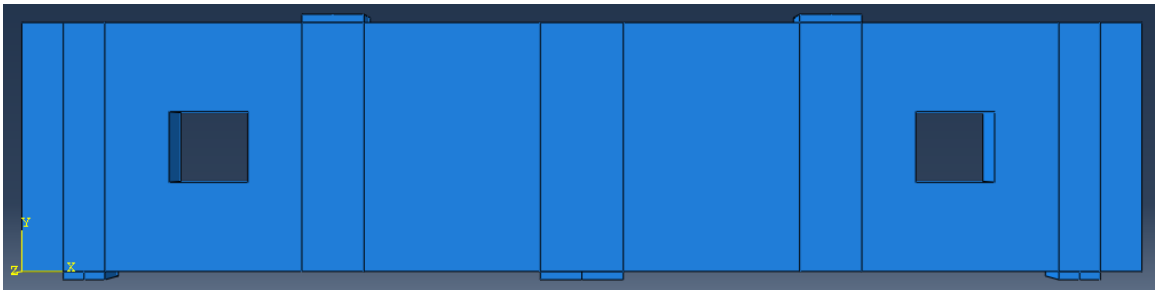

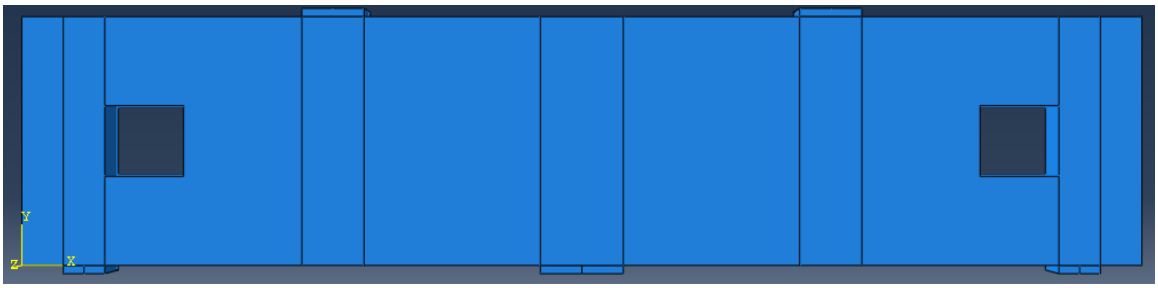

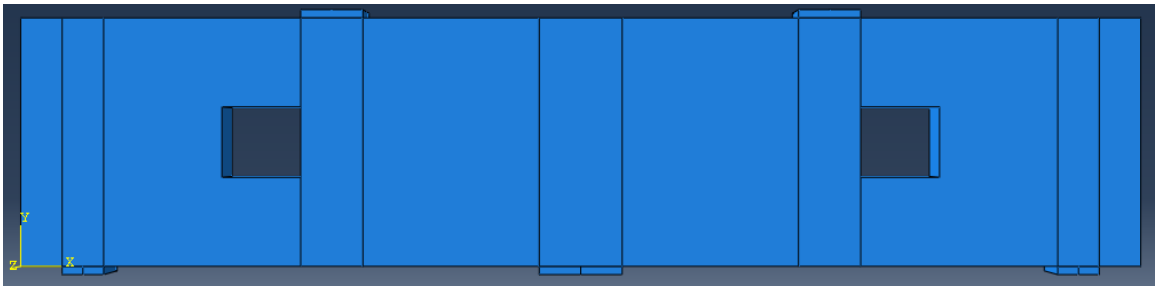

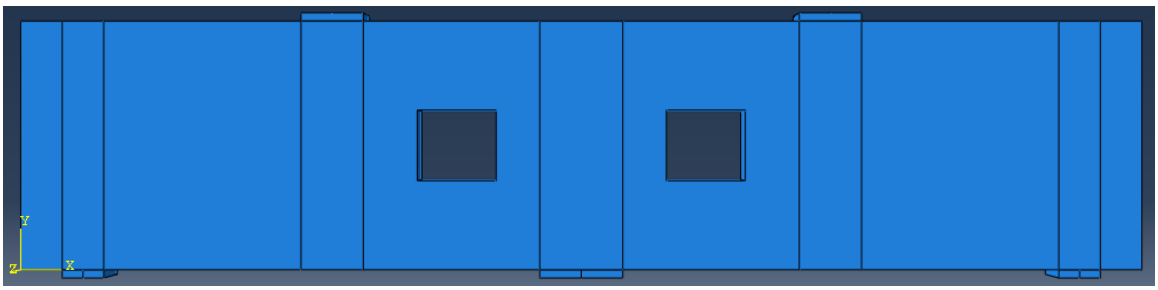

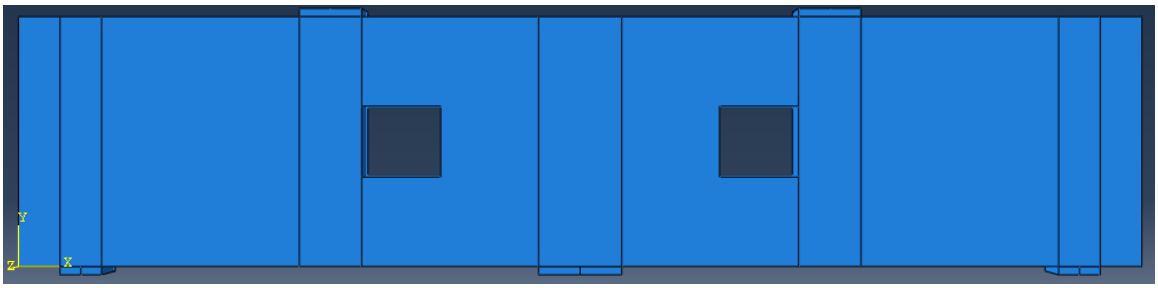

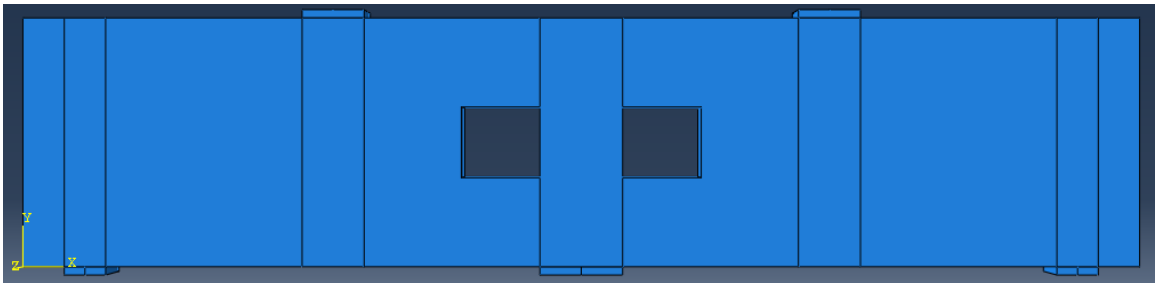

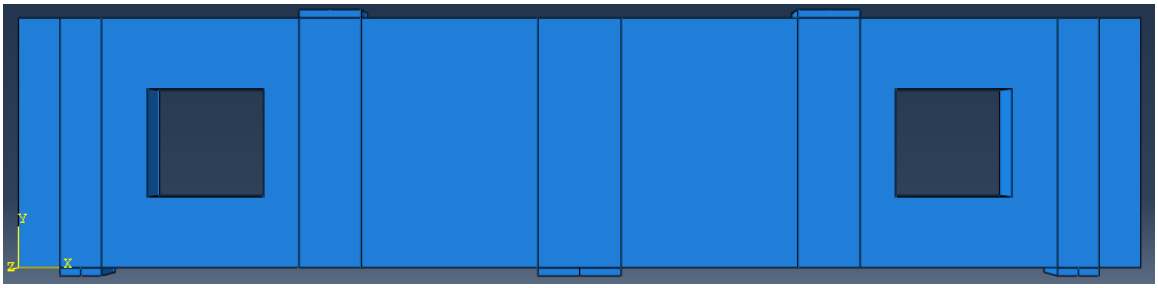

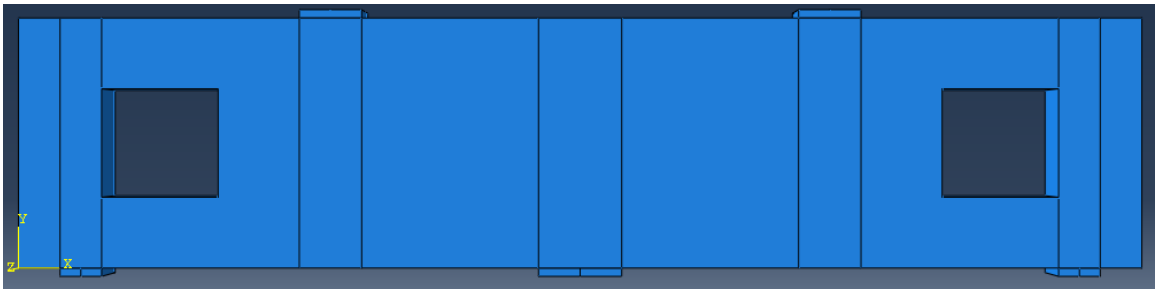

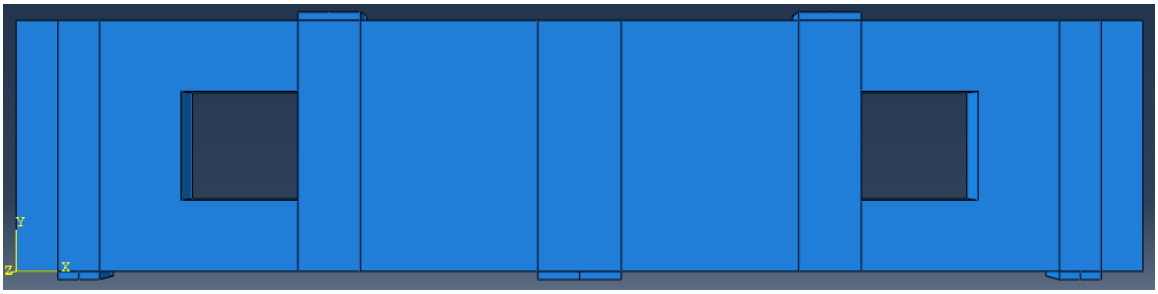

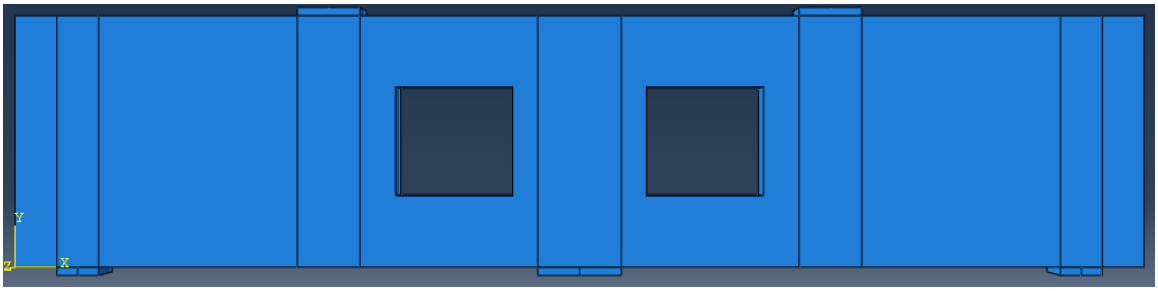

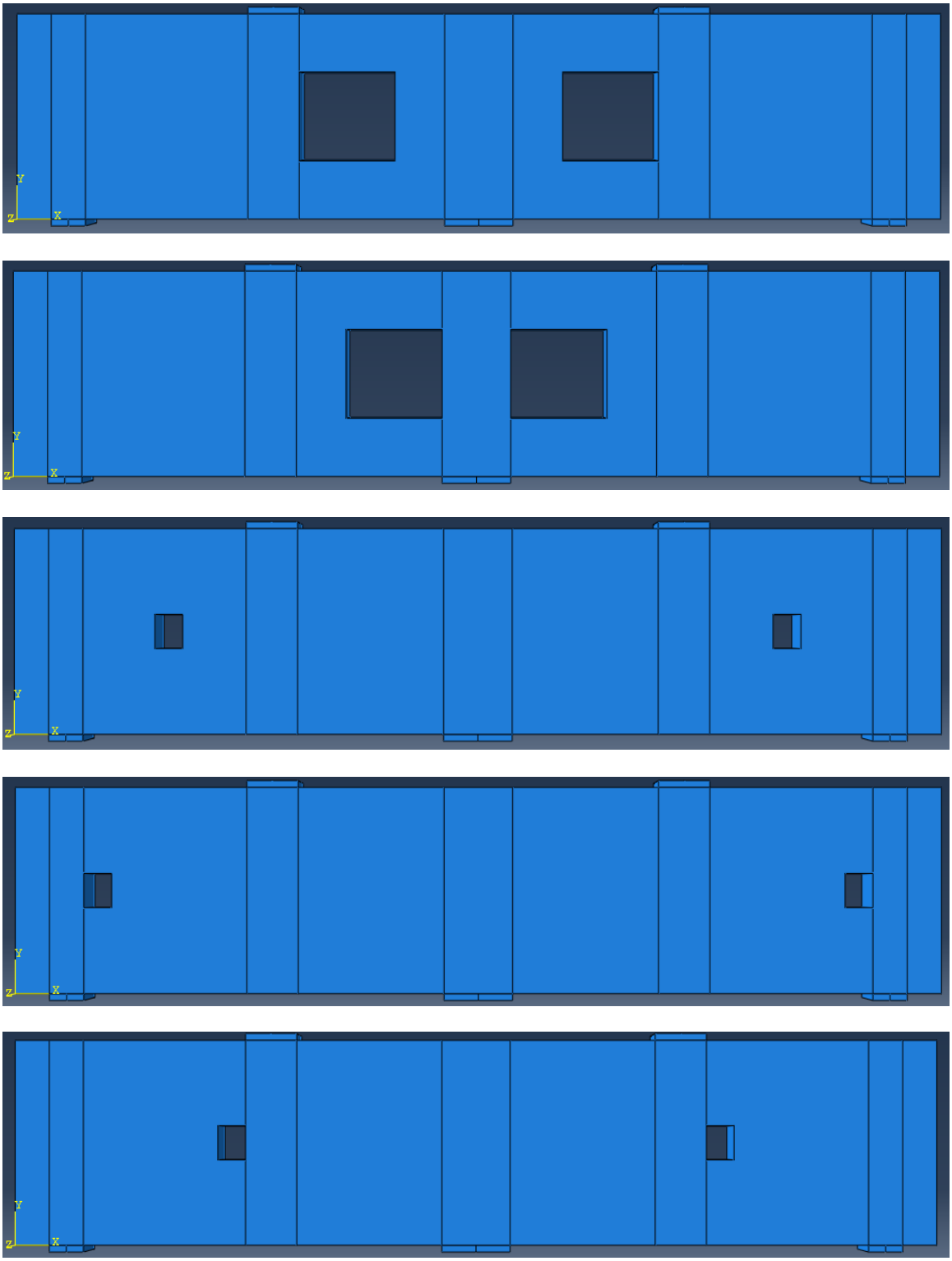

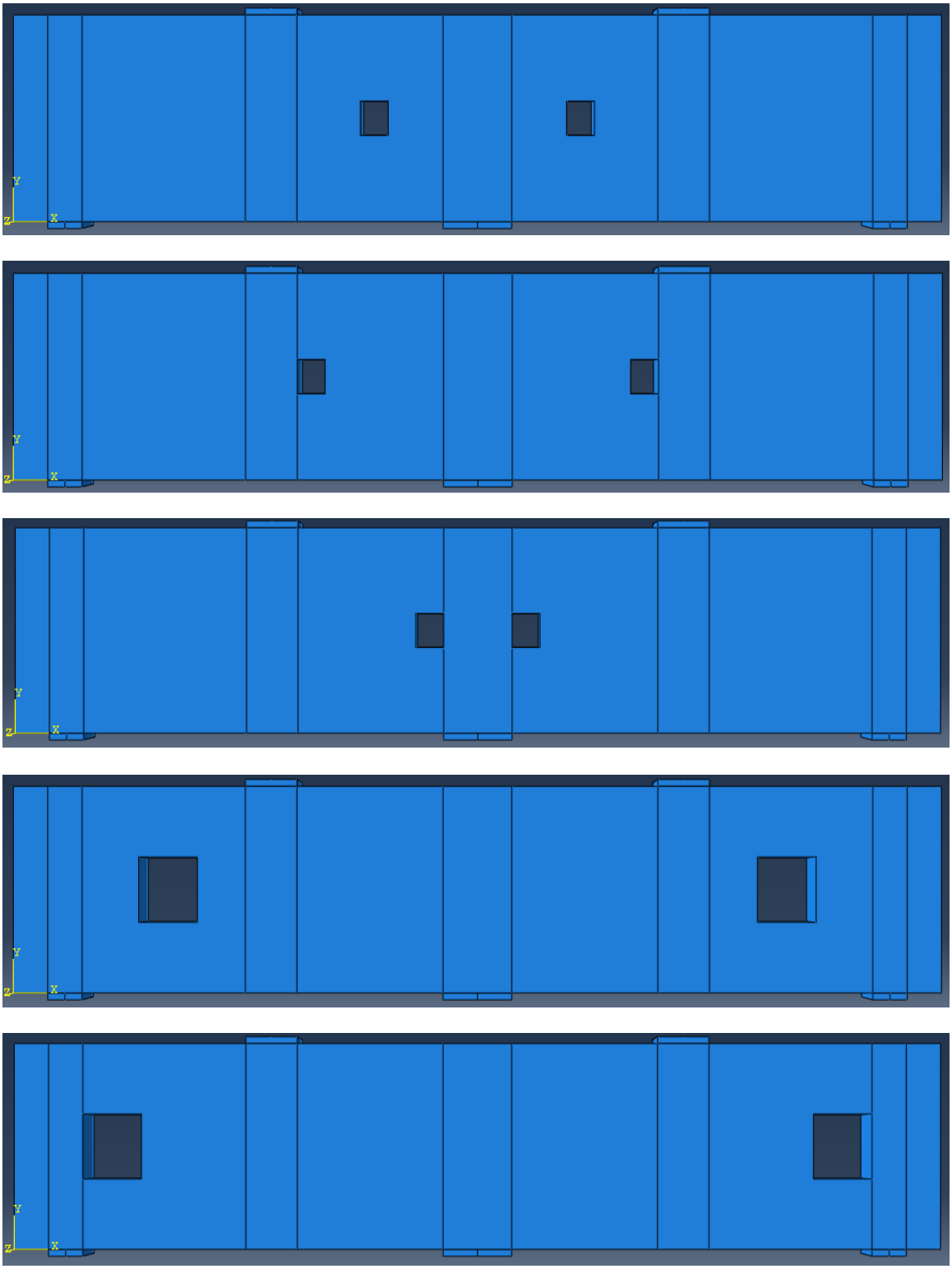

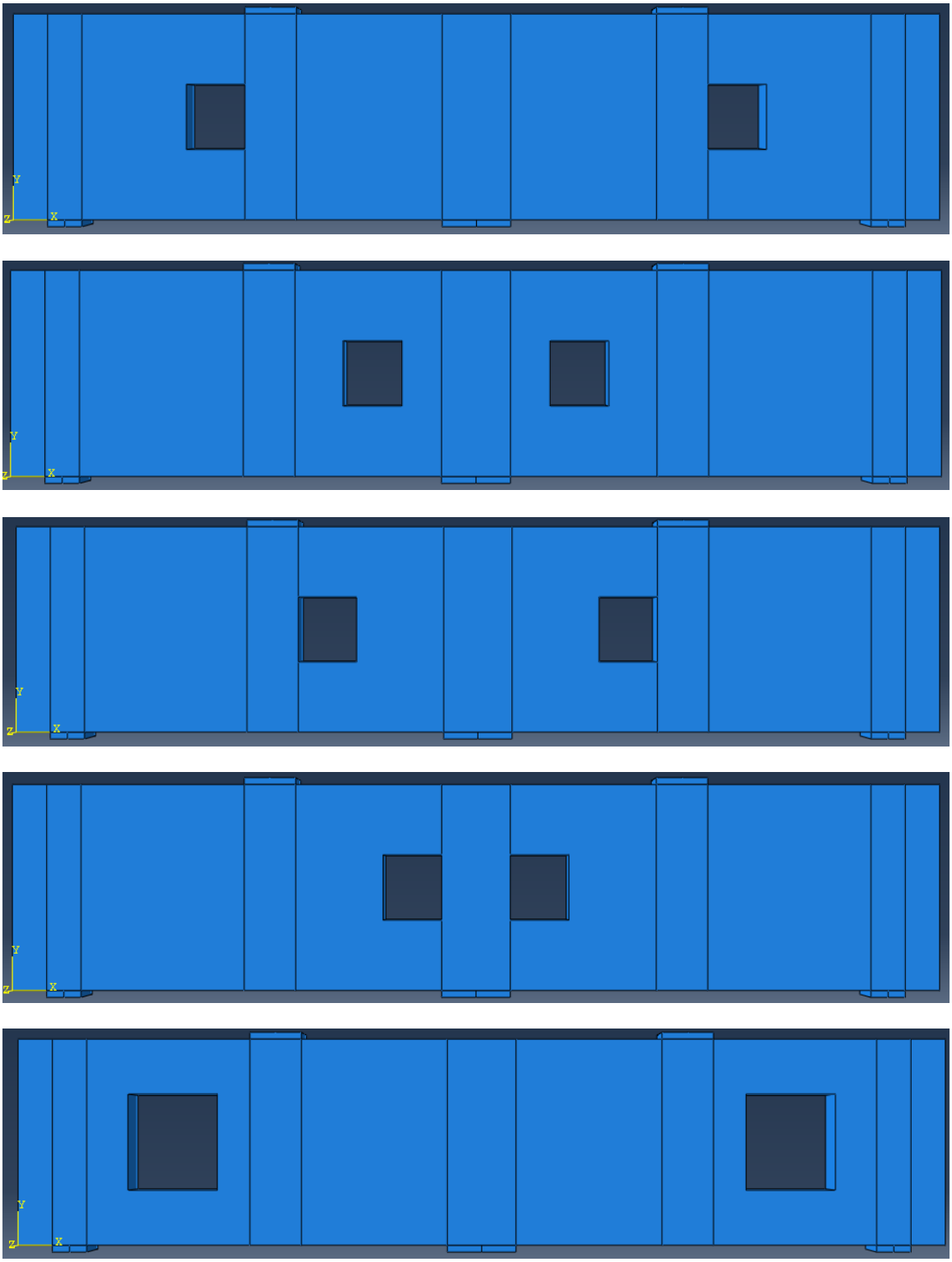

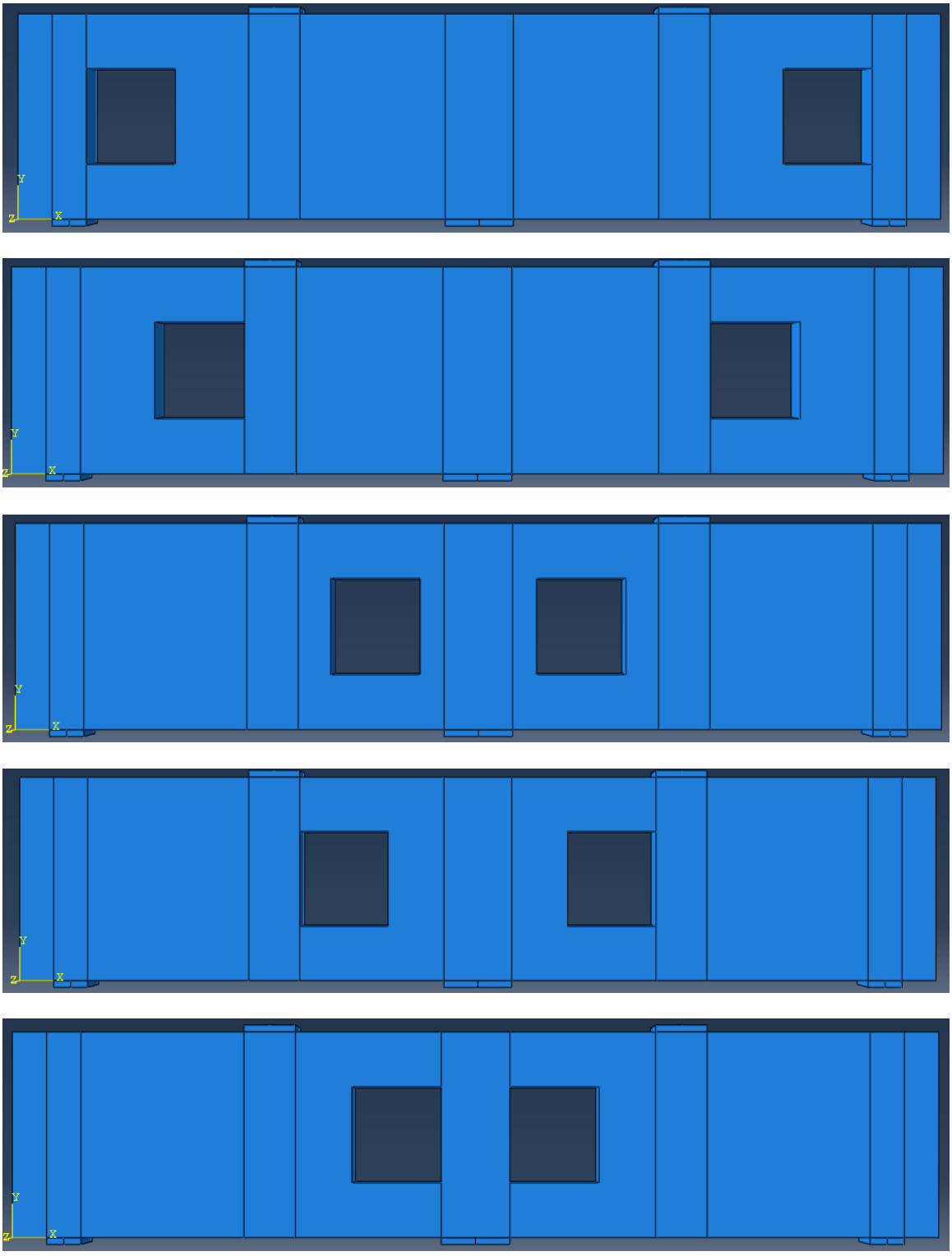

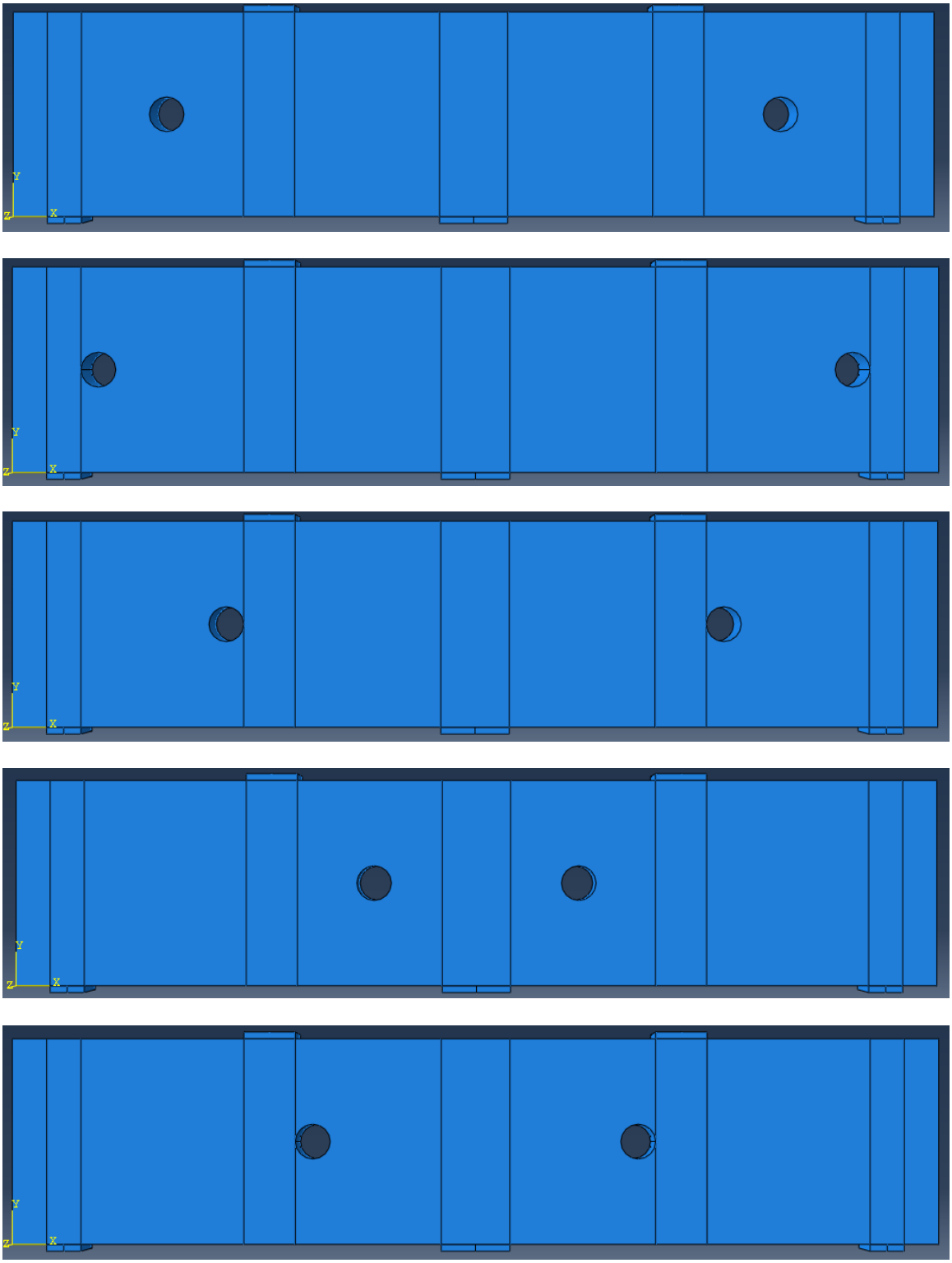

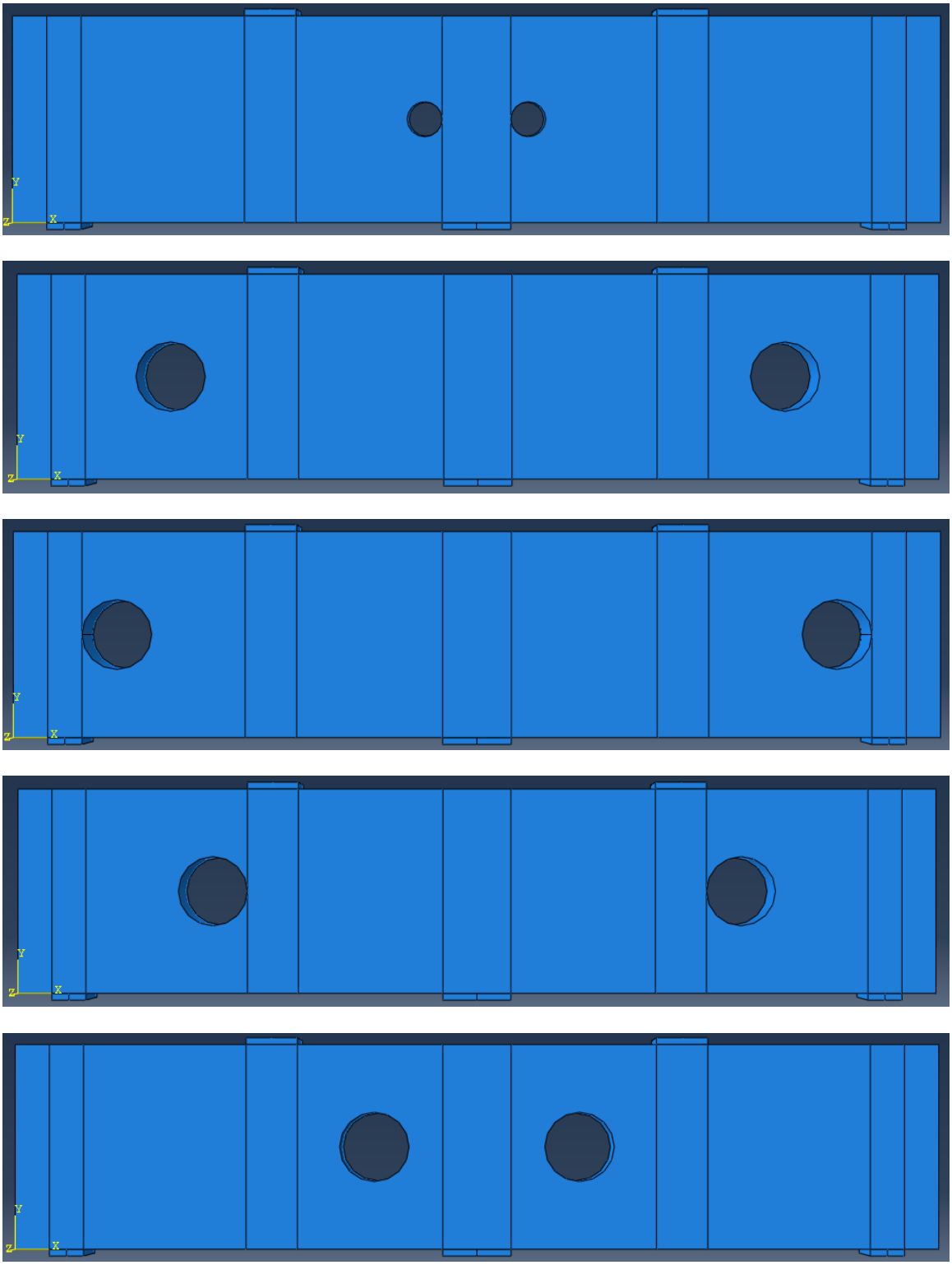

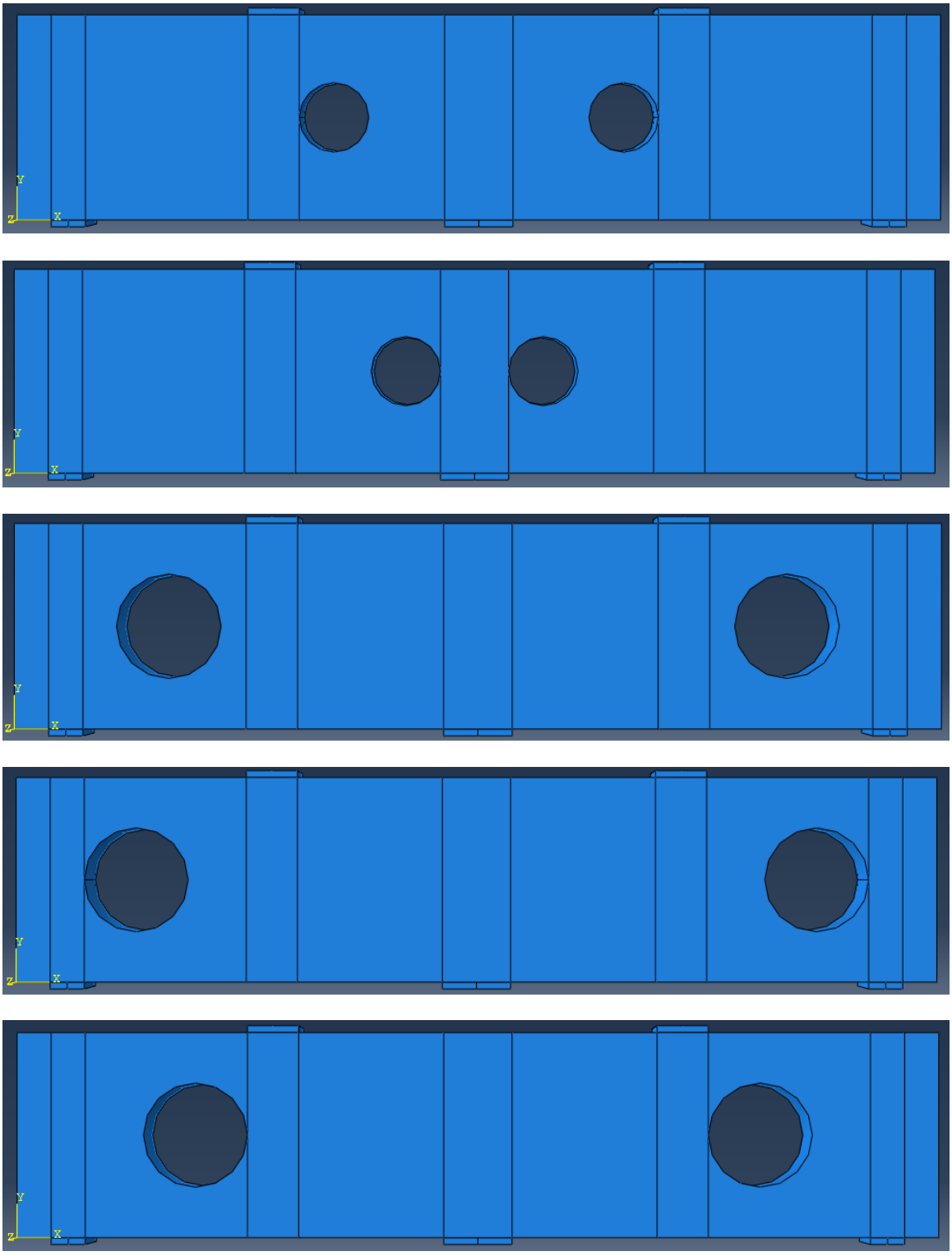

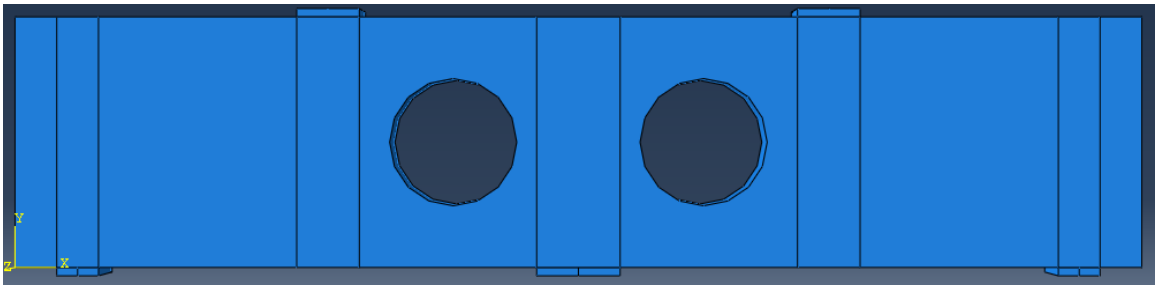
Y
Z
X

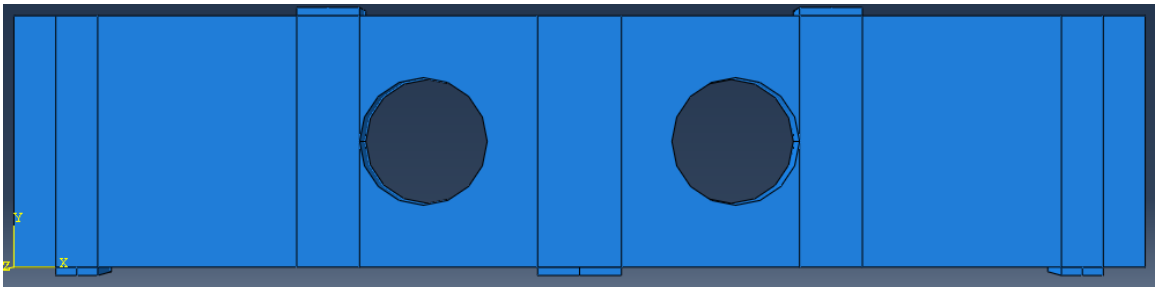
Y
Z
X

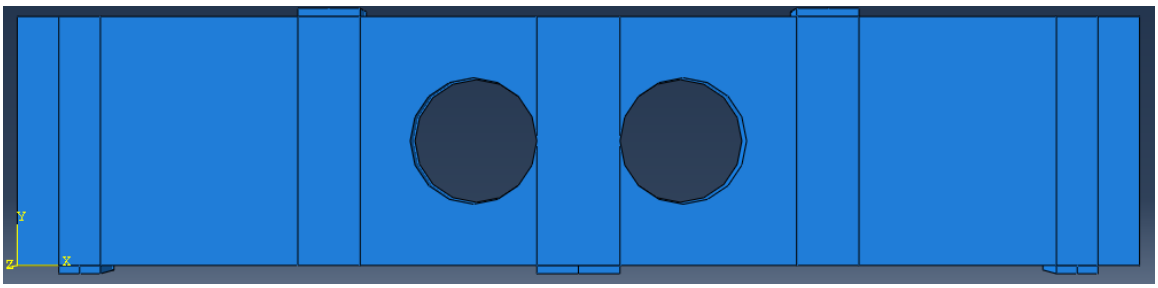
Y
Z
X

APPENDIX C

Table c.1 Total load carrying capacity for all sample models

Beam notation	Ultimate load	Beam notation	Ultimate load	Beam notation	Ultimate load
L10-60	899.82135	B25	893.284241	B49	888.9694824
B1	885.19928	B26	860.600159	B50	857.3739014
B2	844.189026	B27	842.143311	B51	830.3704224
B3	807.308899	B28	794.2448	B52	771.2078
B4	750.91394	B29	726.3738	B53	698.0936
B5	682.777344	B30	621.5916	B54	591.2874
B6	568.772156	B31	863.629	B55	852.6006
B7	838.213257	B32	831.1218	B56	816.9654
B8	794.720215	B33	798.8846	B57	774.0998
B9	743.094299	B34	724.4332	B58	690.0086
B10	668.012695	B35	604.1894	B59	569.8968
B11	542.152954	B36	528.9218	B60	482.9528
B12	439.70874	B37	884.6442	B61	871.2284
B13	855.066223	B38	847.9602	B62	832.3638
B14	826.041687	B39	821.3808	B63	793.7334
B15	762.134766	B40	756.6576	B64	712.9246
B16	676.800476	B41	646.9904	B65	595.3764
B17	558.577881	B42	591.6778	B66	519.2982
B18	452.523254	B43	854.5546	B67	841.382
B19	832.03949	B44	815.4522	B68	796.1552
B20	787.214844	B45	783.829	B69	748.9182
B21	710.145508	B46	702.824	B70	681.3024
B22	666.000061	B47	587.5436	B71	554.7082
B23	538.605652	B48	503.2816	B72	461.2114
B24	428.971619				